

Project ID N°: **101036449**

Call: **H2020-LC-GD-2020-3**

Topic: **LC-GD-8-1-2020** - Innovative, systemic zero-pollution solutions to protect health, environment, and natural resources from persistent and mobile chemicals



Preventing Recalcitrant Organic Mobile Industrial chemicals for Circular Economy in the soil-sediment-water System

Start date of the project: **1st November 2021**

Duration: **42 months**

D4.3 – Recommendations on EAOP-CW based treatment system for water reuse applications

Main authors: **Jessica Meijide Fernández**, Jofre Herrero, Leónidas Pérez-Estrada, Carme Bosch (EURECAT), Dana Pierina Orlando, Rocío Inés Bonansea, Miren López de Alda, Marta Llorca, Marinella Farré, Alicia Cano, Víctor Matamoros (CSIC), Toni Mas, Begoña Martínez, Josep Pascual (CBT), Sandra Valero (CCB), Peter Behnisch, Harrie Besselink (BDS)

Lead Beneficiary: **EURECAT**

Type of delivery: **Report**

Dissemination Level: **PU**

Filename and version: PROMISCES_D4-3_Recommendation-EAOP-CW (version 1)

Website: **<https://promiscses.eu/>**

Due date: M40 (28 February 2025)

This project has received funding from the European Union's Horizon 2020 research and innovation programme under grant agreement N°101036449



© European Union, 2025

No third-party textual or artistic material included on the publication without the copyright holder's prior consent to further dissemination by other third parties.

Reproduction is authorized provided the source is acknowledged

Disclaimer

The information and views set out in this report are those of the author(s) and do not necessarily reflect the official opinion of the European Union. Neither the European Union institutions and bodies nor any person acting on their behalf may be held responsible for the use which may be made of the information contained therein.

Document History

This document has been through the following revisions:

Version	date	Author/Reviewer	Description
V0.1	02/12/2024	Jessica Meijide, Jofre Herrero, Sandra Valero, Toni Mas, Josep Pascual, Marta Llorca, Dana Pierina Orlando, Rocío Inés Bonansea, Miren López de Alda, Alicia Cano, Peter Behnisch	Initial version
V0.2	17/01/2025	Jessica Meijide, Carme Bosch, Miren López de Alda, Begoña Martínez, Toni Mas, Sandra Valero, Victor Matamoros	Initial check
V0.3	10/02/2025	Jessica Meijide, Carme Bosch, Dana Pierina Orlando, Rocío Inés Bonansea, Miren López de Alda, Sandra Valero, Alicia Cano, Victor Matamoros	Document updated after review
V0.4	18/02/2025	Veronika Zhiteneva	Validation
V0.5	26/02/2025	Jessica Meijide, Dana Pierina Orlando, Alicia Cano, Victor Matamoros, Sandra Valero	Final version after validation
V0.6	26/02/2025	Floriane Sermondadaz	Quality control
V1.0	27/02/2022	Julie Lions	Version for submission

Authorisation

Authorisation	Name	Status	Date
Review	M. Sgroi	WP4 participant	22/01/2025
Validation	U. Miehe	WP4 Leader	21/02/2025
Quality Control	F. Sermondadaz	Administrative and financial manager	26/02/2025
Approval	J. Lions	Project coordinator	27/02/2025

Distribution

This document has been distributed to:

Name	Title	Version issued	Date of issue
EURECAT, CSIC, CBT, BDS, KWB	WP4.2 Partners & WP Leader	Version 1	03/03/2025

Executive Summary

The increasing presence of industrial persistent, mobile and toxic compounds (iPM(T)s) and per- and polyfluoroalkyl substances (PFAS), presents a critical barrier to advancing sustainable water management and the circular economy. To address these challenges, the PROMISCES project, part of the Horizon 2020 Green Deal initiative, aims to develop and demonstrate advanced water treatment technologies integrating electrochemical advanced oxidation processes (EAOP) with constructed wetlands (CW) focuses on reducing the concentration of potentially harmful substances in reclaimed water for agricultural irrigation.

This study contributes to the European Union's goals outlined in the Green Deal, the Zero Pollution Action Plan, and the Circular Economy Action Plan by addressing the removal of persistent contaminants from wastewater to enable safe agricultural irrigation. This initiative is particularly significant for water scarce regions such as Catalonia, Spain. The Besòs case study (CS#3) focused on the Montornès del Vallès Wastewater Treatment Plant (WWTP), where approximately 60% of the incoming wastewater flow comes from industrial sources. The PROMISCES project complies with stringent European and Spanish regulations for wastewater treatment and reuse, addressing the demand for advanced systems to adhere to evolving directives, such as the new Urban Wastewater Treatment Directive 2024/3019 and Spanish Royal Decree 1085/2024, approving the EU Water Reuse Regulation (2020/741) in Spain.

This hybrid system combines electrochemical oxidation and ozonation (e-Peroxone or EAOP), generating hydroxyl radicals for the efficient degradation of iPM(T)s and PFAS, while minimizing the energy consumption and reducing the toxic by-product formation. The system also includes a constructed wetland (CW) system, which mimic natural wetlands for pollutant filtration and nutrient absorption. Using plant species such as *Phragmites australis* and *Iris pseudacorus*, CWs serve as a post-treatment stage, enhancing effluent quality and providing additional environmental benefits, including promoting biodiversity.

The CS#3 followed a multi-phase approach, beginning with contaminant screening through non-target and targeted analytical methods, to identify priority contaminants, such as industrial chemicals and pharmaceuticals, in the effluent streams of the WWTP. Next, lab scale testing was conducted to assess the efficiency of ozonation, electrooxidation, and e-Peroxone in removing contaminants from synthetic wastewater. Pilot-scale testing was then conducted at the Montornès del Vallès WWTP to assess the performance of the e-Peroxone process and a wetland system, validating their efficiency under real-world conditions. The final phase involved a crop irrigation study, analyzing the feasibility of using reclaimed water on the growth of *Lactuca sativa* (lettuce) and assessing the potential contaminant uptake.

Key findings include the high performance of the EAOP, which achieved excellent removal efficiencies exceeding 90% for most target iPM(T)s, whereas PFAS removal was negligible, with e-Peroxone outperforming standalone ozonation or electrooxidation. Additionally, the CW system served as an effective post-treatment polishing stage, reducing nutrient levels and improving effluent quality. Reclaimed water also met stringent microbiological and chemical standards for agricultural use, with lettuce metabolomics indicating no significant health risks.

Based on the CS#3 results, this technological integration tackles the water scarcity challenges commonly faced by Mediterranean regions, positioning reclaimed water as a sustainable and viable solution for agricultural irrigation. Ongoing research and investment in such innovations are essential for driving the advancement of circular water economies.

Table of contents

1	Introduction	10
1.1	e-Peroxone treatment: An overview	10
1.2	Nature based treatment: A constructed wetland	11
1.3	The case for combining EAOP and CW	11
1.4	Objectives.....	12
2	Site description	13
2.1	General overview of the WWTP Montornès del Vallès	13
2.2	Infrastructure and layout	13
2.3	Infrastructure Overview.....	14
2.4	Secondary effluent composition.....	14
2.5	Environmental and regulation context.....	15
3	Pilot plant configuration	16
3.1	EAOP prototype	16
3.2	Wetland system	18
4	Methodology.....	19
4.1	Non-target screening of secondary WWTP effluent and target contaminant selection (Subtask 4.2.1)	19
4.2	Testing of technologies at lab-scale (TRL 4/5) (Subtask 4.2.2)	20
4.3	Pilot-scale technology testing (TRL 6) (Subtask 4.2.3)	20
4.4	Analytical methods for pilot monitoring	21
4.4.1	Physicochemical parameters	21
4.4.2	Nutrients	21
4.4.3	iPM(T)s	21
4.4.4	PFAS	23
4.4.5	Inorganic ions.....	24
4.4.6	Toxicological assays	24
4.4.7	Microbiological analysis	25
4.5	Study of the uptake and distribution of contaminants in vegetable crops irrigated with reclaimed water (Subtask 4.2.4)	26
4.6	Criteria for evaluating the use of reclaimed water in irrigation	26
5	Results.....	28
5.1	Non-target screening of secondary WWTP effluent and target contaminant selection	28
5.2	Testing of technologies at lab-scale (TRL 4/5)	30
5.2.1	Synthetic secondary effluent tests	30
5.2.2	Real secondary effluent trials	33

5.2.3	Scaling up: real secondary effluent at larger scale	37
5.3	Challenges and adaptations during pilot plant installation	41
5.4	Pilot-scale technology operation (TRL 6)	42
5.4.1	EAOP system	42
5.4.2	CW system	42
5.4.3	Monitoring	45
5.5	Parameters and removal efficiency of the pilot-scale technology testing (TRL 6).....	45
5.5.1	Physicochemical parameters	45
5.5.2	Nutrients	46
5.5.3	iPM(T)s removal	47
5.5.4	PFAS removal	51
5.5.5	Formation and fate of inorganic ions	52
5.5.6	Energy consumption	54
5.5.7	Toxicological analysis	54
5.5.8	Microbiological and physicochemical analyses analysis.....	55
5.6	Control wetland system - potential for removal of PMTs and PFAS	55
5.6.1	Physicochemical parameters and nutrients	55
5.6.2	iPM(T)s removal	57
5.6.3	PFAS removal	59
5.7	Compliance with Directive (EU) 2024/3019 on urban wastewater treatment	60
5.8	Challenges and adaptations during pilot plant operation	64
6	Use of reclaimed water in vegetable crop irrigation	65
6.1.	Characteristics of the water used for irrigation.....	65
6.2.	Uptake and distribution of contaminants in vegetable crops	66
6.2.1	iPM(T)s	66
6.2.2	PFAS	69
6.3.	Impact on crop yield and quality	70
6.3.1	Crop productivity and quality	70
6.3.2	Crop metabolomics.....	71
6.4.	Environmental and health implications.....	72
6.4.1	iPM(T)s	72
6.4.2	PFAS	75
7	Conclusions and recommendations.....	76
7.1	Key findings on process operation.....	76
7.2	Recommendations for optimizing the treatment and crop studies	76
7.3	Future considerations for system scalability	77
8	References	79

List of figures

Figure 1. Circular Economy Route for Case Study 3 (Source: KWB)	10
Figure 2. Technological treatment train for water reuse for agricultural irrigation (Source: KWB)	12
Figure 3. Location of Montornès del Vallès WWTP	13
Figure 4. Schematic representation of the EAOP prototype	16
Figure 5. EAOP prototype (APRIA Systems, Photobench LED275-8a)	16
Figure 6. P&ID diagram of the EAOP prototype (APRIA Systems, Photobench LED275-8a)	17
Figure 7. CW system (Montornès del Vallès WWTP)	18
Figure 8. Experimental set-up design for the CWs	19
Figure 9. Experimental setup design for testing of technologies at lab-scale	20
Figure 10. Experimental setup depicting the individual containers for cultivating lettuce	26
Figure 11. Sum of peak areas for each sample preparation (SP) method evaluated through suspect screening	28
Figure 12. iPM(T)s removal by ozonation, electro-oxidation and e-Peroxone using synthetic secondary effluent	32
Figure 13. iPM(T)s removed by electro-oxidation and e-Peroxone using real secondary effluent	34
Figure 14. PFAS removal from real secondary effluent using electro-oxidation and e-Peroxone	35
Figure 15. PFAS removal in real secondary effluent using electro-oxidation and e-Peroxone	36
Figure 16. iPM(T)s removal using electro-oxidation and e-Peroxone on real secondary WWTP effluent at larger scale	38
Figure 17. PFAS removal using electro-oxidation and e-Peroxone on real secondary WWTP effluent at larger scale	39
Figure 18. Weekly precipitation (blue bar) and evapotranspiration (orange bar) values (mm) and average weekly temperature (red line) (°C) calculated using data from Parets del Vallès Meteorological Station.	43
Figure 19. Average residence time (green line), irrigation time (red line) and weekly treated water volume for the post EAOP (blue bar) and control (orange bar) CW systems	44
Figure 20. Nutrient removal of the post EAOP CW at Montornès del Vallès WWTP	47
Figure 21. Pharmaceutical removal using e-Peroxone at Montornès del Vallès WWTP	48
Figure 22. Pharmaceuticals removal in the post EAOP CW system at Montornès del Vallès WWTP	48
Figure 23. Pesticides/Drugs of abuse/Others removal using e-Peroxone at Montornès del Vallès WWTP	49
Figure 24. Pesticides/Drugs of abuse/Others removal by post EAOP CW system at Montornès del Vallès WWTP	49
Figure 25. Industrial chemicals removal using e-Peroxone at Montornès del Vallès WWTP	50
Figure 26. Industrial chemical removal in the post EAOPs CW system at Montornès del Vallès WWTP (April: yellow bar, May: blue bar, June: orange bar and July: grey bar)	50
Figure 27. Nutrient removal of control CW at Montornès del Vallès WWTP	57
Figure 28. Pharmaceutical removals by control CW system at Montornès del Vallès WWTP	57
Figure 29. Pesticides/Drugs of abuse/Others removals by control CW system at Montornès del Vallès WWTP (April: yellow bar, May: blue bar, June: orange bar and July: grey bar)	58
Figure 30. Industrial chemical removals by control CW system at Montornès del Vallès WWTP	58
Figure 31. Agronomical parameters of lettuce crops irrigated with different water types (n=10)	70
Figure 32. Score plot with samples normalized using the triphenylamine feature and data scaled via Pareto scaling.	72

List of tables

Table 1. Design values for the Montornès del Vallès WWTP	14
Table 2. Average composition of the secondary effluent during pilot operation (April 1 to July 31, 2024)	15
Table 3. List of target analytes included in the LC-MS/MS-based targeted method developed	22
Table 4. PFAS quantified by IDAEA-CSIC	23
Table 5. Maximum allowable value established for Quality A.A. standards.....	25
Table 6. Soil-grown crops monitoring parameters	27
Table 7. Results obtained from analysis of target compounds in 85 water samples collected during the pilot and field-scale experiments.....	29
Table 8. Target pollutants and their theoretical concentrations in the spiked solution	30
Table 9. EE/O values for each pollutant involved in the treatment processes using spiked synthetic effluent water.....	33
Table 10. Formation of chlorinated by-products using electro-oxidation and e-Peroxone on real secondary effluent.....	36
Table 11. EE/O values for each pollutant involved in the treatment processes for real secondary effluent...	36
Table 12. Formation of chlorinated by-products using electro-oxidation and e-Peroxone on real secondary WWTP effluent at a larger scale	39
Table 13. Formation of brominated by-products using electro-oxidation and e-Peroxone on real secondary WWTP effluent at a larger scale	40
Table 14. EE/O values for each pollutant involved in the treatment processes for real secondary WWTP effluent	41
Table 15. Management of CW system operations and regulation of water inflows and outflows.....	44
Table 16. Average monthly sulfonic PFAS levels before and after e-Peroxone	51
Table 17. Average monthly carboxylic PFAS levels before and after e-Peroxone	51
Table 18. Average monthly sulfonic PFAS levels before/after post e-AOP CW	51
Table 19. Average monthly carboxylic PFAS levels before/after post e-AOP CW.....	52
Table 20. Formation of chlorinated by-products by e-Peroxone at Montornès del Vallès WWTP	52
Table 21. Removal of chlorinated by-products by constructed wetland	53
Table 22. CALUX analysis results of WAX-SPE water sample extracts	54
Table 23. Comparison of physicochemical parameters between CW systems (control vs post-EAOP)	56
Table 24. Average monthly sulfonic PFAS levels before (initial) and after (final) the control CW at Montornès del Vallès.....	59
Table 25. Average monthly carboxylic PFAS levels (initial) and after (final) the control CW at Montornès del Vallès.....	59
Table 26. Summary of iPMTs data: EAOP inlet concentration and removal efficiencies.....	61
Table 27. Summary of PFAS data: EAOP inlet concentration and removal efficiencies	63
Table 28. General water quality parameters for each type of irrigation water (n=5)	66
Table 29. Concentration of iPM(T)s in irrigation waters (n=3) and soil used for crop studies	67
Table 30. Overview of the iPM(T)s compounds in lettuce samples irrigated with bottled water (BW), secondary effluent wastewater (WW), and reclaimed water (RW).....	68
Table 31. Overview of the PFAS compounds in lettuce samples irrigated with bottled water (BW), secondary effluent wastewater (WW), and reclaimed water (RW) (n=10)	69
Table 32. Risk quotient (RQs) values for iPMT compounds detected in untreated wastewater (uWW), secondary effluent wastewater (WW) and reclaimed water (RW)	73
Table 33. Threshold of toxicological concern (TTC) analysis results for detected compounds	75
Table 34. Weekly intake for PFAS (sum of PFOA, PFOS and PFHxS)	75

List of abbreviations

- BOD5:** Biochemical Oxygen Demand (5 days)
- COD:** Chemical Oxygen Demand
- CWs:** Constructed Wetlands
- DO:** Dissolved Oxygen
- DOC:** Dissolved Oxygen Concentration
- DPG:** N,N'-diphenylguanidine
- EAOP:** Electrochemical Advanced Oxidation Processes
- EE/O:** Electrical Energy per Order
- HSSF CWs:** Horizontal Subsurface Flow Constructed Wetlands
- iPM(T):** Industrial Persistent, Mobile, and Potentially Toxic Compounds
- PFAS:** Per- and Polyfluoroalkyl Substances
- SHE:** Standard Hydrogen Electrode
- SP:** Sample Preparation
- SS:** Suspended Solids
- TN:** Total Nitrogen
- TP:** Total Phosphorus
- TRL:** Technology Readiness Level
- WWTP:** Wastewater Treatment Plant

1 Introduction

The presence of per- and polyfluoroalkyl substances (PFAS) and other industrial persistent, mobile, and potentially toxic compounds (iPM(T)s) within natural ecosystems poses a substantial obstacle to advancing the circular economy, due to their harmful impact on both ecological systems and human health. Achieving the objectives set forth by the European Green Deal, alongside the ambitions of the Zero Pollution Action Plan and the Circular Economy Action Plan, calls for cutting edge approaches capable of effectively addressing and removing these contaminants from ecosystems.

The **Besòs case study (CS#3)**, located in the Barcelona Province, Spain, brought together a skilled team of experts from IDAEA-CSIC, CBT, CCB and Eurecat, who assessed the levels of PFAS and other iPM(T)s in wastewater to explore its reuse for agricultural irrigation (**Figure 1**). This initiative holds significant importance in Catalonia's water scarce regions, where persistent droughts often result in strict water restrictions and reduced consumption, severely limiting freshwater resources available for agricultural irrigation.

Given these circumstances, the treated wastewater emerges as a viable alternative for agricultural irrigation. By carefully evaluating and addressing the presence of contaminants, the PROMISCES project aims to contribute to sustainable water management within the Besòs River basin, a key example of a Mediterranean climate watershed, thereby promoting water reuse and supporting agriculture in one of Spain's most drought prone regions.



Figure 1. Circular Economy Route for Case Study 3 (Source: KWB)

1.1 e-Peroxone treatment: An overview

The Electro-Peroxone (e-Peroxone) process merges electrochemical oxidation with ozonation, offering an advanced solution for wastewater treatment. This method efficiently degrades persistent toxic chemicals by generating hydroxyl radicals through an innovative, *in situ* production of H_2O_2 via cathodic oxygen reduction, enhanced by ozone gas sparging. Since hydroxyl radicals ($E_0 = 2.80 \text{ V vs SHE}$, Standard Hydrogen Electrode) are significantly stronger oxidants than ozone ($E_0 = 2.07 \text{ V vs. SHE}$), they can rapidly degrade a wide range of organic pollutants at exceptionally high reaction rates ($\approx 10^{-8} - 10^{10} \text{ M}^{-1} \text{ s}^{-1}$). During the e-Peroxone process, competing reactions at the cathode can hinder efficient H_2O_2 production. Key side reactions include the reduction of water to hydrogen, the further

reduction of electro-generated H_2O_2 back to water, and the reduction of ozone to oxygen. To optimize H_2O_2 generation and enhance the overall efficiency of the process, reducing these competing reactions is crucial for advanced water treatment applications.

The H_2O_2 electro-generation overcomes the limitations of conventional methods, eliminating the need for high doses of H_2O_2 that pose safety risks during storage, transport, and handling. Furthermore, the e-Peroxone system addresses the limitations of traditional ozone treatments. By optimizing ozone mass transfer and utilization, this system boosts treatment efficiency and effectively prevents the unwanted formation of bromate, providing a powerful and reliable solution for advanced wastewater treatment. Therefore, this approach amplifies the oxidation efficiency, enabling contaminant breakdown and improved treated water quality (Wang et al., 2018).

1.2 Nature based treatment: A constructed wetland

Constructed wetlands (CWs) are engineered ecosystems designed to mimic filtration and purification functions of natural wetlands to enhance water quality. These systems are composed of three key components: well-balanced substrates made of sand, gravel, and other materials; diverse populations of microorganisms; and hardy plant species selected for their capacity to absorb pollutants.

These engineered systems can be categorized based on three key criteria: i) hydrology, distinguishing between surface or subsurface flows; ii) plant species type, including emergent, submerged, or free-floating plants; and iii) flow direction, whether horizontal or vertical (Barco and Borin, 2017).

Horizontal subsurface flow constructed wetlands (HSSFCW) are one of the most widely used CW systems across Europe. In this setup, wastewater flows gradually through a porous medium until it reaches the plant substrate, where many pollutants are filtered out before the treated effluent is discharged. The wetland features aerobic zones populated by macrophytes and soil substrates alongside anaerobic zones primarily composed of gravel and sand (Sachdeva et al., 2023).

The selection of the appropriate vegetation is crucial for effective CW design. Two of the most used species are wetland macrophytes *Phragmites australis* and *Iris pseudacorus*, which play a vital role in enhancing the system's performance. These species serve multiple functions including nutrient uptake, oxygen release in the rhizosphere, filtration, providing surfaces for microbial biofilm growth, stabilizing substrates, and aiding in pollutant treatment (Vymazal, 2011).

1.3 The case for combining EAOP and CW

The e-Peroxone process can be combined with complementary treatment technologies, amplifying its overall performance. A prime example is the combination of e-Peroxone with CW systems as a post-treatment stage. This treatment enhances the quality of the treated water by leveraging the natural filtration and adsorption abilities of the CWs, offering a final polishing step to the effluent (**Figure 2**). This innovative combination of e-Peroxone and CWs not only excels at advanced pollutant removal but also brings valuable environmental benefits, like promoting biodiversity and contributing ecosystem services.

Advanced chemical oxidation methods, such as electrooxidation, are highly effective at breaking down persistent contaminants such as PFAS, pesticides, and pharmaceutical residues. However, these methods can lead to the formation of harmful by-products as perchlorate, bromate, and halogenated organic compounds (Yang, 2019). Perchlorate, specifically, acts as an endocrine

disruptor and can accumulate in plants and animals, posing potential health risks to consumers (Kumarathilaka et al., 2016).

To address this risk, the **PROMISCES** project uses e-Peroxone process to leverage hydrogen peroxide to inhibit the formation of toxic by-products (Yao et al., 2019). Coupled with a constructed wetland, this combined process enhances pollutant removal efficiency, reduces overall costs, and minimizes the formation of harmful by-products. Although these hybrid systems have only been tested at the bench scale (Casierra-Martinez et al., 2020; Cedillo-Herrera et al., 2020), they have demonstrated promising potential for effectively removing persistent contaminants.

As pressures on water resources continue to rise and the need for sustainable treatment methods becomes more urgent, this integrated system offers a promising pathway to meet the demand for efficient, eco-friendly wastewater treatment solutions.



Figure 2. Technological treatment train for water reuse for agricultural irrigation (Source: KWB)

1.4 Objectives

The **Besòs case study (CS#3)** focused on developing and demonstrating the combine EAOP with CWs as a nature-based post-treatment solution (TRL 4-6) to (i) remove iPM(T)s and PFAS from WWTP effluent with a high proportion of industrial wastewater and (ii) reduce the transfer of these contaminants during water reuse for agricultural irrigation, ensuring no risk to human health.

The specific performance targets were: (i) removal of over 5 PFAS compounds; (ii) removal of more than 20 iPM(T) substances; and (iii) a PM(T) removal efficiency of over 90%.

2 Site description

2.1 General overview of the WWTP Montornès del Vallès

CS#3 is located at the Montornès del Vallès WWTP in the municipality of Montornès del Vallès, Barcelona, Catalonia, Spain, on the left bank of the Besòs River (**Figure 3**). This treatment plant processes wastewater from multiple nearby areas, including Montornès del Vallès, Parets del Vallès, Vilanova del Vallès, Vallromanes, Montmeló, parts of Granollers and Mollet, as well as Lliçà de Vall and Lliçà d'Amunt. Additionally, wastewater from the industrial zones in these regions is processed, serving a population equivalent of approximately 300,000 inhabitants. The treated effluent is then discharged into the Besòs River.

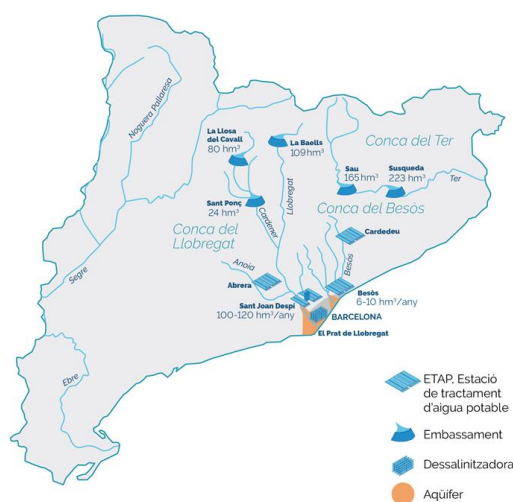


Figure 3. Location of Montornès del Vallès WWTP

The decision to focus on this plant for the PROMISCES project was driven by the fact that around 60% of the incoming water originates from industrial sources, including sectors such as pharmaceuticals, organic chemistry, food processing, metal coating, leather, and textiles.

2.2 Infrastructure and layout

The first phase of the Montornès del Vallès WWTP was constructed in 1994, featuring a primary physical-chemical treatment designed to handle a flow of 30,000 m³/day. The plant was then expanded in 1999 with the addition of a biological process. This process utilizes blowers and fine bubble diffusers to supply air, facilitating the oxidation of organic matter. This organic matter is further eliminated with biomass in reactors populated by microorganisms. After thickening, the resulting sludge is stabilized in an anaerobic digester, significantly enhancing purification efficiency compared to the initial physic-chemical treatment, especially in terms of organic pollution removal.

In 2005, the Montornès del Vallès WWTP underwent further upgrades to rise its capacity to 40,000 m³/day. These upgrades included ammonium and nitrogen removal, as well as an automated air supply control system for the biological reactor, that reduces energy consumption compared to conventional setups (**Table 1**).

The plant's sludge is sourced from two different streams: primary sludge, which is extracted from the bottom of the primary sand trap and concentrated in a gravity thickener, and secondary sludge, which undergoes further thickening in centrifugal units. These sludges are then combined, digested anaerobically, and stabilized, significantly reducing their volume. After digestion, the sludge is dewatered using a three-stage system. The anaerobic digestion process, which occurs in a 5,000 m³ digester, produces methane-rich biogas that is fed to two 250 kW co-generation engines to generate electricity.

Table 1. Design values for the Montornès del Vallès WWTP

Parameter	Design values
Treatment	Biological
Inhabitants' equivalents	300,000
System performance	95%
COD (mg/L)	947
BOD ₅ (mg/L)	310
SS (mg/L)	313
TN (mg/L)	62
TP (mg/L)	8

2.3 Infrastructure Overview

- **Arrival Inlet:** Pumping system to regulate flow into the plant
- **Pre-treatment:** Screening, degritting, and a floatable separator to remove larger solids
- **Primary Treatment:** Primary sedimentation to settle suspended solids
- **Secondary Treatment:** Piston flow system for efficient organic matter removal
- **Decantation:** Concentric decantation to separate remaining solids from treated water
- **Aeration:** Fine bubble diffusers to oxygenate biological reactors, efficient breakdown of organic material.
- **Primary Thickening:** Static gravity thickening for primary sludge concentration
- **Secondary Thickening:** Mechanical centrifuge for additional concentration of secondary sludge
- **Digestion:** Anaerobic digestion for sludge stabilization and biogas production
- **Dewatering:** Centrifuge system to remove excess water from the sludge
- **Service water treatment:** Includes filtration, ultraviolet disinfection, and chlorination for high-quality treated water for non-potable uses

2.4 Secondary effluent composition

Secondary effluent, typically derived from the biological treatment of domestic/industrial wastewater, contains a complex blend of organic and inorganic substances. **Table 2** presents the average composition of the secondary effluent during pilot operation period (April 1 to July 31, 2024). These values are following the standards outlined in the current Council Directive 91/271/EEC (UWWTD), as well as the New Revision of this UWWTD 2024/3019 and Regulation (EU) 2020/741, which lays out the minimum standards for water reuse.

Table 2. Average composition of the secondary effluent during pilot operation (April 1 to July 31, 2024)

Parameter	Secondary effluent WWTP	UWWTD 91/271/ECC	New UWWTD 2024/3019	Regulation (EU) 2020/741	Royal Decree 1085/2024 (Quality A.A)
pH	7.17	n.a.	n.a.	n.a.	*
σ ($\mu\text{S/cm}$)	2,224	n.a.	n.a.	n.a.	*
COD (mg/L)	49	125	125	n.a.	*
TOC (mg/l)	n.a.	n.a.	37	n.a.	*
BOD ₅ (mg/L)	7,72	25	25	<10	<10
SS (mg/L)	6,72	35	35	<10	<10
TN (mg/L)	5.4	10	8	n.a.	*
TP (mg/L)	0.42	1	0,5	n.a.	*
NH ₄ (mg/L)	0.91	n.a.	n.a.	n.a.	*

n.a.: not available Source: Gica0 (Consorti Besòs Tordera)

* **Contaminants:** Generally, only a limited number of contaminants will be regulated in wastewater discharge authorizations to ensure that the production and supply of regenerated water does not negatively impact the receiving environment. This aligns with the regulations outlined in Royal Decree 817/2015 and Royal Decree 1514/2009.

Throughout the operation of the pilot plant, IDAEA-CSIC closely monitored the concentrations of iPMTs and PFAS in the secondary effluent from Montornès del Vallès WWTP. The analysis revealed long-chain PFAS (>C6) concentrations ranged from 0.50-7.67 ng/L, while short-chain PFAS (<C6) varied between 0.70 and 79.87 ng/L.

Additionally, the iPM(T)s monitoring encompassed a diverse array of these compounds—industrial chemicals, pharmaceuticals, drugs of abuse, pesticides and others—each presenting a wide range of concentration levels. These values reflect the variability and complexity of iPM(T)s residues typically found in secondary effluents. For instance, target pharmaceuticals and industrial chemicals showed concentrations spanning from trace amounts up 1.6 $\mu\text{g/L}$, whereas pesticides and drugs of abuse tended to fall within lower ranges, typically in the ng/L scale.

2.5 Environmental and regulation context

The Montornès del Vallès WWTP discharges its treated effluent into the Besòs River, with the riverbed of its tributary, the Congost River, designated as a protected site under the Natura 2000 network. This classification highlights the area as environmentally sensitive.

Given the current hydrological challenges, CBT is actively working to enhance the availability of water resources within its operational area. To this end, the organization is developing a comprehensive Master Plan for Regenerated Water (PDAR), which includes a range of strategies designed to optimize and adapt water management practices for the future.

Due to the ongoing drought, around 90% water in the Besòs basin now originates from treated wastewater. Consequently, treated water must reach higher quality standards to meet environmental regulations and anticipate stricter requirements in upcoming directives, notably the new UWWTD 2024/3019. Additionally, evolving drinking water legislation must be considered, as mounting water stress will necessitate the use of premium-quality regenerated water to address the challenge of supplying pre-drinking water.

3 Pilot plant configuration

3.1 EAOP prototype

The electrochemical advanced oxidation processes (EAOP) prototype (APRIA Systems, Photobench LED275-8a) (Figure 4, Figure 5 and Figure 6) has been designed to integrate three advanced oxidation technologies, each engineered to operate independently or in combination with the others: (i) an ozone generation system equipped with an ozoniser and a Venturi tube; (ii) an annular UV-C LED photoreactor (not used in PROMISCES project); and (iii) an electrochemical cell equipped with BBD (boron-doped diamond) electrodes. This flexible configuration enables for tailored operation depending on the treatment requirements optimizing performance and efficiency in the pollutant degradation.

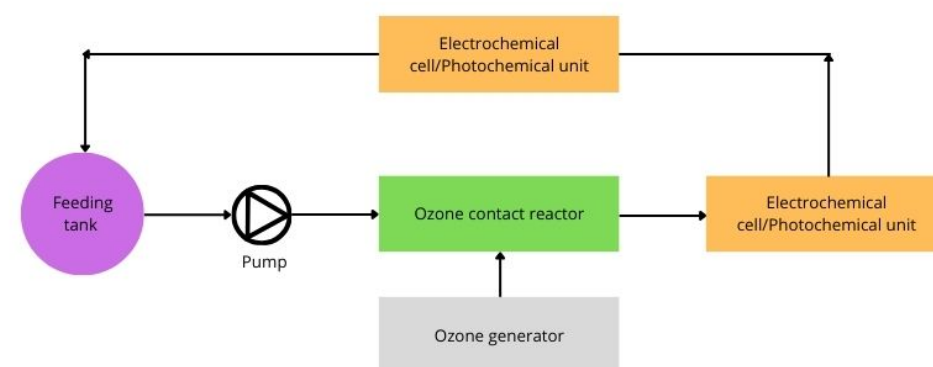


Figure 4. Schematic representation of the EAOP prototype (APRIA Systems, Photobench LED275-8a)



Figure 5. EAOP prototype (APRIA Systems, Photobench LED275-8a)

Ozonation unit

The treatment process initiates by channelling the water into a Venturi tube. As the water flows through this tube, ozone is introduced into the stream. This ozone is generated by the ozoniser at a maximum rate of approximately 7 g/h, using atmospheric air as the feed gas. Subsequently, the ozonated water enters a contact reactor, specifically engineered to promote optical mixing and maximize the interaction between the ozone and water. Within this chamber, contact time is carefully extended, facilitating complete ozone dissolution and enhancing the overall effectiveness of the treatment process. Any remaining ozone in the gas phase is efficiently removed using a thermocatalytic ozone destructor, preventing any excess ozone from being released to the environment. Upon completion of the treatment process, the ozonated water can be either recirculated back to the feed tank for further processing or directed to the following treatment unit for additional treatment steps.

Photochemical unit

In the photochemical treatment, the water undergoes processing within a glass annular photoreactor that consists of two concentric tubes. Water flows through the outer tube while a powerful LED lamp is housed within the inner tube. This light source is composed of 80 UV-C LEDs ($\lambda=275$ nm) distributed across four strips, providing adjustable irradiated power. To achieve the desired treatment dose, either the flow rate of the water or the irradiated power of the lamp must be modified accordingly. Additionally, the photoreactor features an air-cooling system and a temperature probe, ensuring effective temperature monitoring and control throughout the process.

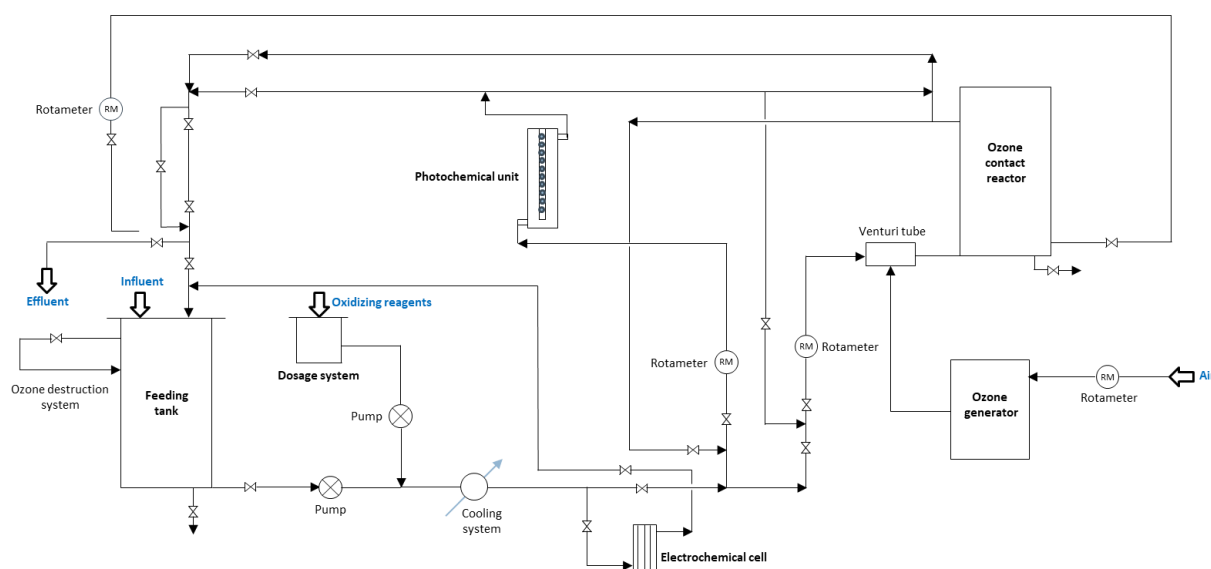


Figure 6. P&ID diagram of the EAOP prototype (APRIA Systems, Photobench LED275-8a)

Electrooxidation unit

The electrochemical cell featured a boron-doped diamond (BDD) anode and a stainless steel (SS) cathode, designed with optimized active surface areas. Each BDD electrode, fabricated with a niobium substrate and double-sided coating, and each SS electrode measured 5×15 cm, providing a total surface area of $150 \text{ cm}^2/\text{electrode}$. The electrodes were assembled in an alternating stack with

a 3 mm gap between them, forming a set of 5 BDD and 6 SS electrodes for an active area of 1500 cm² (excluding the outermost SS electrodes' external surfaces).

Additionally, the system is outfitted with a safety pressure switch which guarantees operations stay within safe limits, with a maximum operating pressure established at 4.5 bar. Temperature, pH, redox potential, dissolved ozone and conductivity values of the treated water are monitored via the PLC screen located on the front of the electrical and control enclosure. Furthermore, the installation features three visual flowmeters and three pressure gauges, each linked to the respective unit, providing real-time flow and pressure readings.

3.2 Wetland system

Two CW channels were designed to maximize their natural filtration capabilities, each measuring 74 cm in width, 47 cm in depth, and 3 meters in length, and employing a horizontal subsurface flow configuration (**Figure 7**). These artificial ecosystems incorporate a layered gravel system (1.5 cm diameter), enhancing water flow and filtration, along with the introduction of two macrophyte species: *Iris pseudacorus* and *Phragmites australis*.



Figure 7. CW system (Montornès del Vallès WWTP)

One of the flumes receives water directly from the outlet of the Montornès del Vallès WWTP, utilizing secondary effluent without prior filtration and the second channel is supplied with water from the EAOP prototype outlet buffer tank, which undergoes both filtration and e-Peroxone process (**Figure 8**).

Both constructed wetlands are fed from the lower section of the flume and function as subsurface horizontal flow systems, with water flowing through a granular medium at a depth influenced by the size and spread of the plant roots. Both CWs operated under the same hydraulic conditions, defined by the volume of water treated by the EAOP. The water produced by the EAOP was stored in multiple buffer tanks to maintain a steady flow. The system operated on a daily irrigation schedule, running for 7 hours from Monday to Friday during working hours, with a flow rate of 0.35 L/min. From Friday to Sunday, the flow rate was reduced to 0.20 L/min for a duration of 66 hours. The average inlet flow rate over the entire period was 0.24 L/min, calculated by dividing the total liters consumed by the total watering hours.

The CWs have an effective porosity of 25% (determined through granulometric analysis, according to Sanders (1998)). The CWs have a maximum capacity of 250 liters and operate under normal conditions with the water filled to one-third of their total depth, which allows them to hold an estimated volume of 80-90 liters. The average hydraulic residence time, calculated based on the typical inlet flow rate and total volume treated, ranges from 5 to 6 hours. However, on sample days, the hydraulic residence time increases to approximately 6 to 7 hours, as the system operates in batch mode to optimize water contact with the rhizomes, processing an average daily volume of 210 liters. This estimation may vary due to multiples factors such as changes in the inflow rates, irrigation durations, evapotranspiration, rainfall, and sampling frequency, all of which influence fluctuations in outflow during the pilot operation.

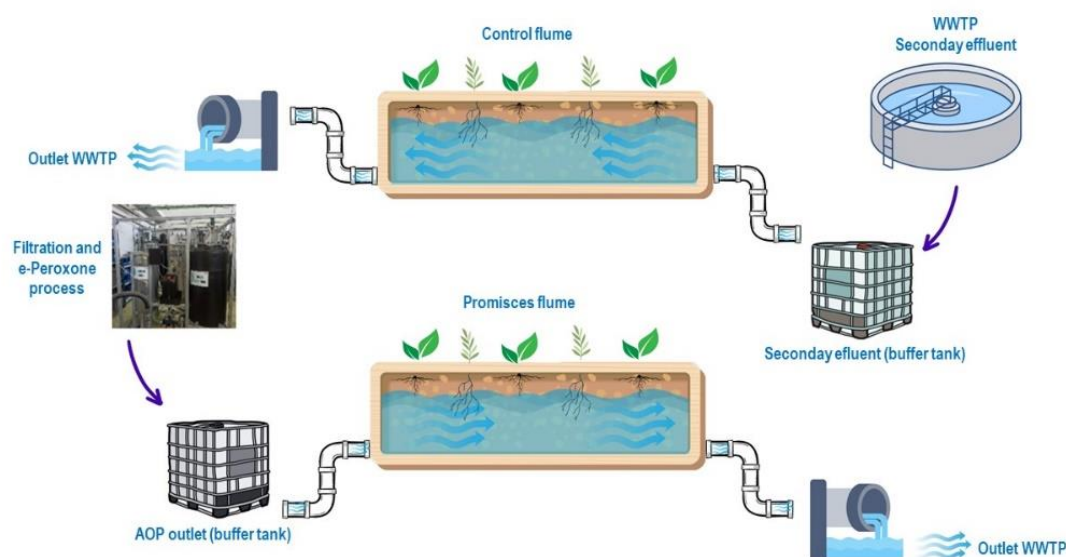


Figure 8. Experimental set-up design for the CWs

4 Methodology

4.1 Non-target screening of secondary WWTP effluent and target contaminant selection (Subtask 4.2.1)

A non-target screening approach of secondary WWTP effluent was conducted using three different sample preparation methods to achieve a comprehensive identification of iPM(T), as detailed in Deliverable D1.4. The identified compounds were then prioritized based on their persistence, bioaccumulation potential, mobility, and toxicity.

Subsequently, the 25 most relevant compounds from this study were selected to develop a target method using liquid chromatography-tandem mass spectrometry with a hybrid quadrupole time-of-flight analyzer (SPE-LC-QToF-MS/MS) in positive ionization mode. This selection was expanded to approximately 40 compounds by including additional compounds of interest identified in previous studies at a wastewater regeneration station.

4.2 Testing of technologies at lab-scale (TRL 4/5) (Subtask 4.2.2)

The technology underwent rigorous testing at the lab-scale, utilizing the batch experimental setup illustrated in **Figure 9**. The ozone generated from compressed oxygen is directed into a specially designed 5L contact tank with an integrated cooling system. This setup optimizes the interaction between ozone and wastewater, keeping temperatures within an ideal range to maximize the efficiency of the oxidation process. The cooling system ensures stable conditions, preventing thermal degradation and sustaining the optimal environment for effective treatment.

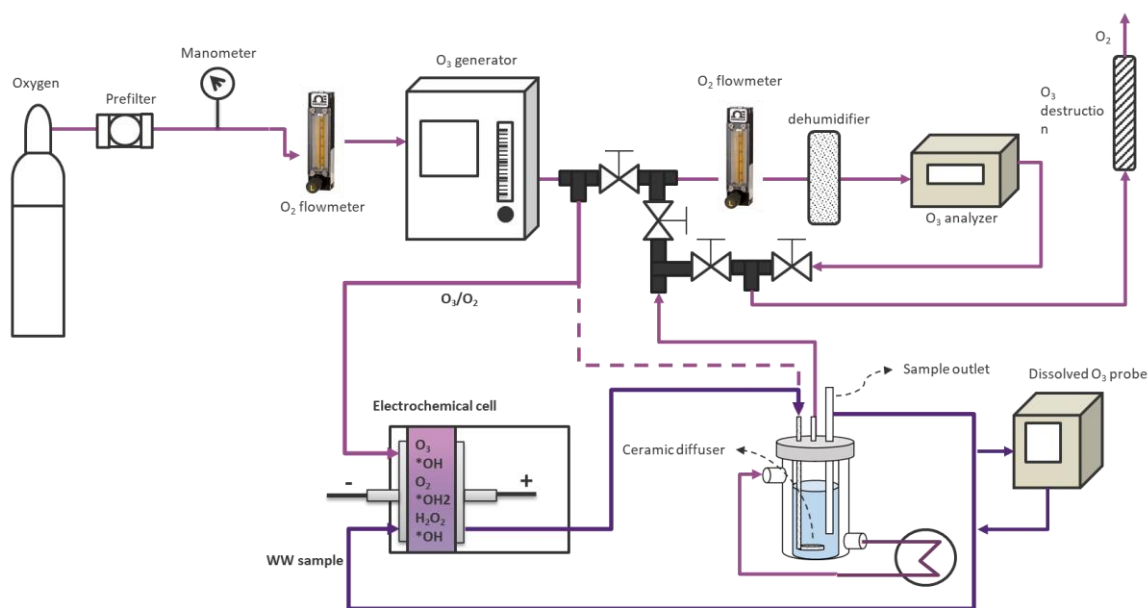


Figure 9. Experimental setup design for testing of technologies at lab-scale

In addition, the system integrates an electrochemical cell that complements the ozone treatment by generating reactive species, enhancing the degradation of these contaminants in the wastewater. This combination establishes a robust, multi-faceted treatment process, enabling a thorough assessment of the technology's performance within a controlled laboratory environment. The system's precise design allows for meticulous monitoring throughout the 240-min treatment period and fine-tuning of operational parameters, yielding valuable insights into the efficiency and overall effectiveness of the treatment approach under evaluation.

4.3 Pilot-scale technology testing (TRL 6) (Subtask 4.2.3)

The pilot scale testing was conducted using the pilot plant configuration, as detailed in chapter 3. Pilot plant configuration. This set-up was specifically designed to evaluate the efficiency and effectiveness of the treatment processes under realistic operational conditions. The operational conditions establish a thorough framework for assessing the technology, including factors such as flow rates, temperature, and specific characteristics of the wastewater.

Throughout the pilot plant operation, the samples were collected from several key points including the outlet of the secondary treatment (which serves as the input to the EAOP prototype), the outlet of the EAOP prototype, the buffer tank supplying treated water from the EAOP prototype to the post EAOP wetland, the buffer tank feeding the control wetland with water from the secondary treatment outlet, and the wetland outlet.

After collecting the samples, sodium thiosulfate (1M) was added to quench the oxidation reaction, using a ratio of 1 mL of sodium thiosulfate per 50 mL of sample. The samples were then refrigerated for 24 hours before being sent to the CSIC facilities. There, they were prepared and conditioned appropriately for subsequent injection.

4.4 Analytical methods for pilot monitoring

4.4.1 Physicochemical parameters

The physicochemical parameters were continuously monitored via the front panel of the electrical cabinet of the EAOP prototype. This interface displayed real-time readings of pH, conductivity, operating temperature and redox potential, measured through dedicated probes. The system automatically recorded the values of all variables over time, ensuring precise tracking of operational conditions. As part of quality control, pH, conductivity, dissolved oxygen, and temperature were measured during each periodic sampling using the Hanna Instruments HI98494 multiparameter device. These manual measurements complemented the automated monitoring system, ensuring the accuracy and reliability of the data collected. In addition, chemical oxygen demand (COD) was determined using Hach LCK314 cuvette test kits (range 15–150 mg/l) with a TR420 Thermoreactor and DR2800 spectrophotometer (Hach Lange, UK).

4.4.2 Nutrients

Ammonium was measured using Hach LCK304 (0.015–2 mg/L) and LCK305 (1–12 mg/L) cuvette test kits, with analysis performed on a DR2800 spectrophotometer (Hach Lange, UK). Nitrate levels were quantified using the Hach LCK339 kit (0.23–13.5 mg/L) on the same spectrophotometer. For total nitrogen and total phosphorus, Hach LCK138 (1–16 mg/L) and LCK349 (0.05–1.5 mg/L) cuvette test kits were used, analyzed with TR420 Thermoreactor and DR2800 spectrophotometer (Hach Lange, UK).

4.4.3 iPM(T)s

Water sample analysis was conducted using an Elute UHPLC system paired with an Impact II Q-TOF mass spectrometer (Bruker Daltonics, Billerica, MA, USA). Detailed chromatographic and mass spectrometric conditions can be found in Deliverable D1.4, sections 2.4.4 and 2.4.5. The method demonstrated robust validation at two concentration levels (0.2 and 2 µg/L), delivering reliable results in terms of sensitivity (LOD ranging from 0.04 to 166 ng/L), reproducibility (RSD <15% for most compounds), and recoveries (absolute values generally between 60% and 140%). **Table 3** provides an overview of the compounds included in the target method.

Table 3. List of target analytes included in the LC-MS/MS-based targeted method developed by CSIC for waters

Nº	Compound	CAS No.	Substance category
1	1,2,3-Benzotriazole	95-14-7	Industrial Chemicals
2	1,8-Diazabicyclo [5.4.0]undec-7-ene	6674-22-2	Industrial Chemicals
3	10,11- Dihydroxycarbamazepine	35079-97-1	Pharmaceuticals (metabolite)
4	2,4-Diaminotoluene	95-80-7	Industrial Chemicals
5	2-Amino-4-cresol + 6-Methyl-2-pyridinemethanol	95-84-1 / 1122-71-0	Industrial Chemicals
6	2-Aminophenol	95-55-6	Personal Care Products
7	2-Ethyl-1,5-dimethyl-3,3-diphenylpyrrolinium	21409-27-8	Pharmaceuticals (metabolite)
8	2-Ethylhexyl diphenyl phosphate	1241-94-7	Industrial Chemicals
9	2-Methoxy-5-methylaniline	120-71-8	Industrial Chemicals
10	3,5-di-tert-Butyl-4-hydroxybenzoic acid	1421-49-4	Industrial Chemicals
11	(4+5)-Methylbenzotriazole	29878-31-7	Industrial Chemicals
12	6-Methoxyquinoline	5263-87-6	Industrial Chemicals
13	Bis(2-ethylhexyl)amine	106-20-7	Industrial Chemicals
14	Caffeine	58-08-2	Others
15	Caprolactam	105-60-2	Industrial Chemicals
16	Carbamazepine	298-46-4	Pharmaceuticals
17	Carbendazim	10605-21-7	Pesticides
18	Dibutyl adipate	105-99-7	Personal Care Products
19	Dibutyl hydrogen phosphate	107-66-4	Industrial Chemicals
20	Dibutyl phthalate	84-74-2	Industrial Chemicals
21	Diethyl phthalate	84-66-2	Personal Care Products
22	Diuron	330-54-1	Pesticides
23	Flecainide	54143-55-4	Pharmaceuticals
24	Galaxolidone	507442-49-1	Personal Care Products
25	MDMA	42542-10-9	Drugs of abuse
26	Melamine	108-78-1	Industrial Chemicals
27	N,N'-Diphenylguanidine	20277-92-3	Industrial Chemicals
28	N-Phenyl-1-naphthylamine	90-30-2	Industrial chemicals
29	O-Desmethyl Venlafaxine	93413-62-8	Pharmaceuticals (metabolite)
30	Ofloxacin	82419-36-1	Pharmaceuticals
31	Sebumenton	26259-45-0	Pesticides
32	Sitagliptin	486460-32-6	Pharmaceuticals
33	Sulpiride	15676-16-1	Pharmaceuticals
34	Temazepam	846-50-4	Pharmaceuticals
35	Terbutryn	886-50-0	Pesticides
36	Theophylline	58-55-9	Others (metabolite)
37	Tributyl phosphate	126-73-8	Industrial Chemicals
38	Tributylamine	102-82-9	Industrial Chemicals
39	Triethyl phosphate	78-40-0	Industrial Chemicals
40	Tris(2-butoxyethyl) phosphate	78-51-3	Industrial Chemicals
41	Venlafaxine	93413-69-5	Pharmaceuticals

For lettuce analysis, a complementary method was developed, involving sample extraction via QuEChERS and subsequent analysis using the same conditions applied for water samples. This method has also been validated, and the results from its application to lettuce samples in this project are slated for publication.

4.4.4 PFAS

The analysis of PFAS and related compounds through suspect screening builds on IDAEA-CSIC's previous experience with other compound groups. The workflow facilitates the tentative identification of PFAS and related compounds with a confidence level of up to 2, as defined by Schymanski et al. (2014) and scale and refine to level 1 for the PFASs for which CSIC possesses the standard (**Table 4**), as outlined in Deliverable D1.4.

Sample purification and pre-concentration. Water samples were centrifuged at 2000 rpm for 10 min at room temperature before extraction. Subsequently, 200 mL of water was transferred to a PET container and spiked with a mixture of surrogate internal standards in methanol, achieving a final concentration of 10 pg/mL in sample. The extraction protocol was adapted from a previously developed method by IDAEA-CSIC (Barbosa et al., 2023).

In summary, solid-phase extraction (SPE) cartridges were conditioned sequentially with 2 mL of methanol and 2 mL of ultrapure water under gravity conditions. Samples comprising 200 mL of surface water and 100 mL of wastewater were loaded under vacuum conditions through PEEK capillary tubes at a controlled flow rate of 1 mL/min. The cartridges were then dried under vacuum for 15 min, and PFASs were eluted using 8 mL of methanol (0.1% NH₄OH) into polypropylene tubes. The eluates were evaporated nearly to dryness under a gentle nitrogen stream, transferred into LC vials with 250 µL inserts, and reconstituted in 100 µL of ultrapure water/methanol (90:10). To ensure the reliability of the process, an SPE blank sample was processed alongside real samples to monitor potential cross-contamination.

Table 4. PFAS quantified by IDAEA-CSIC

Carboxylic acids	Sulfonic acids & sulfonamides	New PFAS
PFBA	PFBS	6:2 diPAP
PFPeA	PFPeS	8:2 diPAP
PFHxA	PFHxS	ADONA
PFHpA	PFHpS	EtFOSA
PFOA	PFOS	EtFOSAA
PFNA	PFNS	FOSAA
PFDA	PFDS	MeFOSAA
PFUnA	PFDoS	MeFOSA
PFDoA	FOSA	HFPO-DA (Gen-X)
PFTTrDA	Fluorotelomer sulfonic acids	PFMOAA
PFTeDA	4:2 FTSA	PFMOPrA
PFHxDA	6:2 FTSA	PFMOBA
PFODA	8:2 FTSA	PFO ₂ HxA
	10:2 FTSA	PFO ₃ OA
		PFO ₄ DA

Instrumental Analysis: Chromatographic separation is performed using an Acquity LC system (Waters, Milford, MA, USA) coupled with a C18 Hypersil GOLD PFP LC analytical column (50x3 μm) (Thermo Fisher Scientific, San Jose, CA). The mobile phase consists of (A) 20 mM aqueous ammonium acetate and (B) 20 mM methanol ammonium acetate. The elution gradient starts at 20% B, which increases to 80% B within 5 minutes. In the following 5 minutes, the gradient rises to 90% B, which is maintained for 2 more minutes. The initial conditions are restored within 1 minute and maintained for another minute, completing a total run time of 12 minutes per injection at a flow rate of 0.2 mL/min. The optimal injection volume is 10 μL .

The chromatographic system is integrated with a Q-Exactive hybrid quadrupole-Orbitrap mass spectrometer (Thermo Fisher Scientific), equipped with an electrospray ionization (ESI) source, operating in negative ionization mode. Data acquisition is performed in full scan (FS) mode (90-1500 Da) with a resolution of 70,000 FWHM, alongside data-dependent scans (ddS) targeting the most intense ions, at a resolution of 15,000 FWHM. The entire system is managed through Xcalibur 4.1 software.

The total ion chromatograms (TIC), generated from FS acquisitions, are then processed with Xcalibur software for the quantification of CSIC's available standards (level 1 confidence).

4.4.5 Inorganic ions

The quantification of the chlorinated and brominated ions was conducted using a DIONEX ICS-2100 ion chromatography system. This analysis was performed with a high-performance ion-exchange column, using a gradient elution of H_2O and KOH at a flow rate of 1 mL/min, ensuring precise separation and quantification of the target ions. To guarantee optimal analysis quality, samples were filtered through 0.45 μm nylon membrane prior to injection, removing any particulate matter, which could interfere with the chromatography process.

4.4.6 Toxicological assays

The samples were divided for extraction using two different SPE columns. A general extraction was performed using the HLB-SPE column, while a PFAS specific extraction was carried out with the WAX-SPE column. The eluates from both extractions were evaporated under a gentle stream of N_2 and further reconstituted in the appropriate volume of DMSO, based on the extraction method used.

Serial dilutions of all sample extracts were prepared in DMSO and then analysed for their potential to disrupt with T_4 -TTR binding (PFAS CALUX), $\text{ER}\alpha$ -receptor activation ($\text{ER}\alpha$ CALUX), PXR-receptor activation (PXR CALUX), cytotoxicity (Cytotox CALUX), AR-receptor antagonism (anti-AR CALUX), and PPAR γ -receptor antagonism (anti-PPAR γ CALUX).

TTR-Binding Assay. Serial sample dilutions were incubated overnight at 4°C in Tris-buffer (pH 8.0) with TTR (0.058 μM) and a fixed concentration of T_4 (0.052 μM) (3.2% of the sample dilution in the incubation mixture). After incubation, TTR-bound and free T_4 were separated using a Bio-Gel P-6DG column. The eluate was then transferred into the assay medium, and TR β CALUX cells were exposed for 24 hours.

CALUX Bioassays. CALUX cells were seeded in 96-well plates with assay medium. After exposing the CALUX cells to serial sample dilutions in triplicate (PFAS CALUX: dilutions after TTR-binding assay; other CALUX: dilution series of sample extracts), the induction of luciferase production was measured by luminescence using a Berthold luminometer following the addition of luciferin substrate. On each

96-well plate, complete calibration curves for each bioassay are also analysed using the relevant reference compounds.

Data analysis. The analysis results of sample extracts, presented as induction relative to the standard reference compound, were interpolated into the calibration curves of each respective bioassay for quantitative assessment of disruptive potential. This process was carried out using the statistical software package GraphPad Prism V5.03. Only dilutions without any signs of cytotoxicity were considered for the final evaluation of the analysis. All findings are expressed as the equivalent amount of reference compound per liter of processed water.

4.4.7 Microbiological analysis

The treated water was analysed for microbiological parameters, including *E. coli*, *Legionella*, and eggs of parasitic helminths (both *Taenia* and nematodes), to confirm compliance with the requirements set by Royal Decree 1085/2024 This Spanish regulation establishes the Water Reuse Regulation and introduces several amendments to other decrees about water management.

The analysis was carried out by an external laboratory to evaluate whether the treated water complies with Quality A.A. standards for irrigation of vegetable crops, particularly those consumed raw, as established by the Spanish Royal Decree 1085/2024. These crops, where the edible part comes into direct contact with the reclaimed water, require a higher level of safety to prevent any health risks. The laboratory tests aim to verify if the water meets the specific microbiological and chemical criteria outlined for this quality level (**Table 5**), ensuring its safety for agricultural use in food production.

Table 5. Maximum allowable value established for Quality A.A. standards

Parameter	Maximum allowable value
<i>E. coli</i> (CFU/100 mL)	10
Turbidity (NTU)	5
SS (mg/L)	10
DBO ₅ (mg/L)	10
Intestinal nematodes (egg/L)	1
<i>Legionella spp.</i> ^a (CFU/L)	< 1000
<i>T. saginata</i> and <i>T. solium</i>	-
Contaminants ^b	-

^a *Legionella spp.*: Compliance with **Royal Decree 487/2022**, which established health requirements for the prevention and control of Legionella, will also be required.

^b The restricted contaminants listed in the wastewater discharge authorization will be monitored to ensure the production of reclaimed water does not lead to deterioration of the receiving environment. This aligns with the requirements set forth in **Royal Decree 817/2015**, establishes the monitoring and assessment criteria for surface water status and environmental quality standards, and **Royal Decree 1514/2009**, regulates the protection of groundwater against contamination and degradation.

4.5 Study of the uptake and distribution of contaminants in vegetable crops irrigated with reclaimed water (Subtask 4.2.4)

The experiments were carried out in a temperature-controlled growth room at CSIC facilities, maintaining an average temperature of 25.4 ± 1.5 °C and relative humidity of $60.2 \pm 4.9\%$. Experimental units consisted of 2.5 L cylindrical amber glass pots (15 cm diameter, 20 cm height) equipped with bottom outlets connected to drainage tubes (3 cm diameter). Each pot was filled with 2.3 kg of air-dried soil, sieved to 2 mm, and mixed with washed sand (2 mm) in a 70/30 ratio. The soil, sourced from the surface horizon of a pristine mountain area 20 km from Barcelona, featured a loamy sandy texture (77.5% sand, 9.9% silt, 12.6% clay), a pH of 8, and an electrical conductivity measuring 0.14 dS/m. The soil contained 3.6% organic carbon (dry weight, dw), 0.38% nitrogen (Kjeldahl method), and 14.4 mg/kg of phosphorus. The cation concentrations were 181 mg/kg for K^+ , 4698 mg/kg for Ca^{2+} , 231 mg/kg for Mg^{2+} , and 269 mg/kg for Na^+ , all measured on a dry weight basis. At the beginning of the study, all pots were supplemented with a 0.1% organic NPK fertilizer.

The horticultural crop selected was *Lactuca sativa* L. cv. Maravilla de Verano. A total of 30 plants were grown individually in the prepared amber glass pots. The crops were irrigated with three different water types ($n = 10$): secondary-treated wastewater (WW) from CS#3 in Montornès del Vallès; reclaimed water (post EAOP CW); and control water (control) sourced from bottled pristine groundwater. **Figure 10** illustrates the experimental setup.



Figure 10. Experimental setup depicting the individual containers for cultivating lettuce at harvest

4.6 Criteria for evaluating the use of reclaimed water in irrigation

The technologies evaluated in CS#3 present a valuable opportunity to minimize crop exposure to iPM(T)s. Thoroughly evaluating their impact on crop productivity, quality, and metabolism, as well as evaluating the potential buildup of residual PMTs in crop tissues to ensure food safety and protect human health from potential risks, is crucial.

Lettuce (*Lactuca sativa*) was chosen for this study due to its high consumption and role as a fresh food staple, serving as an ideal indicator crop to evaluate the safety and quality of reclaimed water in irrigation practices.

To ensure realistic conditions, the greenhouse study was conducted using loamy sandy soil, typical of Mediterranean agricultural fields. This approach ensured a practical framework for examining the effects of reclaimed water on crops in environments like real world farming scenarios.

The evaluation of reclaimed water use in irrigation is based on an in-depth analysis of agronomical, chemical, and biological parameters (**Table 6**), offering a comprehensive understanding of its impact and feasibility for sustainable agricultural practices.

Table 6. Soil-grown crops monitoring parameters

Agronomical part	Chemical part	Biological part
Wet and dry weight/crop yield	PFAS and iPM(T)s	Crop metabolomics (leaves)
Chlorophyll content		
Number of leaves		
Lipid content		
Carbohydrate content		

The dry and fresh biomass, as well as the number of lettuce leaves were measured at the end of the productive life cycle. Chlorophyll content in leaves and biomass weight were evaluated in-situ using a chlorophyll meter (Opti-Sciences, Hudson, NH, USA). Lipid and carbohydrate levels were quantified using the method described by Margenat et al. (2018). Metabolomic analysis was carried out following the methodology detailed by Matamoros et al. (2022).

5 Results

5.1 Non-target screening of secondary WWTP effluent and target contaminant selection

In the suspect screening analysis of WWTP effluent water samples collected in January, 2022, and processed using three different sample preparation methods, a total of 119 compounds were detected in at least one sample (**Figure 11**), with 22 of them confirmed through reference standards.

Industrial application-related compounds constituted the second most prevalent category of contaminants, accounting for 33 compounds and metabolites. These industrial chemicals were subsequently prioritized for targeted analysis to better understand their behaviour, considering key environmental factors such as persistence and mobility.

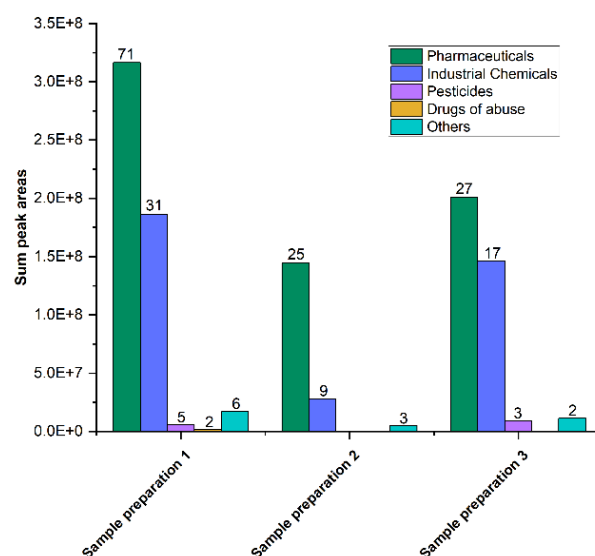


Figure 11. Sum of peak areas for each sample preparation (SP) method evaluated through suspect screening (SP-1 freeze-drying preconcentration, SP-2 direct injection and SP-3 online preconcentration). The number above each bar corresponds to the number of compounds detected.

For the pilot-scale experiments, a total of 85 water samples were analysed, encompassing influent and effluent water from the treatment plant, along with reclaimed water collected at various stages of the pilot plant operating under different conditions.

Table 7 presents the findings, detailing the limits of detection and quantification (LODs/LOQs), detection frequencies, and the average, minimum, and maximum concentrations of the target compounds. Out of the 41 analysed compounds, 39 were detected in the samples. Among these, galaxolidone (a metabolite of the personal care product galaxolide), 1,2,3-benzotriazole (used as an anti-corrosion and anti-fogging agent), and tributyl phosphate (a flame retardant and plasticizer) were the most prevalent, based on their average concentrations and detection frequencies.

Table 7. Results obtained from analysis of target compounds in 85 water samples collected during the pilot and field-scale experiments

	LOD (ng/L)	LOQ (ng/L)	Average (ng/L)	Min (ng/L)	Max (ng/L)	Frequency of detection (Pos/85)
Galaxolidone	5.9	20	2.7E+03	5.5E+02	8.3E+03	85
1,2,3-benzotriazole	1.3	4.3	2.4E+03	1.5E+02	7.4E+03	85
Tributyl phosphate/triisobutyl phosphate	0.36	1.2	1.8E+03	1.0E+01	4.9E+04	85
10,11-Dihydro-10,11-dihydroxycarbamazepine	32	105	9.9E+02	2.0E+02	2.1E+04	85
(4+5)-Methylbenzotriazole	1.9	6.2	6.7E+02	2.5E+01	1.5E+03	85
Ofloxacin	4.0	13	3.0E+02	2.5E+01	3.8E+03	85
6-Methyl-2-pyridinemethanol+ 2-Amino-4-cresol	1.3	4.4	3.0E+02	3.0E+01	1.5E+03	85
N,N'-Diphenylguanidine (DPG)	0.07	0.23	2.4E+02	7.4E-01	1.5E+03	85
Triethyl phosphate	0.27	0.88	5.8E+01	8.6E+00	5.5E+02	85
Temazepam	3.3	11	4.2E+01	1.7E+01	3.4E+02	85
Tributylamine	0.05	0.16	1.9E+01	3.8E-01	6.7E+01	85
Bis(2-ethylhexyl)amine	0.34	1.1	1.3E+01	3.3E+00	5.2E+01	85
(EDDP) / 2-ethyl-1,5-dimethyl-3,3-diphenylpyrrolinium	0.14	0.46	2.4E+01	1.2E+00	1.9E+02	84
Sitagliptin	1.7	5.5	6.1E+02	2.1E+01	2.8E+03	82
Tris(2-butoxyethyl) phosphate	0.64	2.1	3.3E+02	6.8E+01	1.3E+03	82
Flecainide	0.09	0.29	1.9E+02	1.1E+01	2.3E+03	82
MDMA	0.06	0.20	3.3E+03	2.1E+00	1.2E+05	81
Diuron	2.2	7.4	1.7E+01	5.9E+00	7.3E+01	81
Caffeine	21	70	1.6E+03	6.4E+01	2.4E+04	79
Carbamazepine	0.99	3.3	4.4E+01	6.5E+00	1.1E+02	79
O-Desmethyl venlafaxine	0.31	1.0	6.1E+02	6.0E-01	2.3E+03	78
Venlafaxine	0.12	0.38	2.4E+02	2.3E-01	6.6E+02	77
2-Aminophenol	3.3	11	1.7E+03	3.1E+01	2.8E+04	75
Dibutyl phthalate	0.05	0.16	1.3E+03	2.7E+00	4.4E+04	73
Diethyl phthalate	1.1	3.7	1.6E+03	1.2E+01	1.2E+04	72
Terbutryn	0.34	1.1	3.0E+01	1.4E+00	8.3E+01	72
Sulpiride	0.44	1.4	2.4E+02	3.4E+00	1.2E+03	71
Carbendazim	0.03	0.09	1.9E+01	1.8E-01	1.3E+02	70
Dibutyl hydrogen phosphate	0.29	0.97	3.1E+03	3.8E+00	5.8E+04	69
Melamine	0.97	3.19	1.9E+02	4.8E+01	3.5E+02	65
3,5-di-tert-Butyl-4-hydroxybenzoic acid	18	61	4.7E+02	8.2E+01	4.7E+03	61
Caprolactam	0.19	0.63	6.5E+02	1.2E+01	8.5E+03	59
2,4-Diaminotoluene	14	46	6.5E+03	7.2E+01	5.1E+04	48
Theophylline	17	56	1.8E+03	1.1E+02	2.0E+04	46
1,8-Diazabicyclo [5.4.0]undec-7-ene (polycat dbu)	0.04	0.13	3.3E+01	1.1E+00	1.4E+02	28
6-Methoxyquinoline	0.88	2.9	2.4E+01	1.6E+01	3.3E+01	11
Dibutyl adipate	0.97	3.2	4.1E+01	8.3E-01	8.1E+01	10
Secbumeton	0.15	0.50	1.9E+01	1.0E+00	9.5E+01	6
2-Ethylhexyl diphenyl phosphate	10	34	1.1E+04	5.0E+03	1.7E+04	2
2-Methoxy-5-methylaniline	0.63	2.1	ND	ND	ND	ND
N-Phenyl-1-naphthylamine	3.3	11	ND	ND	ND	ND

5.2 Testing of technologies at lab-scale (TRL 4/5)

5.2.1 Synthetic secondary effluent tests

The synthetic secondary effluent tests were designed to replicate WWTP effluent by introducing sodium chloride into deionized water. This methodology created a controlled environment that reduced the variability inherent in treated wastewater, enabling a more precise assessment of various treatment processes under consistent conditions. By mimicking the ionic composition achieving a representative conductivity of 2500 $\mu\text{S}/\text{cm}$ —typical of secondary effluents—these tests provide valuable insights into treatment efficiency, paving the way for optimized strategies in real-world applications.

The performance of the oxidation processes was meticulously assessed, particularly regarding the removal efficiencies of PFAS, represented by a mix of three specific compounds, and iPM(T)s, which included a combination of nine unique substances. **Table 8** provides detailed information on these compounds, along with their theoretical concentrations in the spiked solution. In these assays, the solution was spiked with a PFAS concentration 10 times higher due to the detection limit of the analytical methods. This adjustment was necessary as the methods could not accurately measure lower PFAS concentrations, to ensure that the results were detectable and provide a reliable assessment of treatment efficiency under the experimental conditions.

Table 8. Target pollutants and their theoretical concentrations in the spiked solution

Type of contaminant	Contaminant	CAS number	Concentration ($\mu\text{g}/\text{L}$)
iPM(T)s	1,4- Dioxane	123-91-1	10.24
	1,2,3-Benzotriazole	95-14-7	10.60
	2,4- Diaminotoluene	95-80-7	10.31
	4-methyl-1H-benzotriazole	29878-31-7	10.34
	N,N'-Diphenylguanidine (DPG)	102-06-7	10.07
	Tris(2-butoxyethyl) phosphate	78-51-3	9.69
	2-Aminophenol	95-55-6	10.30
	Melamine	108-78-1	10.58
	5-Methyl-1H-benzotriazole	136-85-6	10.10
PFAS	PFHxA	307-24-4	100.26
	PFBS	375-73-5	100.31
	PFHxS	355-46-4	100.19

These experiments examined three advanced treatment technologies aimed at removing specific target pollutants: ozonation, electro-oxidation, and e-Peroxone, a hybrid method combining the first two technologies. To enhance the effectiveness of these treatments, two key operational parameters were systematically investigated. For both electro-oxidation and e-Peroxone, the applied current intensity was adjusted to evaluate its influence on oxidant production and pollutant degradation efficiency. Similarly, ozone concentration in the ozonation and e-Peroxone processes was varied to evaluate its role in the contaminant breakdown and its interaction with the electrochemical system.

Despite adjusting the ozone dose, with 384 mg/L as the estimated upper limit, to optimize conditions during ozonation process (**Figure 12**), the removal efficiency for iPM(T)s consistently underperformed, falling short of anticipated levels. Notably, melamine exhibited lower removal rates, highlighting its resistance to ozonation under the tested conditions. These results suggest while

ozonation is effective in removing 4-methylbenzotriazole and N,N'-diphenylguanidine, the process remains insufficient for addressing several compounds with significant resistance to oxidative degradation. Nevertheless, no 5-methylbenzotriazole removal was detected, despite Béalu et al. (2024) reporting its moderate elimination by ozonation using 0.5 mg O₃/mg DOC. In this case, drawing comparisons with literature values is challenging, as the O₃ dose per mg of DOC cannot be calculated due to the extremely low DOC concentrations. Given these results, ozonation was not tested further due to its limited effectiveness in synthetic water. The low removal efficiency observed in controlled conditions suggested ozonation might not perform well in real-world scenarios where the complexity of the effluent influences the treatment's effectiveness.

In electro-oxidation, a current intensity of 15 A proved insufficient to achieve effective degradation of the contaminants (**Figure 12**). Thus, in the subsequent stages, only current intensities of 30 A were evaluated to improve the efficiency of pollutant removal and degradation, ensuring better alignment with the treatment objectives.

Subsequently, e-Peroxone was evaluated by testing the influence of the applied current intensity and ozone concentration, to analyze their impact on the effectiveness of pollutant removal and degradation.

As can be seen in **Figure 12**, using the estimated maximum ozone dosage (384 mg O₃/L) enhances performance compared to utilizing half the estimated maximum ozone concentration (192 mg O₃/L). This underscores the crucial role of the ozone dosage in maximizing the e-Peroxone efficiency, demonstrating its potential as complementary technology for advanced water treatment. Although initial results suggested that electro-oxidation performed better than e-Peroxone at higher current intensities, both technologies were further evaluated to test their effectiveness in treating secondary effluent.

Afterwards, experiments were conducted to study the degradation of PFAS both individually and in competitive settings to assess competitive oxidation. These tests also evaluated the effects of ozone dosage and current intensity, like the approach used for iPM(T)s. Despite starting with an initial concentration about 100 ppb each individual PFAS compound, the results revealed significantly higher concentrations than anticipated. At this point, the cleaning protocols between experiments were revised to prevent any carryover of concentrations from prior tests. This adjustment was essential to eliminate residual contamination that could affect the results, ensuring that each experiment started under controlled conditions for a more accurate evaluation of removal efficiency.

In terms of energy consumption, the **electrical energy per order (EE/O)** was calculated for each pollutant involved in the treatment process. This parameter is defined as the electrical energy required (measured in KWh) to achieve one-order-of-magnitude reduction in the concentration of a specific pollutant within 1 m³ of contaminated water (Singh et al., 2020). This metric is crucial for evaluating the efficiency of the treatment process, as lower energy usage indicates more effective and sustainable methods for pollutant removal.

The EE/O values were calculated based on the specific operational conditions of these assays (**Table 9**). These values are representative solely of the experimental setup, including the initial concentrations used, and may not apply to other scenarios or operational parameters.

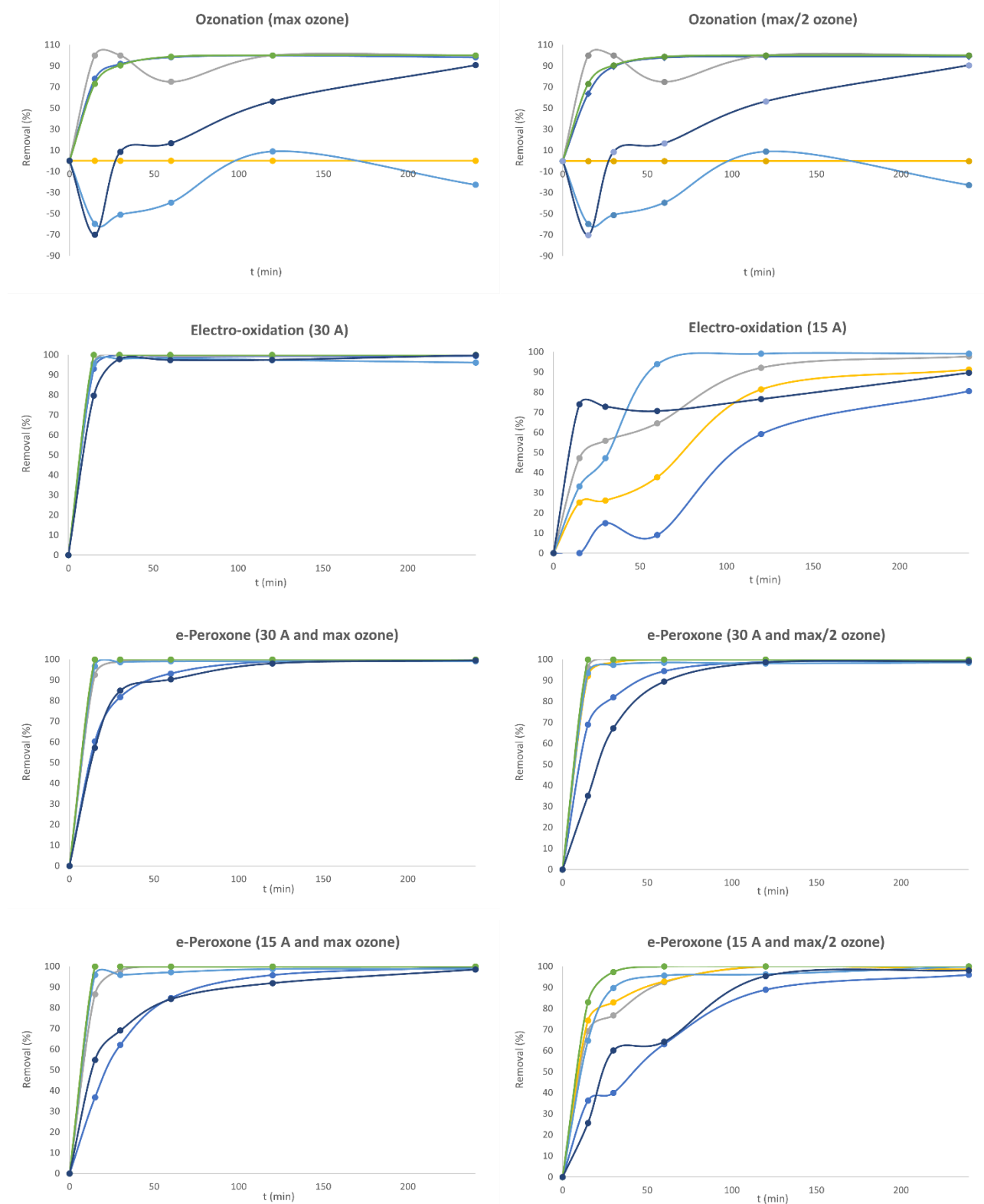


Figure 12. iPM(T)s removal by ozonation, electro-oxidation and e-Peroxone using synthetic secondary effluent (1,2,3-benzotriazole: blue line, 4-methylbenzotriazole: grey line, 5-methylbenzotriazole: yellow line, melamine: light blue line N,N'-diphenylguanidine (DPG): green line, and tris(2-butoxyethyl) phosphate: navy blue line)

Table 9. EE/O values for each pollutant involved in the treatment processes using spiked synthetic effluent water

Type of contaminant	Contaminant	Ozonation EE/O (kWh/m ³)	Electro-oxidation EE/O (kWh/m ³)	e-Peroxone EE/O (kWh/m ³)
iPM(T)s	1,4- Dioxane	n.a.	n.a.	n.a.
	1,2,3-Benzotriazole	10.1-11.3	17.5	62.4-88.6
	2,4- Diaminotoluene	n.a.	n.a.	n.a.
	4-methyl-1H-benzotriazole	n.a.	14.6-78.0	12.5-37.5
	N,N'-Diphenylguanidine	10.7-19.1	n.a.	n.a.
	Tris(2-butoxyethyl) phosphate	n.a.	24.4-170	63.4-81.1
	2-Aminophenol	n.a.	160-205	n.a.
	Melamine	n.a.	15.2-35.3	7.7-21.2
	5-Methyl-1H-benzotriazole	n.a.	12.9-162	18.1-36.7
PFAS	PFHxA	n.a.	n.a.	n.a.
	PFBS	n.a.	n.a.	n.a.
	PFHxS	n.a.	n.a.	n.a.

n.a.: not available

For ozonation, EE/O values cannot be calculated because the 90% removal threshold was not reached within the operational timeframe (**Table 9**). Conversely, in the electro-oxidation and e-Peroxone processes, the removal efficiency for some contaminants exceeded 90% well in advance of collecting the first sample. The results offer a general indication of performance but cannot be directly compared due to the absence of precise 90% removal values. This limitation arises from the insufficient number of samples available, which prevents accurate data fitting and interpolation to refine the analysis.

5.2.2 Real secondary effluent trials

Following the lab-scale analysis of iPM(T)s and PFAS removal using a synthetic effluent, additional experiments were conducted with real secondary WWTP effluent. This was intended to assess the impact of the liquid matrix on the iPM(T)s and PFAS removal efficiencies. By comparing all the results from synthetic and real effluents, deeper insights into the complexities introduced by several constituents present in secondary effluent can be obtained. This comprehensive approach helps identify potential challenges and optimize treatment strategies for real-world applications.

These experiments analysed both doped and undoped scenarios to evaluate how the presence of multiple contaminants influences the oxidation process. In the doped experiments, known iPM(T)s and PFAS concentrations were used to test the system's ability to effectively remove these compounds under controlled conditions. In contrast, the undoped experiments measured removal efficiencies in natural settings, without the addition of specific contaminants.

Additionally, in this stage, the effectiveness of the oxidation processes was thoroughly evaluated, with a specific focus on the removal efficiencies of PFAS—using a combination of three PFAS compounds—and iPM(T)s, which comprised a mix of nine distinct compounds. The details of these compounds, with their respective theoretical concentrations in the spiked solution, are presented in **Table 8**. Note that at this point, the concentration of PFAS was reduced to 10 ppb by performing a pre-concentration step during the sample analysis.

The subsequent monitoring performed by IDAEA-CSIC revealed only five of the nine iPM(T) compounds spiked into the real secondary effluent could be successfully quantified. The method

successfully enabled the quantification of **1,2,3-benzotriazole**, **2-aminophenol**, **(4+5)-methylbenzotriazole**, **N,N'-diphenylguanidine (DPG)**, and **tris(2-butoxyethyl) phosphate**.

Despite being introduced at the same concentrations, four compounds could not be quantified during the analysis. **2,4-diaminotoluene** exhibited concentration increases over time, even in unspiked samples where the initial concentration was nearly zero. In contrast, **melamine** showed no significant differences between the spiked and unspiked samples. The initial concentrations were practically the same, indicating that spiking did not influence the levels of these compounds in the analysed system. Additionally, the detection of **1,4-dioxane** was not feasible because its analysis requires positive ionization mode, whereas the rest of the compounds were measured using negative ionization mode.

Despite the analytical challenges encountered in these experiments, higher removal percentages were achieved using e-Peroxone process (operating at 30 A and an estimated ozone dosage of 384 mgO₃/L) compared to electro-oxidation alone (**Figure 13**). Furthermore, as anticipated, the oxidative treatment proved more effective at elevated contaminant concentrations. As a result, these findings confirm the performance of the e-Peroxone process to treat real secondary effluent at the laboratory scale.

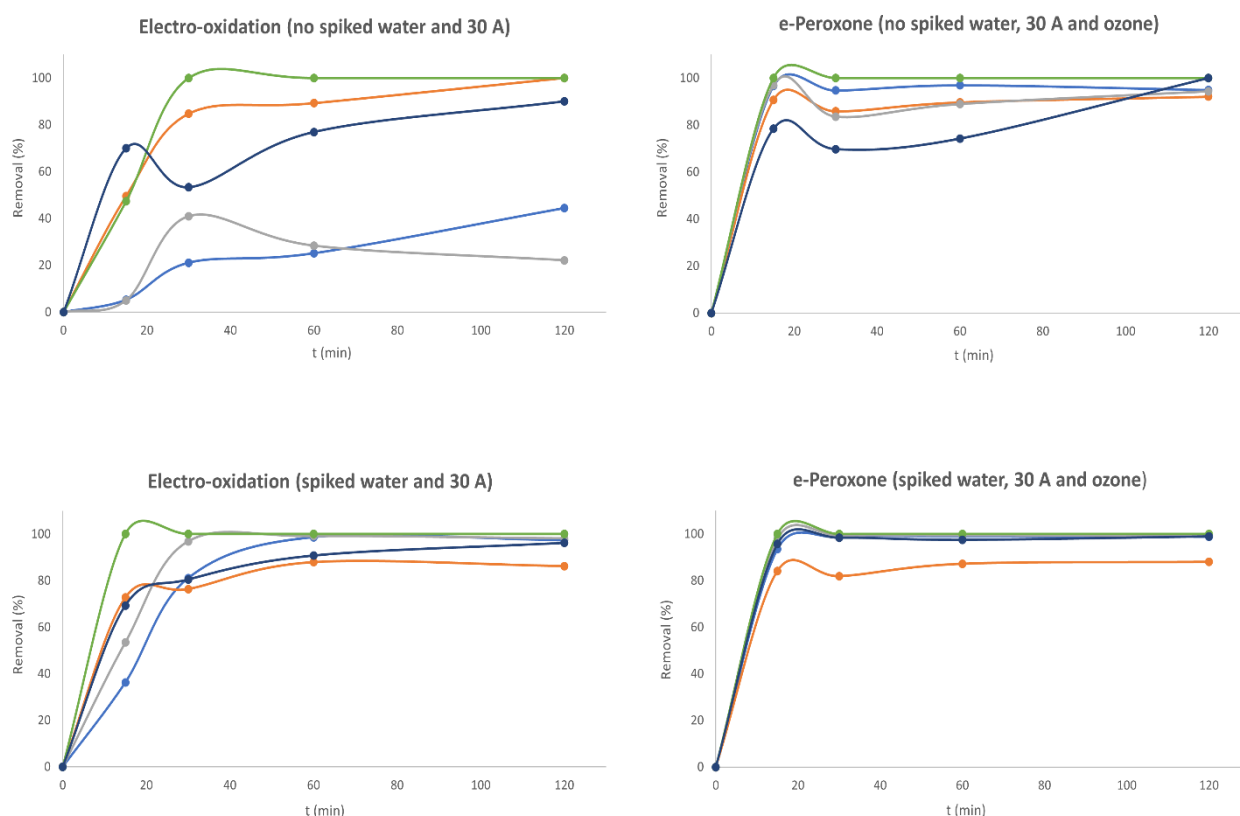


Figure 13. iPM(T)s removed by electro-oxidation and e-Peroxone using real secondary effluent (1,2,3-benzotriazole: blue line, 2-aminophenol: orange line, (4+5)-methylbenzotriazole: grey line, N,N'-diphenylguanidine (DPG): green line and tris(2-butoxyethyl) phosphate: navy blue line)

Unfortunately, in the described experiments, the target compounds PFBA, PFPeA and PFOA were not detected in either the spiked or non-spiked assays, suggesting their concentrations were below the detection limits of the analytical method. Similarly, 6:2 FTS remained below the quantification limit in both cases, further complicating the assessment of its removal efficiency within the oxidation

process. Notably, these four contaminants were not initially included in the spiked mixture. However, interestingly, PFOS -also absent from the spiked mixture- was detected in both experiments. This result suggests potential cross-contamination or residual presence of PFOS in the liquid matrix or containers used for the experiments. Nevertheless, cross-contamination during chemical analysis has been ruled out by using control blanks in parallel during the entire chemical extraction and analysis to monitor for any possible contamination.

In the spiked experiments, four target PFAS contaminants, PFHxA, PFBS, PFHxS, and PFOS were detected; however, their concentrations deviated from the expected theoretical values, hindering an accurate evaluation of the removal efficiency for these compounds. This inconsistency impacts the ability of drawing definitive conclusions about the effectiveness of the treatment process. As can be seen in **Figure 14**, the fluctuations in the PFAS removal over time did not exhibit a significant trend.

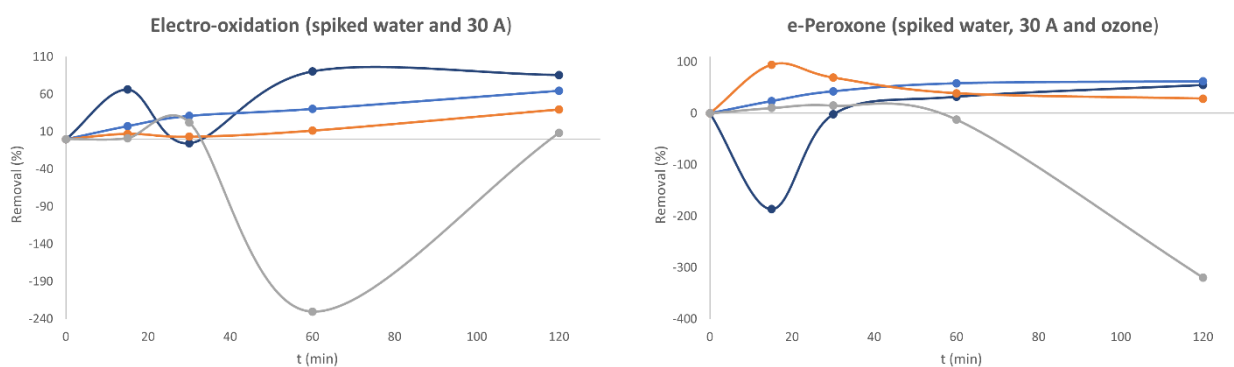


Figure 14. PFAS removal from real secondary effluent using electro-oxidation and e-Peroxone (PFHxA: navy blue line, PFBS: blue line, PFHxS: orange line, PFOS: grey line)

Furthermore, at this stage, none of the PFAS were detected in the non-spiked experiments, indicating a challenge for scaling up the process at the WWTP Montornès del Vallès. Therefore, the sample volume for PFAS analysis was adjusted. Given that the initial experimental setup involved a 5L reactor with only 50 mL/sample available, the sample volume was increased to 500 mL. This adjustment was conducted to enable pre-concentration before analysis, allowing for more precise PFAS quantification. Looking ahead, future experiments must be conducted without spiking the samples to gain a more accurate understanding of removal efficiencies.

To evaluate the feasibility of the e-Peroxone process for effective PFAS removal, Eurecat outsourced the detailed analysis of specific compounds -PFHxA, PFBS and PFHxS- to a specialized commercial laboratory. The experiment was conducted under the same operational conditions as previous ones, by spiking these compounds to simulate real-world contamination levels.

As can be seen in **Figure 15**, a notable reduction in long-chain PFHxA and PFHxS was observed over time, while the removal efficiency for short-chain compounds progressively diminished. This decline is attributed to the breakdown of long-chain PFAS, which generates short-chain PFAS as by-products. As a result, the concentration of short-chain PFAS increases, making their removal less efficient over time. This highlights the complex dynamics of PFAS degradation during the e-Peroxone process.

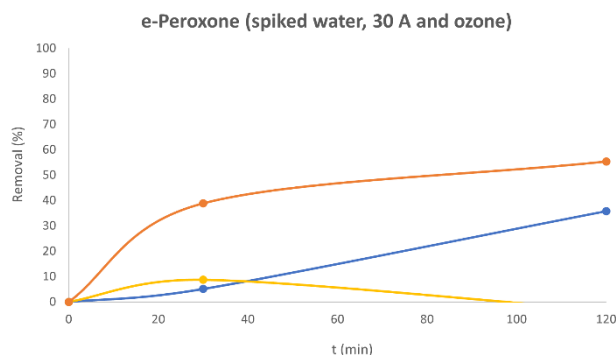


Figure 15. PFAS removal in real secondary effluent using electro-oxidation and e-Peroxone (PFHxA: navy blue line, PFBS: yellow line and PFHxS: orange line)

The generation of ions following the oxidative treatment was analysed, revealing the formation of chlorate (**Table 10**). The analytical method was not sufficiently optimized for quantifying these ions at the observed concentrations. To address this, Eurecat laboratory personnel modified the method to reduce the detection limits by tenfold to 0.5 mg/L and developed a perchlorate method, considering the presence of chlorate could indicate the potential formation of perchlorate as well.

Table 10. Formation of chlorinated by-products using electro-oxidation and e-Peroxone on real secondary effluent

Treatment	Chloride (mg/L)		Chlorite (mg/L)		Chlorate (mg/L)	
	Initial	Final	Initial	Final	Initial	Final
Electro-oxidation	336	22	< 5	< 5	< 5	69
e-Peroxone	337	26	< 5	< 5	< 5	75

In terms of energy consumption, the **electrical energy per order (EE/O)** was calculated for each pollutant involved in the treatment process (**Table 11**).

Table 11. EE/O values for each pollutant involved in the treatment processes for real secondary effluent

Type of contaminant	Contaminant	Electro-oxidation EE/O (kWh/m ³)	e-Peroxone EE/O (kWh/m ³)
iPM(T)s	1,2,3-Benzotriazole	n.a.	19.8
	2,4- Diaminotoluene	n.a.	43.4
	N, N'-Diphenylguanidine	n.a.	n.a.
	Tris(2-butoxyethyl) phosphate	165.2	17.1
	2-Aminophenol	88.3	194.9
	Melamine	n.a.	n.a.
	(4+5)-Methyl-1H-benzotriazole	n.a.	n.a.
PFAS	PFHxA	n.a.	n.a.
	PFBS	n.a.	n.a.
	PFHxS	n.a.	n.a.

n.a.: not available

The EE/O values were determined under the specific operational parameters of these assays (**Table 11**). These values are representative solely of the experimental setup, including the initial concentrations, and may not apply to other scenarios or operational parameters. Similarly to the experiments conducted with synthetic effluent, the results provide a general performance indication

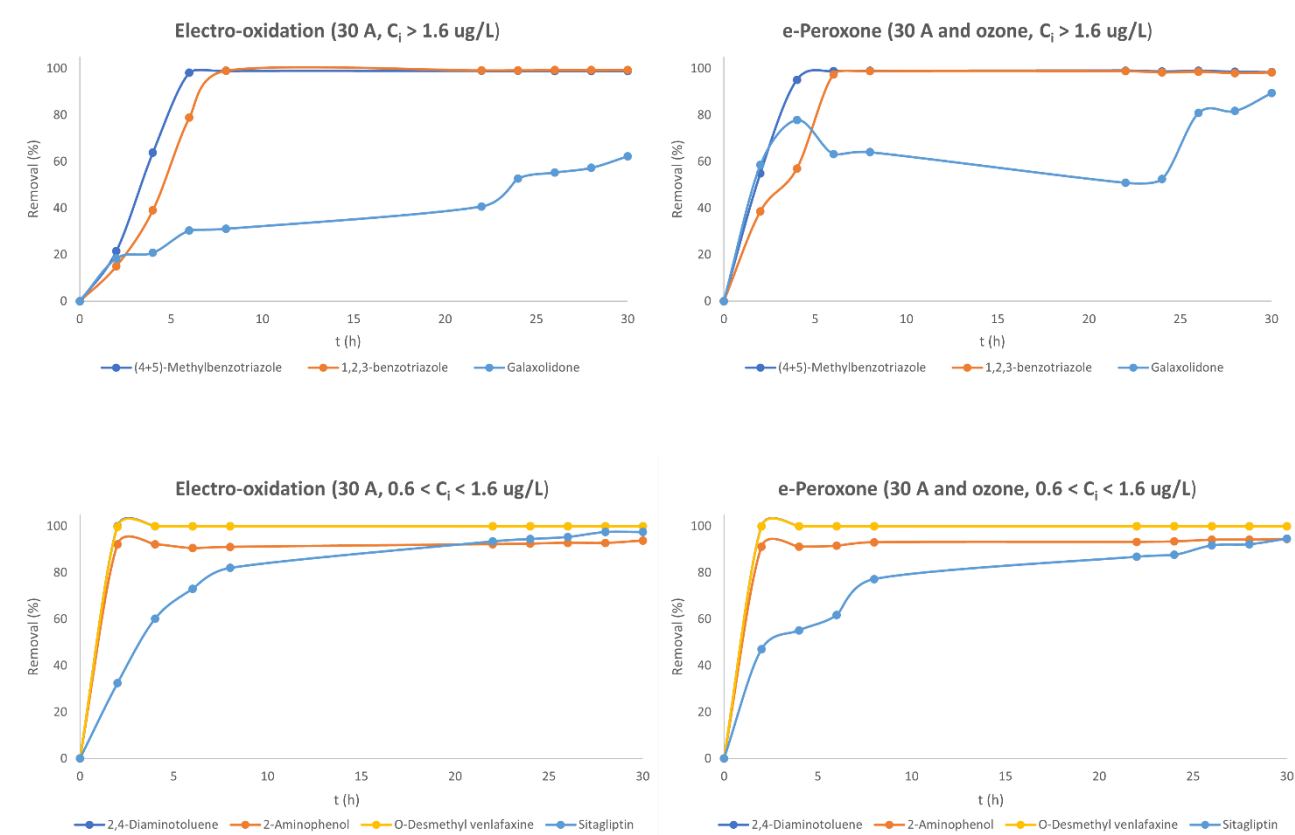
but lack direct comparability due to the unavailability of precise 90% removal values. This limitation stems from an insufficient sample size, hindering accurate data fitting and interpolation needed for more detailed analysis.

5.2.3 Scaling up: real secondary effluent at larger scale

Prior to scaling up the e-Peroxone treatment at the WWTP, Eurecat carried out a series of experiments using the EAOP prototype at their premises in July-August 2023. To evaluate the system's performance at a larger scale, electro-oxidation and e-Peroxone runs were conducted over a total of 30 hours. The tests were divided into two 8-hour operational sessions, spaced across consecutive days (day 1: 8 hours of operation, 14-hour pause, and day 2: an additional 8 hours). This approach allowed for a comprehensive analysis of the treatment duration and system efficiency under extended operational conditions.

Notably, the EAOP prototype is not designed for continuous operation due to the absence of an emergency stop mechanism for handling potential ozone leaks. As a result, some additional safety measures were implemented to ensure secure and controlled operation.

During these experiments, the focus was placed exclusively on monitoring iPM(T)s and PFAS removal (**Figure 16** and **Figure 17**), and ion formation (**Table 12** and **Table 13**) over time, as these are critical parameters for the implementation of the EAOP prototype at the WWTP. Given the varying properties and origins of the iPM(T)s analysed by IDAEA-CSIC, these compounds were grouped based on their initial concentration in the influent. Consequently, these target pollutants were classified into five concentration ranges, spanning from values above 1.6 $\mu\text{g/L}$ to as low as 0.06 $\mu\text{g/L}$.



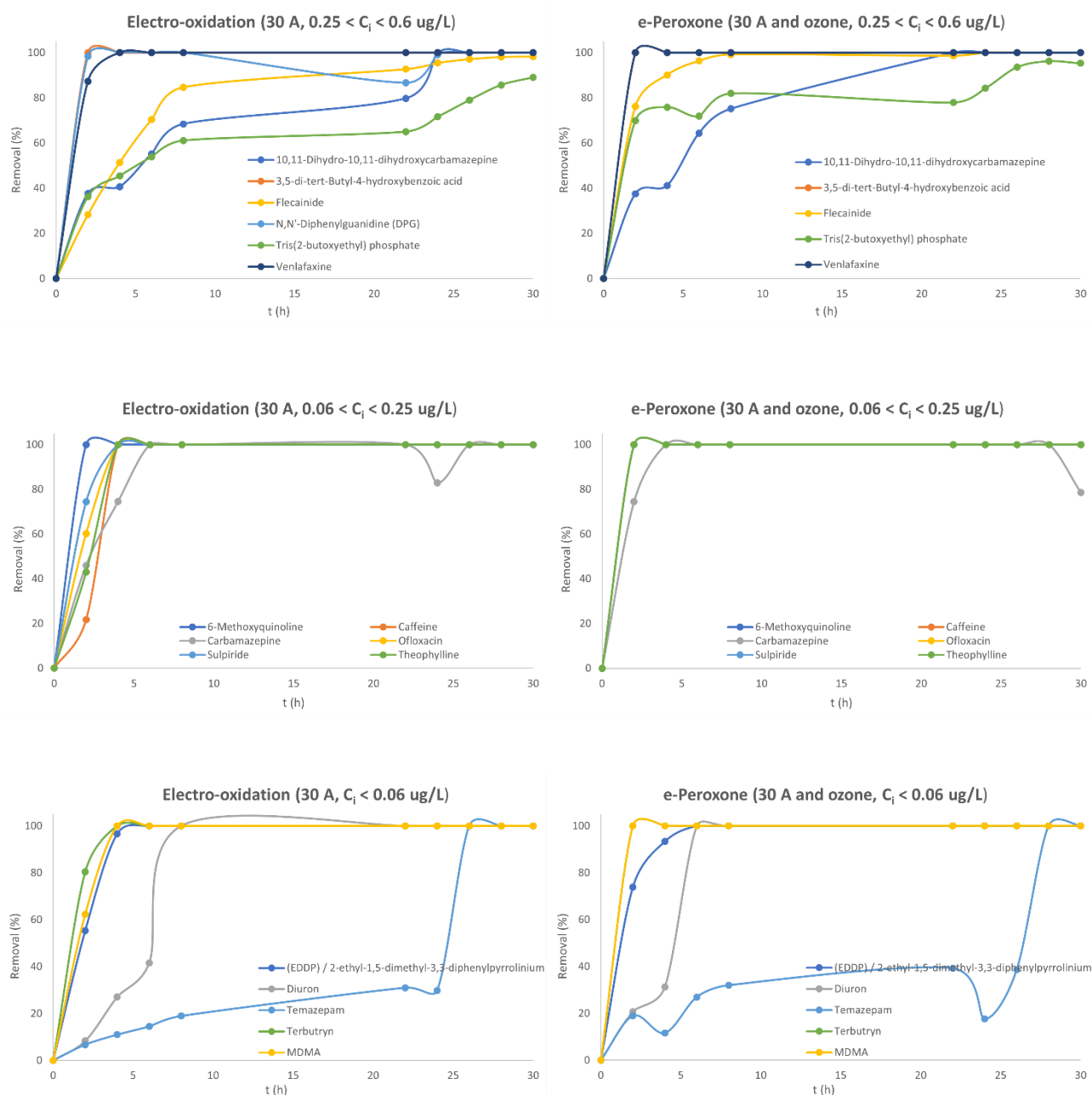


Figure 16. iPM(T)s removal using electro-oxidation and e-Peroxone on real secondary WWTP effluent at larger scale

As can be seen in **Figure 16**, the removal efficiency of iPM(T)s fluctuated considerably based on the functional groups within the molecules and their initial concentration. This variation highlights the importance of these factors in optimizing treatment processes for effective contaminant reduction. Although no significant differences were noted between the electro-oxidation process and the e-Peroxone system for many compounds, the introduction of ozone resulted in a slight improvement in the removal of specific substances.

To determine the ideal treatment duration for practical applications, a compromise was established between pollutant removal efficiency and the energy consumption associated with the treatment time. This detailed analysis identified 360 minutes as the optimal timeframe for reaching effective results.

Unfortunately, no significant removal of PFAS was observed, as depicted in **Figure 17**, since the initial and the final concentrations at different times are virtually identical. This outcome raises important considerations regarding the efficiency of the treatment process.

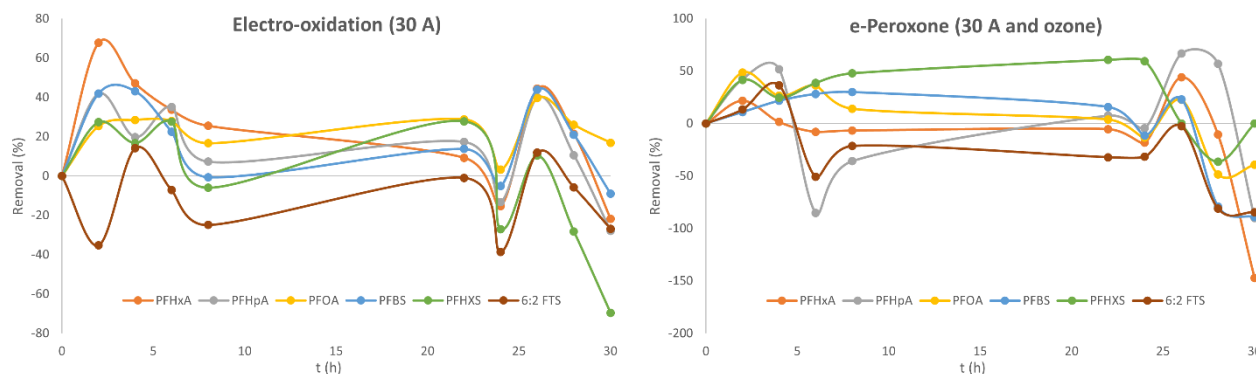


Figure 17. PFAS removal using electro-oxidation and e-Peroxone on real secondary WWTP effluent at larger scale

Several publications reported that oxidation processes involving long-chain PFAS produce short-chain PFAS as by-products. This transformation can result in a relatively stable concentration of short-chain PFAS if the reaction time is inadequate for achieving complete mineralization (Barisci and Suri, 2020; Radjenovic et al., 2020; Mirabediny et al., 2023).

The lack of significant changes in PFAS concentrations suggests that either the current treatment parameters are not adequately optimized to effectively target these persistent compounds, or the analytic methods used for quantification are challenged by interferences in the liquid matrix. Considering these insights, the optimal operational parameters for the AOP prototype were defined so that effective removal of iPM(T)s could be reached.

Additionally, during the oxidation process, halides (chlorides and bromides) may undergo reactions leading to the generation of chlorinated and brominated by-products (**Table 12** and **Table 13**). This fact not only impacts the overall chemical composition of the effluent but also raises environmental concerns regarding the potential toxicity of these compounds. Furthermore, the formation of such by-products may affect compliance with discharge limits, necessitating careful monitoring to ensure that the treated water meets regulatory standards before being released into the environment.

Table 12. Formation of chlorinated by-products using electro-oxidation and e-Peroxone on real secondary WWTP effluent at a larger scale

Treatment	Chloride (mg/L)		Chlorite (mg/L)		Chlorate (mg/L)		Perchlorate (mg/L)	
	Initial	Final	Initial	Final	Initial	Final	Initial	Final
Electro-oxidation	367	329	< 0.5	< 0.5	1.3	85	2.8	219
e-Peroxone	386	253	< 0.5	< 0.5	0.5	57	< 0.5	169

The production of chlorinated compounds during the oxidation process was quantified at EURECAT's laboratory (refer to section 4.6, Quantification of inorganic ions). The analysis revealed a significant increase in chlorate and perchlorate ions following oxidation treatment, attributable to the anodic

oxidation of chloride ions (Amado-Piña et al., 2022). As illustrated in **Table 12**, the electro-oxidation process resulted in a greater formation of these ions compared to the e-Peroxone technology.

The generation of inorganic oxychlorines during the e-Peroxone process has been explored by Lin et al. (2016). The anodic oxidation plays a crucial role in the conversion from chloride to oxychlorines, particularly during the initial stage of chloride transformation into hypochlorous acid/hypochlorite and the final stage of chlorate conversion into perchlorate. Although ozone and hydroxyl radicals do not directly oxidize chloride, they can oxidize hypochlorite (ClO^-) into higher oxychlorines once they are electrochemically generated at the anode (Lin et al., 2016). On the other hand, electro-generated hydrogen peroxide plays a key role in reducing hypochlorite back to chloride and transforming chlorate radicals into chlorate ions, thus helping to minimize the formation of oxychlorines.

Table 13. Formation of brominated by-products using electro-oxidation and e-Peroxone on real secondary WWTP effluent at a larger scale

Treatment	Bromide (mg/L)		Bromate (mg/L)	
	Initial	Final	Initial	Final
Electro-oxidation	< 1	< 0.5	< 0.5	< 0.5
e-Peroxone	< 0.5	< 0.5	< 0.5	< 0.5

Bromate formation is practically negligible at low specific ozone doses ($< 0.5 \text{ mgO}_3/\text{mg DOC}$) during the ozonation process. Nevertheless, its formation poses a notable risk when higher ozone doses are applied during ozonation, particularly at or above $1.0 \text{ mgO}_3/\text{mg DOC}$. Even moderate bromide levels in water (as low as $50 \text{ } \mu\text{g/L}$) may trigger significant bromate production, raising both operational and environmental challenges (von Gunten, 2003).

The e-Peroxone process effectively reduces bromate formation in bromide-containing water by reducing ozone's lifetime and neutralizing hypobromous acid (HBrO), which is a key reaction intermediate in bromate production during ozone-based reactions.

The formation of brominated compounds was quantified in EURECAT's lab. As shown in **Table 13**, the quantification limits of the method were insufficient to accurately measure the levels of bromide and bromate present in both the influent and effluent, respectively. Moving forward, the bromate concentration was analysed in a commercial laboratory with a lower quantification limit of $1 \text{ } \mu\text{g/L}$.

In terms of energy consumption, the **electrical energy per order (EE/O)** was calculated for each pollutant involved in the treatment process (**Table 14**).

Table 14. EE/O values for each pollutant involved in the treatment processes for real secondary WWTP effluent

Type of contaminant	Contaminant	Electro-oxidation EE/O (kWh/m ³)	e-Peroxone EE/O (kWh/m ³)
iPM(T)s	(4+5)-Methyl-1H-benzotriazole	4.55	4.35
	1,2,3-Benzotriazole	5.21	5.42
	Galaxolidone	n.a.	n.a.
	2,4- Diaminotoluene	n.a.	n.a.
	2-Aminophenol	2.46	2.72
	o-desmethyl venlafaxine	1.05	n.a.
	Sitagliptin	14.10	18.07
	10,11-Dihydro-10,11-dihydroxycarbamazepine	21.01	n.a.
	3,5-di-tert-butyl-4-hydroxybenzoic acid	n.a.	n.a.
	Flecainide	12.90	5.69
	N, N'-Diphenylguanidine	1.50	4.33
	Tris(2-butoxyethyl) phosphate	n.a.	15.62
	Venlafaxine	3.02	n.a.
	6-Methoxyquinoline	n.a.	n.a.
	Carbamazepine	n.a.	n.a.
	Sulpiride	n.a.	n.a.
	Caffeine	n.a.	n.a.
	Ofloxacin	n.a.	n.a.
	Theophylline	n.a.	n.a.
	EDDP/2-ethyl-1,5-dimethyl-3,3-diphenylpyrrolinium	3.61	4.85
	Diuron	n.a.	n.a.
	Temazepam	n.a.	n.a.
	Terbutryn	n.a.	n.a.
	MDMA	n.a.	n.a.

The primary component of operating costs in oxidation processes stems from the electrical energy required per order. As mentioned above, this metric is defined as the amount of electrical energy (in kWh) needed to achieve a one-order-of-magnitude reduction in the concentration of a specific pollutant within 1 m³ of contaminated water. A lower electrical energy per order indicates a more efficient treatment method, highlighting the efficacy of the process in removing pollutants. This focus on optimizing energy consumption not only improves the economic viability of the treatment system but also aligns with sustainability goals by reducing the overall environmental footprint.

5.3 Challenges and adaptations during pilot plant installation

The installation of the pilot plant presented a multifaceted challenge, requiring careful adjustments and innovative solutions to ensure successful execution. From logistical constraints to unforeseen technical difficulties, this section delves into the key challenges encountered during the installation phase into the pilot framework.

- (i) Administrative issues arose from the necessity to secure **an insurance policy for the transportation and operation of the EAOP prototype outside of Eurecat's facilities**. This requirement, mandated by Eurecat, was crucial for ensuring the safety and protection of the equipment during transit and operation. The need for insurance not only added complexity to the logistical planning but also necessitated additional coordination with insurance providers to meet Eurecat's safety standards.
- (ii) **Two smaller wetlands**, compared to those at the Urban River Lab, were designed to ensure they received exclusively treated water from the EAOP prototype, preventing any mixing of secondary water and oxidized water within the same flume. This intentional design preserved the integrity of the water treatment process by creating a dedicated flow of treated water specifically for the wetlands, which enhanced the monitoring and evaluation of their effectiveness in contaminant removal.
- (iii) During lab-scale batch operations, EURECAT detected a **notable increase in water temperature** following its passage through the electrochemical cell, mainly due to the Joule effect. This effect occurs when an electric current passes through a conductor, generating heat as a by-product of the electrical resistance. Consequently, the increase in temperature raised important concerns regarding the scalability of the e-Peroxone system for real-world applications. Therefore, it was essential to implement effective cooling strategies and continuously monitor water temperature throughout the operation. Potential solutions may also involve integrating heat exchangers or adjusting flow rates to prevent excessive heat accumulation. By addressing these temperature-related concerns, the e-Peroxone system can be optimized for larger-scale wastewater treatment applications.
- (iv) To guarantee the optimal electrochemical cell operation, a **filtration system** was established to reduce the concentration of total dissolved solids in the secondary effluent to below 1 mg/L. This advanced setup features a two-stage filtration process: first, a washable 150-micron filter effectively captured larger particles, followed by a finer 25-micron filter for polishing the water for improved clarity.
- (v) The initial strategy for **quantifying the ozone dose** during the pilot plant operation included the installation of an ozone analyzer. APRIA Systems, the ozone generator supplier, clarified that its ozone analysers are specifically designed for commercial use and are incompatible with our EAOP prototype setup. This limitation restricted our ability to quantify ozone levels accurately during the pilot plant operation.

5.4 Pilot-scale technology operation (TRL 6)

5.4.1 EAOP system

Pilot-scale operations at the wastewater treatment plant (WWTP of Montornès del Vallès) commenced on April 9, 2024, and concluded on July 23, 2024, covering a total of 15 weeks. The system initially operated at a treatment capacity of 300 L/day. However, on May 7, the treatment volume was increased to 600 L/day, accompanied by a reduced treatment duration of 180 minutes. This adjustment was made to ensure adequate water production for crop irrigation.

5.4.2 CW system

Located outdoors and operating as a biological treatment unit, the CWs are inherently influenced by weather conditions (**Figure 18**). Data from the Parets del Vallès weather station 3 km away highlighted the impact of meteorological factors. Four weeks during the monitoring period had

rainfall exceeding 20 mm, with a maximum of 51.1 mm recorded on April 29, 2024 (week 3). To prevent overflow, water input to the wetland was suspended during heavy rain events.

Temperature patterns revealed a temperate climate during the initial weeks (13–18°C from weeks 1 to 7), rising to averages above 25°C in July. Evapotranspiration rates, calculated by the Catalan meteorological network using temperature and solar radiation data, consistently exceeded 30 mm per week, further shaping the system's performance.

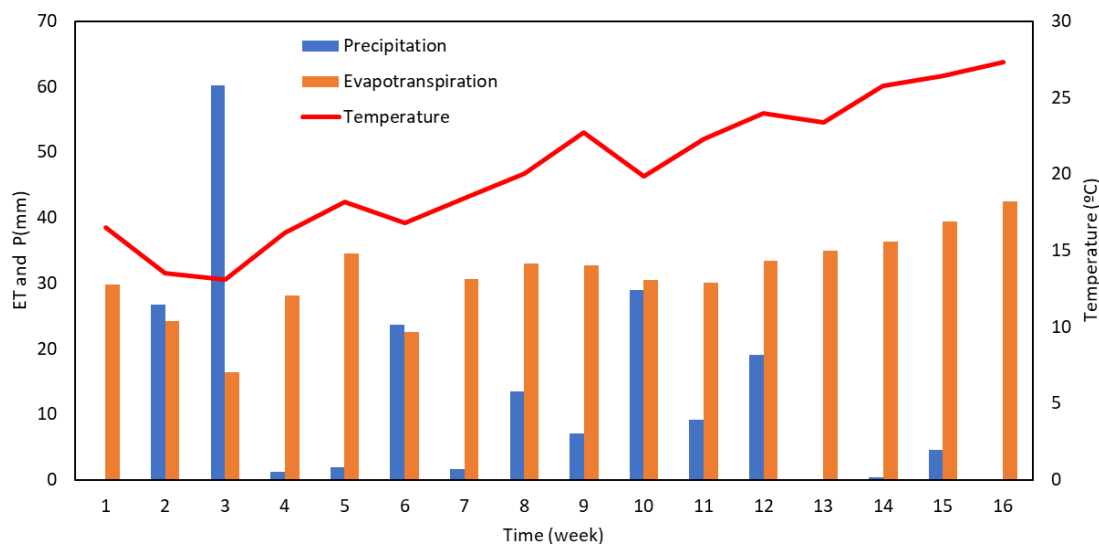


Figure 18. Weekly precipitation (blue bar) and evapotranspiration (orange bar) values (mm) and average weekly temperature (red line) (°C) calculated using data from Parets del Vallès Meteorological Station.

Two CW systems were operated in parallel under identical flow inputs and irrigation time schedules, both tailored to the volume treated by EAOP (**Figure 19** and **Table 15**). Their operation may be categorized into three distinct periods:

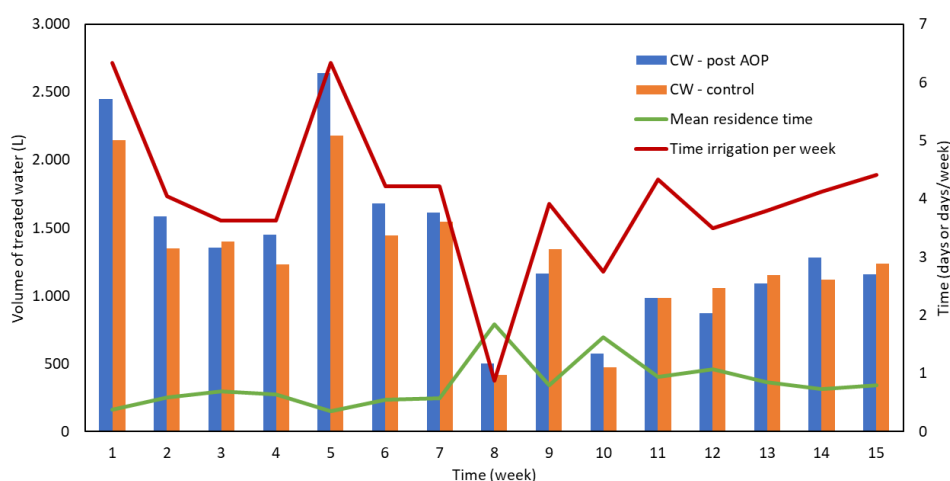
- 1. Initial Period (Weeks 1–7):** During this phase, weekly water treatment volumes ranged from 1,500 to 2,500 liters, with residence times spanning 0.4 to 0.7 days and irrigation schedules set for 4 to 6.5 days per week.
- 2. Rainfall-Impacted Period (Weeks 8–10):** Intense rainfall during this phase reduced irrigation times and treatment volumes, which in turn led to extended residence times. The samples were collected exclusively on non-rainy days to prevent dilution caused by rainfall. This approach ensured the samples accurately represented the actual conditions and were not influenced by the addition of extra water, preserving the precision and reliability of the analyses.
- 3. Stabilization Period (Week 10–15):** The treated volume stabilized at 900 to 1,300 liters per week, with residence times of 0.7 to 1.1 days and irrigation durations between 3.5 and 4.4 days per week.

Outflow from the CWs was estimated based on inflow data and a water balance accounting for evapotranspiration. The percentage of treated water occasionally exceeded 100% during weeks with heavy rainfall but decreased during periods where evapotranspiration surpassed 30 mm. However, water losses attributed to evapotranspiration may be underestimated, which could potentially affect the accuracy of these calculations.

Table 15. Management of CW system operations and regulation of water inflows and outflows.

Week	Date	CW - post AOP				CW - control				P-ET	Time irrigation per week
		Inlet volume	Outlet volume	% treated water	Mean residence time	Inlet volume	Outlet volume	% treated water	Mean residence time		
		L	L		d	L	L		d	L	d
1	09/04/2024	2.449	2.383	97	0,4	2.144	2.078	97	0,4	-57,6	6,3
2	16/04/2024	1.583	1.588	100	0,6	1.350	1.356	100	0,7	-49,5	4,0
3	23/04/2024	1.355	1.467	108	0,7	1.400	1.504	107	0,7	31,3	3,6
4	30/04/2024	1.451	1.401	97	0,6	1.229	1.186	96	0,8	60,0	3,6
5	07/05/2024	2.640	2.568	97	0,4	2.180	2.108	97	0,4	-68,8	6,3
6	14/05/2024	1.682	1.684	100	0,6	1.445	1.448	100	0,6	1,7	4,2
7	21/05/2024	1.615	1.551	96	0,6	1.545	1.480	96	0,6	-63,9	4,2
8	28/05/2024	504	492	98	1,8	420	408	97	2,2	-47,5	0,9
9	04/06/2024	1.163	1.106	95	0,8	1.343	1.286	96	0,7	-75,2	3,9
10	11/06/2024	574	582	101	1,6	475	483	102	2,0	20,5	2,8
11	18/06/2024	984	938	95	0,9	984	938	95	0,9	-48,6	4,3
12	25/06/2024	870	838	96	1,1	1.058	1.027	97	0,9	-47,3	3,5
13	02/07/2024	1.091	1.013	93	0,9	1.153	1.076	93	0,8	-59,2	3,8
14	09/07/2024	1.283	1.203	94	0,7	1.116	1.036	93	0,8	-79,9	4,1
15	16/07/2024	1.159	1.082	93	0,8	1.234	1.157	94	0,8	-75,8	4,4
16	23/07/2024	552	485	88	1,7	481	414	86	1,9	-94,0	1,0

P-ET: precipitation – evapotranspiration


Figure 19. Average residence time (green line), irrigation time (red line) and weekly treated water volume for the post EAOP (blue bar) and control (orange bar) CW systems

The primary goal of these CW systems was to remove nutrients from the secondary WWTP effluent. For the post-EAOP CW, the focus was to evaluate the ability to eliminate oxidation by-products, including remaining iPM(T)s, short-chain PFAS, and newly generated inorganic ions. Meanwhile, the objective of the control CW was to replicate the CW previously studied and optimized by Urban River Labs (URL), where CBT is involved. This would enable an assessment of its effectiveness in removing iPM(T) and PFASs, as well as examining potential differences in plant growth between the two CW systems.

5.4.3 Monitoring

The monitoring of the AOP and constructed wetland pilot commenced in mid-April, featuring a weekly sampling regimen. The analysis of PFAS and iPM(T)s was conducted by IDAEA-CSIC, both before and after treatment (EAOP prototype in/out, wetland in/out, control wetland in/out). iPM(T)s were monitored weekly until May 31, 2024, after which the frequency shifted to a biweekly schedule. PFAS were assessed biweekly. EURECAT analysed the formation of inorganic ions such as bromate, chlorite, chlorate, and perchlorate during the pilot plant operation, as well as their removal in constructed wetlands. CBT and CCB analysed pH, conductivity, nutrients (ammonium, nitrate, total nitrogen, total phosphorous) and COD decay.

5.5 Parameters and removal efficiency of the pilot-scale technology testing (TRL 6)

5.5.1 Physicochemical parameters

Throughout the operation of the pilot plant, the continuous monitoring of critical physicochemical parameters, including inlet water temperature, pH, conductivity, oxidation reduction potential (ORP), and chemical oxygen demand (COD) were vital to assess system performance. By tracking these parameters, Eurecat, CBT and CCB have ensured the optimal conditions for water treatment, enabling an effective adjustment and maintaining the system effectiveness during the operation. The data collected from these measurements was recorded regularly to assess the treatment's progress and outcomes.

Based on these results, a noticeable increase in the water temperature was observed during the oxidation stage, rising from 18-20°C to around 36°C due to the Joule effect (see Challenges and adaptations during pilot plant installation). At these high temperatures, ozone decomposition is not anticipated, meaning the system's performance remains stable under these conditions.

Although pH and conductivity offered valuable information on the chemical stability and ionic balance of the treated water, minimal changes in these parameters during the pilot operation may be attributed to the specific characteristics of the secondary WWTP effluent. During the ozonation process, unexpected slight variations in pH and conductivity were recorded, primarily driven by the generation of oxygen species radicals and the limited formation of carboxylic acids, stemming from the low organic matter content (only trace amounts of target pollutants).

ORP is influenced by the presence of oxidative substances (DO, nitrate, nitrite and oxygen reactive species), alongside reductive compounds (ammonium and organic matter). Positive ORP values observed following EAOP treatment indicated a surplus of oxidizing agents in the EAOP effluent, highlighting an enhanced capacity for oxidation reactions. This aligns with the presence of hydroxyl radicals ($\bullet\text{OH}$), signalling an oxidative environment capable of efficiently breaking down pollutants. As a result, ORP values effectively capture the dynamic interplay of oxidation-reduction reactions that take place along the oxidation process, providing valuable insight into the system's redox balance.

The pH within the CW system stabilized between 8.0 and 8.3, effectively adjusting the pH of the inlet water, which ranged 7.3 to 8.7. Meanwhile, no discernible trend was observed in the evolution of electrical conductivity, which remained between 1,500 and 2,400 $\mu\text{S}/\text{cm}$ at both the inlet and outlet points. The CW system also demonstrated its ability to restore sporadic low dissolved oxygen levels detected in the inlet water, maintaining dissolved oxygen levels consistently between 90% and 100%.

5.5.2 Nutrients

The oxidation of key nutrients, particularly nitrogen and phosphorous, was thoroughly investigated during the pilot plant's operation. Ammonium exhibited substantial oxidation during the e-Peroxone treatment, leading to an average removal rate above 76%. This oxidation process leads to the formation of nitrate, which had an average concentration of 2.30 mg/L and reflecting nitrate formation efficiency of 60%. Additionally, nitrite was completely oxidized to nitrate, with negligible traces remaining in the effluent.

In terms of total nitrogen—including nitrate nitrogen ($\text{NO}_3\text{-N}$), nitrite nitrogen ($\text{NO}_2\text{-N}$), ammoniacal nitrogen ($\text{NH}_3\text{-N}$), and organic nitrogen compounds—the mass balance remained coherent, revealing a 10% overall nitrogen removal. This indicates nitrogen was transformed among different species, with losses attributed to either as nitrogen gas and/or through struvite precipitation. Similarly, total phosphorous—including phosphate, condensed phosphates and organic phosphorous—experienced a removal rate of 8%, largely due to the struvite precipitation.

Struvite deposition in the EAOP prototype -pipes, pumps and electrodes of the electrochemical cell- represents a common issue in wastewater management, especially in areas with hard water containing elevated ammonium and magnesium levels (Santos Sanchez and Martins, 2021) (see Challenges and adaptations during pilot plant operation).

Orthophosphate can interact with ammonium in the presence of magnesium to produce struvite (eq. 1). Alternatively, orthophosphate can react with potassium, replacing ammonium in the crystal lattice and resulting in the formation of the potassium struvite (eq. 2). Nevertheless, potassium struvite only precipitates at low ammonium concentrations,



The potential for struvite formation (SPP) is assessed by comparing the ionic product of the solution ($[\text{Mg}^{2+}][\text{PO}_4^{3-}][\text{NH}_4^+]$) to struvite's solubility product ($\text{pK}_{\text{sp}} = 12.6$). Struvite precipitates once the ionic product exceeds the K_{sp} , while dissolution occurs when the product is lower. The SPP is determined by adjusting the struvite concentration in the solution and recalculating the ionic product until it aligns with the solubility product. A positive SPP means potential for struvite formation (expressed in mg/L), whereas a negative value indicates no likelihood of struvite forming (Jaffer et al., 2002). Even with a high SPP value, struvite crystal formation is not solely dependent on this factor. The process is significantly impacted by ionic strength, pH, temperature, and the presence of other foreign ions. Each of these variables plays a vital role in controlling both the rate and extent of struvite precipitation, highlighting the complexity of the crystallization process (Kékedi-Nagy et al., 2020).

The post EAOP CW system demonstrated an organic matter (COD) and nutrient removal capacity equal to or surpassing expectations (control CW, section Control wetland system - potential for removal of PMTs and PFAS). Specifically, the CW effectively removed organic matter, total nitrogen, nitrate, and total phosphorus (**Figure 20**). Due to the previous EAOP treatment, ammonium levels were negligible, except for in July (removal of 77%), when the EAOP treatment did not operate

properly. Key removal efficiencies include a 19% reduction in Chemical Oxygen Demand COD, reaching a final average concentration of 32.2 mg O₂/L; a 33% reduction in nitrate, with a final concentration of 1.5 mg N/L; a 21% reduction in total nitrogen, with a final concentration of 3.7 mg N/L; and a 36% reduction in total phosphorus, reaching a final concentration of 0.20 mg P/L.

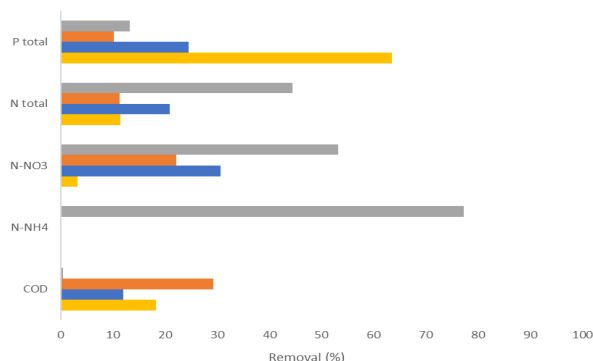


Figure 20. Nutrient removal of the post EAOP CW at Montornès del Vallès WWTP (April: yellow bar, May: blue bar, June: orange bar and July: grey bar)

5.5.3 iPM(T)s removal

The effective removal of iPMTs during the pilot plant operation is crucial for achieving optimal water treatment. By managing operational parameters such as ozone dosage, current intensity, and treatment duration, the EAOP prototype has been designed to maximize the iPM(T)s removal. Insights from prior pilot-scale tests conducted at Eurecat facilities revealed that optimal conditions for iPM(T)s removal occurred when current intensity of 30 A was combined with estimated ozone dosing (384 mg O₃/L) for 360 minutes.

Following various operational challenges related to the working schedules of the WWTP personnel (see Challenges and adaptations during pilot plant operation), the EAOP prototype was successfully operated using 30 A applied current intensity with ozone for 180 min.

The monitoring of iPM(T)s by IDAEA-CSIC enabled the assessment of process efficiency throughout the pilot operation at Montornès del Vallès WWTP. The analysed compounds were categorized based on their application (industrial chemicals, pharmaceuticals, pesticides and drug of abuse/others), and monthly average removal percentages were calculated to identify potential efficiency losses in the process. A potential decrease in efficiency prior to the electrochemical cell cleaning was not easily identifiable. In April, the system operated for 360 min per cycle, notably longer than the subsequent 180 min per cycle. The transition to shorter treatment cycles blurred the distinction between efficiency losses stemming from operational adjustments and those caused by system start up, complicating the efforts to isolate the impact of each factor.

Pharmaceuticals

Following secondary treatment at the Montornès del Vallès WWTP, pharmaceutical compounds were detected and further quantified using the target analysis developed by IDAEA-CSIC, including sitagliptin (antidiabetic), ofloxacin (fluoroquinolone antibiotic), flecainide (antiarrhythmic), carbamazepine (antiepileptic), venlafaxine (antidepressant), theophylline (bronchodilator), temazepam (sedative), and sulpiride (antipsychotic). Most of these compounds exhibited high removal rates, even at 180 min of operation, achieving >80% removal during the e-Peroxone treatment (**Figure 21**). This outcome highlights the process effectiveness in removing contaminants within this treatment time, underscoring its potential for impactful water treatment applications.

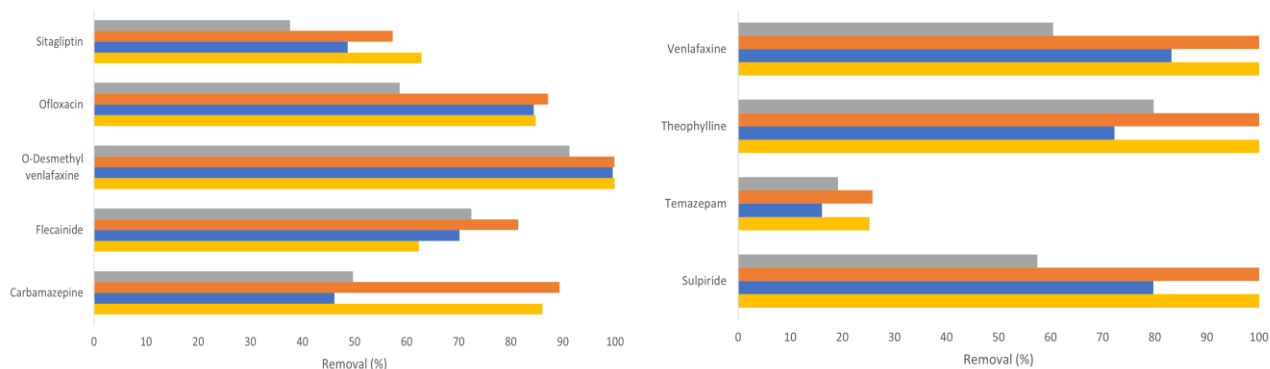


Figure 21. Pharmaceutical removal using e-Peroxone at Montornès del Vallès WWTP (April: yellow bar, May: blue bar, June: orange bar and July: grey bar)

Nevertheless, compounds such as sitagliptin, and especially temazepam, had lower removal rates by e-Peroxone process, even at six hours of treatment, suggesting operational limitations in the technology's effectiveness for persistent substances. This fact underscores the potential need for targeted optimization to effectively address specific pharmaceutical contaminants, rather than focusing on improving the removal of all studied compounds, to reduce the treatment time and energy consumption of the e-Peroxone process.

The operation of post EAOP CW system depends on the e-Peroxone process. High removal efficiencies in the EAOPs involve minimal further removal of compounds was seen in the CW, as most of the contaminants were already removed in the EAOPs (**Figure 22**). Nevertheless, compounds as sitagliptin and flecainide, with 60-70% removal during the e-Peroxone process (**Figure 21**), showed additional removal within the CW systems. These substances were 50-80% removed in the CW, demonstrating that the CW does provide additional compound removal. This revealed the CW's complementary role in treating certain compounds resistant to complete degradation by the oxidation process.

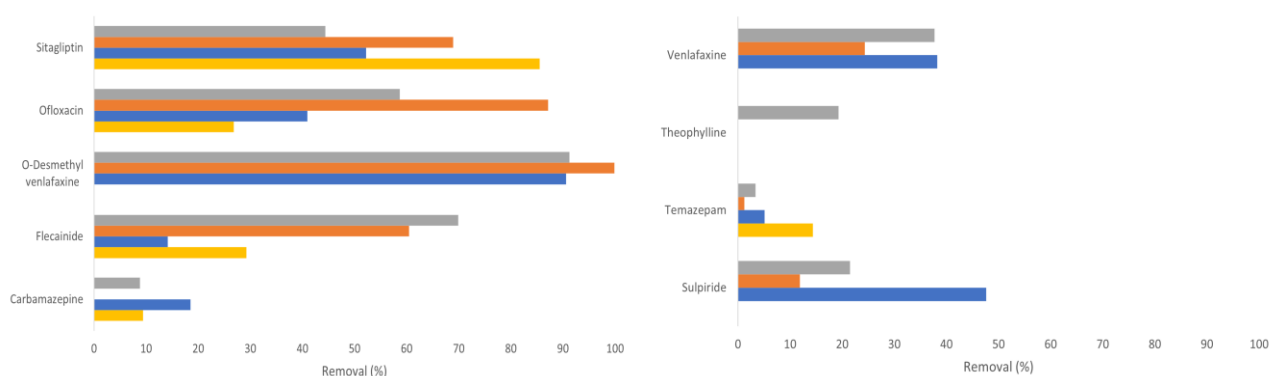


Figure 22. Pharmaceuticals removal in the post EAOP CW system at Montornès del Vallès WWTP (April: yellow bar, May: blue bar, June: orange bar and July: grey bar)

Pesticides/Drugs of abuse/Others

As was anticipated, the removal rates varied significantly, with terbutryn (used as a biocide) and MDMA (commonly known as ecstasy) removed >95% after 180 min of treatment (**Figure 23**). Nevertheless, other compounds such as EDDP (a metabolite of methadone) and carbendazim (a fungicide) demonstrate notable removal differences between the 180-min and 360-min treatment, with removal rates falling below 50% at 180 min.

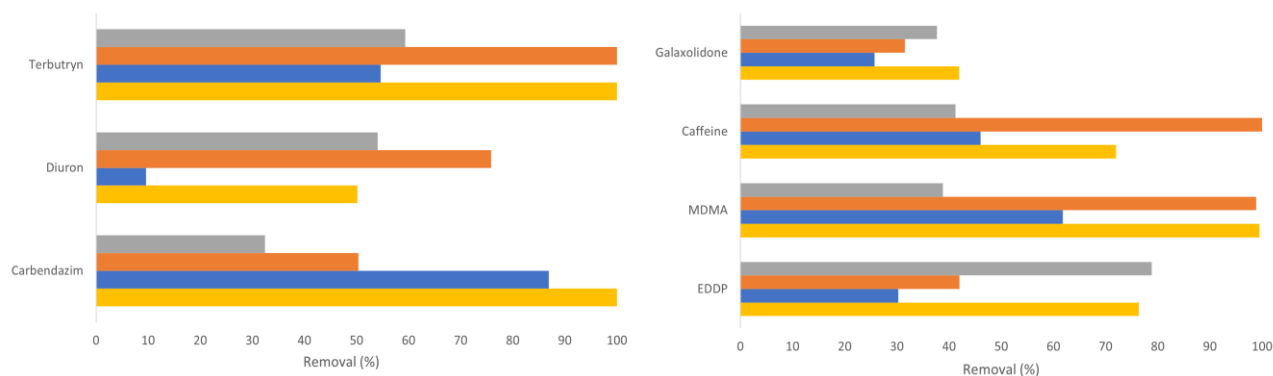


Figure 23. Pesticides/Drugs of abuse/Others removal using e-Peroxone at Montornès del Vallès WWTP (April: yellow bar, May: blue bar, June: orange bar and July: grey bar)

The higher removal observed for diuron and caffeine in June, despite a shorter treatment time, could be due to their concentration dependant behaviour during the treatment process. Besides, seasonal or operational factors could influence pollutant levels and reaction kinetics, adding variability to removal efficiency between months. This suggests that e-Peroxone process may achieve higher removal rates when higher pollutant concentrations are present, even with shorter operational times, while lower concentrations might need extended treatment to reach similar efficiencies.

The post EAOP CW system showed lower removal for pesticide and illicit drug compounds (**Figure 24**) compared to the pharmaceuticals previously discussed. This is due to the high removal of these substances during the oxidation process (**Figure 23**). For example, carbendazim exhibited high removal in CW system during June, coinciding with the lower removal efficiencies observed in the e-Peroxone process for the same compound. In contrast, no removal was detected in April, when the e-Peroxone process effectively eliminated nearly 100% of the carbendazim, leaving a lower concentration in the influent to the CW.

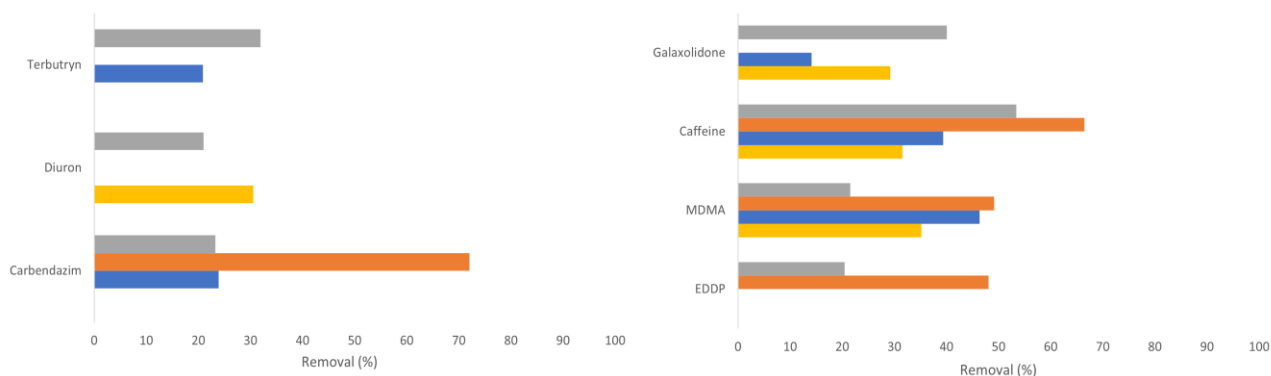


Figure 24. Pesticides/Drugs of abuse/Others removal by post EAOP CW system at Montornès del Vallès WWTP (April: yellow bar, May: blue bar, June: orange bar and July: grey bar)

Industrial chemicals

The most prevalent iPM(T)s detected in the secondary effluent of the WWTP include industrial chemicals such as phthalates, aminophenols, benzotriazole, phosphates, and various amines. Phthalates, aminophenol and tributylamine were removed >90% during 180 min of e-Peroxone treatment (**Figure 25**). This can be likely attributed to their chemical structures, which are more amenable to oxidation processes and can be effectively broken down by the active species generated during treatment.

Organic molecules derived from benzotriazole, more specifically 1,2,3-benzotriazole and (4+5)-methylbenzotriazole) demonstrate relatively low removal percentages. Benzotriazoles possess robust aromatic rings, which make them more resistant to removal by reactive species, leading to only partial removal during the treatment process. According to the literature, compounds like atenolol and benzotriazole, which are more resistant to ozone oxidation, can be progressively eliminated as the ozone dose increases, achieving over 85% removal with a moderate dose (around 0.6 g O₃/g DOC) (Hollender et al., 2009).

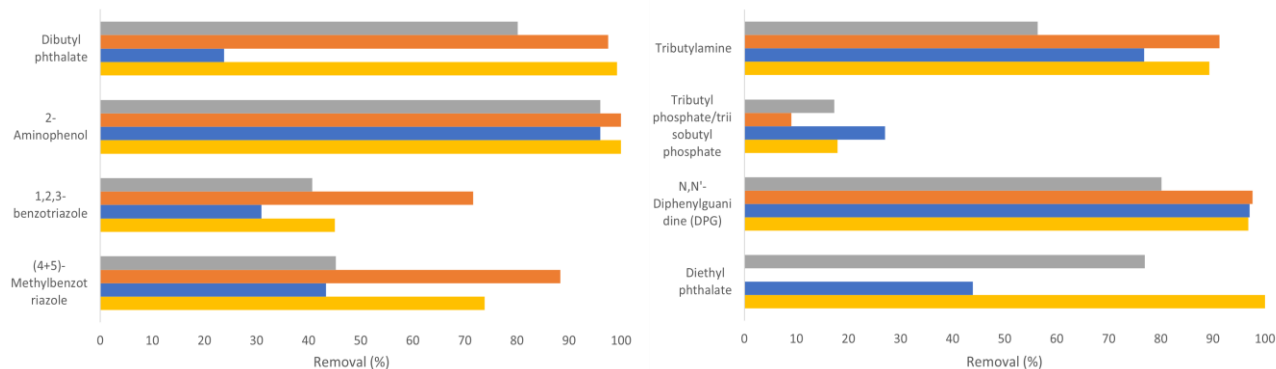


Figure 25. Industrial chemicals removal using e-Peroxone at Montornès del Vallès WWTP (April: yellow bar, May: blue bar, June: orange bar and July: grey bar)

The operation of the post EAOP CW system revealed that most industrial compounds, except for dibutyl phthalate (72±35%), exhibited removal percentages below 60% (i.e., 56±6% for N,N'-DPG or 14±5% for (4+5)-methylbenzotriazole) (**Figure 26**). Despite the effective removal in the EAOP, these compounds demonstrated limited additional removal in the CW system, highlighting the challenges of further treating pollutants already efficiently degraded in the initial oxidation stage. Compounds resistant to oxidation, such as 1,2,3-benzotriazole, exhibited relatively higher removal in the CW during April. This performance compensated for the lower elimination efficiencies achieved during the oxidation process.

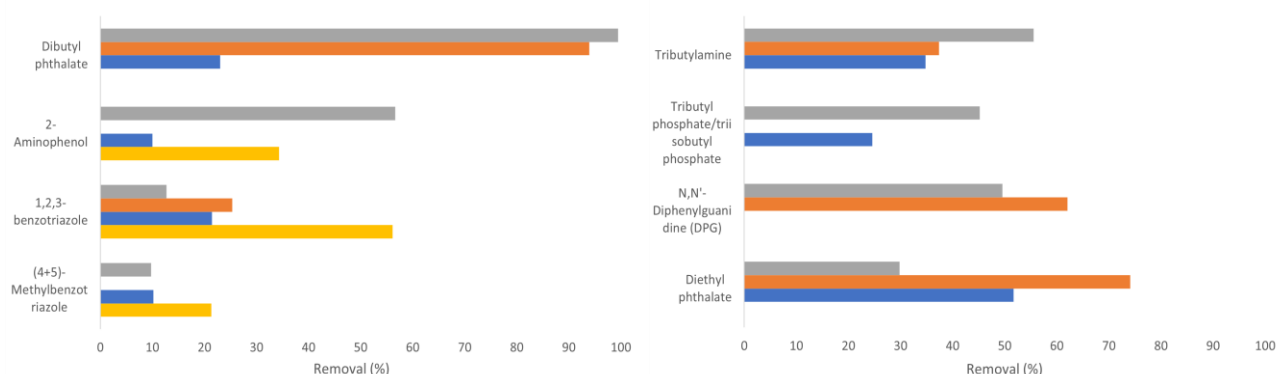


Figure 26. Industrial chemical removal in the post EAOPs CW system at Montornès del Vallès WWTP (April: yellow bar, May: blue bar, June: orange bar and July: grey bar)

5.5.4 PFAS removal

The PFAS removal in the e-Peroxone process was difficult to evaluate. The average monthly concentrations of 6:2 FTS revealed unexpected increases, deviating from the anticipated degradation pathway for this compound. Moderate removal rates for PFOS (**Table 16**) highlight the system's effectiveness in targeting and degrading this compound. By contrast, PFOA exhibits a lower removal when subjected to the same treatment conditions (**Table 17**). However, the data fails to show a clear trend in the removal or formation of short-chain PFAS, which complicates the ability to draw definitive conclusions from these results. This uncertainty may arise from various factors, such as the inherent variability of the process and the ever-changing interactions of PFAS within the system.

Table 16. Average monthly sulfonic PFAS levels before and after e-Peroxone at Montornès del Vallès

Months	6:2 FTS (ng/L)		PFOS (ng/L)		PFHxS (ng/L)		PFBS (ng/L)	
	Initial	Final	Initial	Final	Initial	Final	Initial	Final
April	41.2	74.1	36.8	6.6	< LOD	< LOD	149.7	157.4
May	19.0	40.2	33.3	14.7	< LOD	< LOD	132.7	143.4
June	< LOD	11.2	14.4	20.9	11.0	12.5	277.9	231.2
July	27.9	28.7	54.2	35.3	6.8	6.7	61.3	52.7

Table 17. Average monthly carboxylic PFAS levels before and after e-Peroxone at Montornès del Vallès

Months	PFNA (ng/L)		PFOA (ng/L)		PFHxA (ng/L)		PFBA (ng/L)	
	Initial	Final	Initial	Final	Initial	Final	Initial	Final
April	4.5	1.7	20.4	15.9	< LOD	34.0	< LOD	< LOD
May	2.1	9.5	18.8	14.3	< LOD	31.5	< LOD	< LOD
June	3.2	3.5	17.5	16.0	18.4	18.8	17.7	14.2
July	7.5	6.2	15.9	13.4	20.1	18.2	23.1	46.2

The post EAOP CW system demonstrated low efficiency in removing short-chain PFAS compounds, as indicated by the similarity in concentrations between the inlet and outlet (**Table 18** and **Table 19**). This outcome suggests that short-chain PFAS, due to their high solubility and low adsorption potential, are less likely to be retained or degraded within the CW system. Unlike their long-chain counterparts, which may adhere more readily to organic matter or biofilms within the CW system, short-chain PFAS remain largely mobile, passing through the system without significant alteration. Furthermore, the limited removal observed may be attributed to the lack of sufficient biological and/or chemical mechanisms (e.g. adsorption, phytoremediation) capable of effectively removing these persistent compounds. This emphasizes a major challenge in treating short-chain PFAS in CWs and highlights the need for long-term monitoring of full-scale CWs treating real wastewater for collecting additional data to support the development and validation of models (Savvidou et al., 2024).

Table 18. Average monthly sulfonic PFAS levels before/after post e-AOP CW at Montornès del Vallès

Months	6:2 FTS (ng/L)		PFOS (ng/L)		PFHxS (ng/L)		PFBS (ng/L)	
	Initial	Final	Initial	Final	Initial	Final	Initial	Final
April	74.1	37.3	6.6	34.93	< LOD	< LOD	157.4	166.4
May	40.2	51.8	14.7	36.2	< LOD	< LOD	143.4	143.1
June	11.2	< LOD	20.9	14.4	12.5	11.6	231.2	227.5
July	28.7	19.7	35.3	45.5	6.7	7.4	52.7	59.5

The results also reveal inconsistent removal of long-chain PFAS within the CW system. This irregularity could be attributed to several factors, including the desorption of these compounds from accumulated particulate matter or other wetland matter, or insufficient retention time for thorough degradation. Although the PFAS results are not consistent, PFNA concentrations exhibited an unexpected increase at the wetland outlet compared to the inlet throughout the duration of pilot plant operation, indicating potential contamination occurring within the wetland itself.

Table 19. Average monthly carboxylic PFAS levels before/after post e-AOP CW at Montornès del Vallès

Months	PFNA (ng/L)		PFOA (ng/L)		PFHxA (ng/L)		PFBA (ng/L)	
	Initial	Final	Initial	Final	Initial	Final	Initial	Final
April	1.7	< LOD	15.9	13.5	34.0	< LOD	< LOD	< LOD
May	9.5	51.5	14.3	21.6	31.5	35.9	< LOD	< LOD
June	3.5	7.5	16.0	16.3	18.8	17.4	14.2	15.0
July	6.2	227.4	13.4	12.1	18.2	17.2	46.2	15.2

Among the analysed PFAS compounds, only 12 were quantified and included into PFOA-equivalents calculation. This methodology ensures a systematic assessment: however, the inconsistencies in PFAS levels between the influent and effluent across most compounds indicate potential variability in the data, limiting the ability to accurately reflect the overall PFAS burden.

5.5.5 Formation and fate of inorganic ions

Chlorinated ions, such as chlorite, chlorate, and perchlorate, were tracked throughout the e-Peroxone treatment to assess the monthly average generation of these inorganic by-products alongside chloride removal.

As illustrated in **Table 20**, chloride ions decrease, accompanied by a corresponding rise in chlorate and, most notably, perchlorate ions—the highest oxidation state of chlorine. The significant perchlorate levels observed underscore the strong oxidative conditions in the e-Peroxone process, where reactive oxygen species, mainly hydroxyl radicals, facilitate the stepwise oxidation of the chloride ions to its most stable form, perchlorate.

Table 20. Formation of chlorinated by-products by e-Peroxone at Montornès del Vallès WWTP

Months	Chloride (mg/L)		Chlorite (mg/L)		Chlorate (mg/L)		Perchlorate (mg/L)	
	Initial	Final	Initial	Final	Initial	Final	Initial	Final
April	216.3	152.7	n.a.	n.a.	1.8	8.8	< 2.0	42.8
May	305.8	220.8	n.a.	n.a.	3.0	9.9	13.5	39.9
June	129.0	123.0	n.a.	n.a.	< 0.2	9.6	< 2.0	32.0
July	166.3	138.0	n.a.	n.a.	< 0.2	4.7	< 2.0	18.0

n.a.: not available

This generation of oxidized chlorine ions presents operational challenges for discharging the treated effluent. Chlorate and perchlorate are subject to regulation due to their potential impacts on the aquatic ecosystems and human health. These compounds, as final oxidation products, are resistant to further breakdown and thus accumulate, posing potential compliance issues for wastewater discharge.

Preliminary results suggest the nature-based post-treatment system effectively reduces concentrations of residual inorganic byproducts from the treated effluent (**Table 21**). By capturing these persistent ions before discharge, the wetland system slightly mitigates potential environmental impacts, reducing the risk of accumulation in downstream ecosystems. Altogether, this layer enhances water quality protection and strengthens the overall environmental resilience of the treatment train.

Table 21. Removal of chlorinated by-products by constructed wetland at Montornès del Vallès WWTP

Months	Chloride (mg/L)		Chlorite (mg/L)		Chlorate (mg/L)		Perchlorate (mg/L)	
	Initial	Final	Initial	Final	Initial	Final	Initial	Final
April	153	118	n.a.	n.a.	8.8	6.5	42.8	37.2
May	221	166	n.a.	n.a.	9.9	5.7	39.9	30.8
June	123	102	n.a.	n.a.	9.6	1.7	32.0	24.5
July	138	138	n.a.	n.a.	4.7	2.5	18.0	21.0

n.a.: not available

At present, no specific regulations or limits exist for chlorate and perchlorate in surface water and reclaimed water. The WHO sets the reference levels for chlorate and perchlorate in drinking water at 700 and 70 µg/L (WHO, 2016a; WHO, 2016b). However, both substances have established residue limits in food products. The Commission Regulation (EU) 2020/749 amends Annex III to Regulation (EC) No 396/2005, setting maximum residue levels for chlorate in certain food items. Similarly, Commission Regulation (EU) 2023/915 defines the maximum permissible levels for contaminants, including perchlorate, in food. These regulations set a maximum residue limit for chlorate and perchlorate, ranging from 0.05 to 0.75 mg/kg of food, depending on the product in question. Therefore, the use of non-chlorinated water for irrigation is recommended.

Analogously, brominated ions like bromate were monitored throughout the e-Peroxone treatment to evaluate the monthly average formation of these inorganic by-products alongside bromide reduction. However, unlike chloride, bromide concentrations remained below 1 mg/L, providing a lower baseline for bromate formation. Despite this, careful monitoring remains essential given the potential environmental and health impacts associated with brominated by-products.

Bromate ion quantification was done by a commercial laboratory to improve the detection accuracy by lowering the quantification limits for bromate. The results revealed bromate concentrations below the detection threshold of 10 ppb (parts per billion), confirming the absence of bromate formation in the process.

Furthermore, as expected, the nitrate ions were generated during the oxidation process, leading to an increase in concentration to average values around 9.8 mg/L. According to Regulation (EU) 2020/741, surface water is considered affected by nitrates if the concentration exceeds 25 mg/l. Therefore, despite the increase in concentration, the level does not exceed the threshold.

5.5.6 Energy consumption

In terms of energy consumption, determining the electrical energy per order (EE/O) for the pilot-scale experiments at the Montornès del Vallès WWTP was unfeasible. This is primarily due to the absence of time-series data and the unknown time required to achieve a 90% reduction for each compound. As a result, energy consumption estimates are instead based on the total energy demands of the entire treatment. This includes the ozone generator, the electrochemical cell, and the pumping systems used for both filling and emptying the prototype's feed tank, as well as the pump dedicated to wetland filling.

The cell operates at approximately 30 A and 10 V, while the ozone generator has a nominal power rating of 1000 W. During the operation of the pilot, the ozone generator operates at a current of 0.5 A, and consumes an actual power of 110 W, despite having a nominal power rating of 1000 W. The pump in the oxidation prototype consumes 0.6 kW over a 3-hour cycle. With these parameters, the total energy consumption of the oxidation prototype reaches 3 kWh.

Water transfer and irrigation were handled by a range of specialized pumps. A stainless-steel submersible pump, with a maximum absorbed power of 0.95 kW and nominal motor power of 0.45 kW, was used to move water from the secondary treatment stage to the oxidation equipment. System drainage was managed by a centrifugal pump with a 0.96 kW power capacity. For wetland irrigation, a high-efficiency circulator pump with a permanent magnet motor, operating at 25 W input power, was employed.

In total, the system required 3.81 kWh per cycle, equating to an energy consumption of 12.7 kWh per cubic meter. Considering the EU average price for non-household consumers of 0.2008 €/kWh in the second half of 2023, the energy cost for operating the plant is 2.54 €/m³.

5.5.7 Toxicological analysis

Evaluating toxicity of samples was essential, as the removal of certain substances may inadvertently lead to the formation of more toxic by-products. CALUX methods were used to assess the toxicity of the samples, extending beyond the mere quantification of the target contaminants. By focusing on both the removal and the resulting toxicity, the CALUX method contributes to the development of more effective and environmentally treatment strategies.

A reduction of approximately 90% PFAS activity was observed throughout the entire treatment process, as determined using the CALUX method (**Table 22**). This result highlights the effectiveness of the treatment in reducing the presence of these contaminants.

Table 22. CALUX analysis results of WAX-SPE water sample extracts

Sample	PFAS CALUX	
	activity	LOQ
Inlet EAOPs	620	0.69
Outlet EAOPs	170	0.68
Buffer tank	180	0.68
Outlet PROMISCES wetland	65	0.68
Outlet control wetland	330	0.67

5.5.8 Microbiological and physicochemical analyses analysis

The microbiological analysis of samples was conducted to verify compliance with Quality Standard AA, as specified for irrigation of vegetable crops under Royal Decree 1085/2024.

The secondary effluent is currently unsuitable for irrigation due to *E. coli* concentrations exceeding 250,000 CFU/100 mL, well above the regulatory limit of 100 CFU/100 mL for AA water quality (**Table 5**). Interestingly, an unexpected increase in *E. coli* concentrations was observed after the filtration step, just before the e-Peroxone treatment. This increase may be linked to biofilm formation within the filtration system, potentially causing *E. coli* to be released back into the effluent, or to inadequate filter washing cycles, leading to microbial buildup and breakthrough.

Nevertheless, the e-Peroxone process proved effective in eliminating *E. coli* from the treated water (close to 100%). In contrast, the CW resulted in a slight increase in *E. coli* concentrations (4 CFU/ 100 ml), though it still complied with the regulatory limits.

Regarding *Legionella spp.*, the secondary effluent from Montornès del Vallès WWTP also exceeded the regulatory limits. However, unlike *E. coli*, complete removal takes place during the filtration step just before the e-Peroxone treatment. As for eggs of parasitic helminths, from both the nematode and *Taenia* genera, the secondary effluent meets the specifications outlined in Royal Decree 1085/2024. No further changes in concentrations were observed throughout the treatment process in the pilot plant.

The key physicochemical parameters for irrigation consideration are turbidity and suspended solids. The secondary effluent had turbidity of approx. 2.3 NTU, which slightly increased during the e-Peroxone treatment. This increase can be attributed to the formation of microaggregates and the destabilization of particles during oxidation, which may cause previously settled or colloidal particles to resuspend in the water. Once the water passed through the constructed wetland, turbidity decreased again. This is due to the wetland's role as a natural filtration system, where plants, sediments, and microbial activity remove particles and reduce turbidity.

These findings align with the observed trends in suspended solids (SS) concentrations across the samples. The fluctuations in the turbidity correspond closely to the changes in SS, reflecting a similar pattern throughout the treatment process.

5.6 Control wetland system - potential for removal of PMTs and PFAS

5.6.1 Physicochemical parameters and nutrients

As described in section 5.4. Pilot-scale technology operation (TRL 6) , both CW systems operated under similar flow conditions, and identical design specifications and climatic factors. The key difference was their inlet water: in the case outlined in section 5.5. Parameters and removal efficiency of the pilot-scale technology testing (TRL 6) , the post-EAOP CW received EAOP effluent, while the control CW was supplied with secondary WWTP effluent (i.e. the same water entering the EAOP).

The physicochemical parameters of the inlet water for both CW systems were closely aligned (see pH, electrical conductivity and dissolved oxygen in **Table 23**). The organic matter, measured as COD, was higher in the CW control (47.4 mg O₂/L) compared to the post EAOP CW system (39.7 mg O₂/L) Despite this, the post EAOP CW demonstrated greater degradation rate, achieving a final COD concentration of 32.2 mg O₂/L. The total nitrogen levels in the inlet and outlet were comparable, with nitrogen removal rates ranging from 21% to 24% in both CW systems (**Table 23**). A notable distinction

between the two systems is their nitrogen removal mechanisms: the control CW primarily targeted ammonium removal (69%), while the post-EAOP CW focused on nitrate removal (34%). The low concentrations of ammonium in the post-EAOP CW were attributed to its oxidation to nitrate during the e-Peroxone process. Total phosphorous removal was also measured, with the post EAOP CW (36%) outperforming the control (17%).

Table 23. Comparison of physicochemical parameters between CW systems (control vs post-EAOP)

		Control CW						Post EAOP CW					
		Inlet channel			Outlet channel			Inlet channel			Outlet channel		
		Av.	Min.	Max.	Av.	Min.	Max.	Av.	Min.	Max.	Av.	Min.	Max.
pH		7.97	7.71	8.20	8.06	7.77	8.21	8.19	7.25	8.74	8.11	7.87	8.30
Electrical Conductivity	μS/cm	2,180	1,756	2,534	2,148	1,645	2,602	2,034	1,544	2,300	2,046	1,502	2,380
Dissolved Oxygen	mg/L	9.6	7.9	11.2	9.4	8.3	10.5	9.5	8.2	11.4	9.2	8.0	10.7
COD	mg O ₂ /l	47.4	36.8	57.6	41.2	26.7	52.4	39.7	34.9	43.5	32.2	28.0	36.7
COD removal	%				13	8	27				19	15	25
N-NH ₄ ⁺	mg N/l	1.18	0.39	3.19	0.34	0.11	1.02	0.17	0.01	0.41	0.26	0.07	0.62
N-NH ₄ ⁺ decline	%				69	45	96				0		
N-NO ₃ ⁻	mg N/l	0.56	0.28	0.80	1.01	0.51	1.98	2.29	1.65	2.61	1.51	0.91	1.97
N-NO ₃ ⁻ decline	%				0						34	15	60
N total	mg N/l	4.96	3.70	6.60	3.73	2.46	5.95	4.74	4.24	5.72	3.70	3.12	4.01
N decline	%				24	9	56				21	11	38
P total	mg P/l	0.39	0.18	1.22	0.32	0.09	0.78	0.33	0.22	0.56	0.20	0.07	0.31
P decline	%				17	-22	65				36	18	67

In summary, the physicochemical parameters measured in both CW systems showed no significant differences (**Table 23**, **Figure 20** and **Figure 27**). Further investigation is needed to determine whether variations exist in the water temperature and oxidation reduction potential (ORP) of the EAOP-treated water. A key difference between the two systems was inorganic nitrogen: ammonium dominated in the control CW, whereas nitrate was dominant in the post-EAOP CW. Furthermore, the hydrochemical profile of the EAOP-treated water, including the presence of newly generated ions

such as chlorate, perchlorate, and bromate, showed no discernible impact on the nutrient removal efficiency of the CW systems.

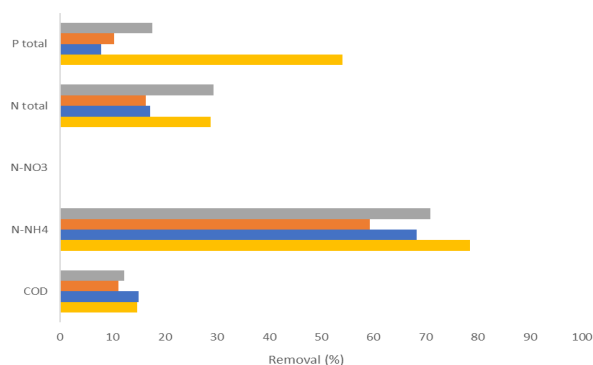


Figure 27. Nutrient removal of control CW at Montornès del Vallès WWTP (April: yellow bar, May: blue bar, June: orange bar and July: grey bar)

5.6.2 iPM(T)s removal

Pharmaceuticals

The removal of pharmaceuticals in the control CW revealed that compounds were partially retained by adsorption to the substrate, uptake by vegetation and microbial degradation in the root zone (**Figure 28**). Venlafaxine and theophylline, both characterized by high hydrophobicity, exhibited a strong affinity for the adsorption to the wetland's organic matter and substrate particles. This binding mechanism limits their mobility within the control CW, resulting in higher removal. This natural retention process is more pronounced in the control CW compared to the post EAOP CW, where e-Peroxone has already degraded a substantial portion of these compounds before they enter the wetland.

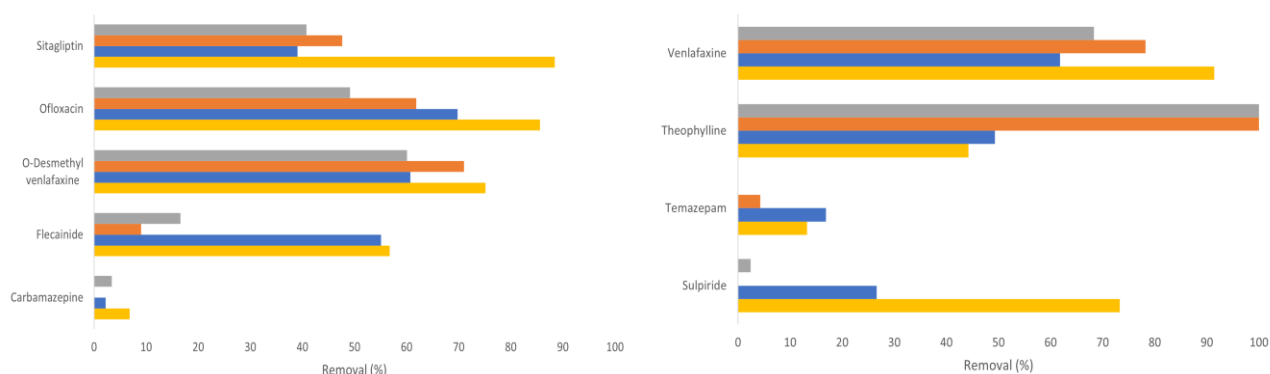


Figure 28. Pharmaceutical removals by control CW system at Montornès del Vallès WWTP (April: yellow bar, May: blue bar, June: orange bar and July: grey bar)

Pesticides/Drugs of abuse/Others

Unlike pharmaceuticals, pesticides exhibited poor removal in the control CW system (**Figure 29**). Despite the moderate/high hydrophobicity of these compounds, their removal can be influenced by multiple factors. Based on the previous studies, carbendazim exhibits different primary species at varying pH levels (Furini et al., 2016). At relatively higher pH values, the solubility of carbendazim strongly decreases, and the predominant species is anionic, leading to weaker soil adsorption. Like

diuron, a systemic herbicide, carbendazim removal likely occurs through mechanisms such as plant uptake and sorption in the root zone might typically be anticipated. Nevertheless, no measurable reduction of diuron concentrations was observed within the control and post EAOP CW systems. This outcome could be attributed to the relatively short hydraulic retention time of the wetland (6h approximately) due to the small size of the wetland.

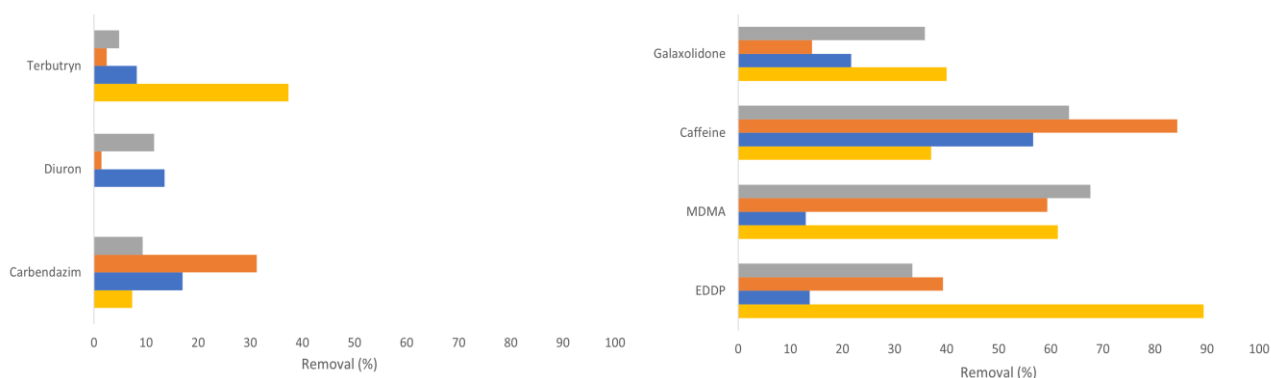


Figure 29. Pesticides/Drugs of abuse/Others removals by control CW system at Montornès del Vallès WWTP (April: yellow bar, May: blue bar, June: orange bar and July: grey bar)

Like pharmaceutical behaviour, the removal of drug of abuse in the control CW was higher (**Figure 29**) than in the post EAOP CW system (**Figure 24**). The lack of oxidative by-products, which are present in post EAOP system and may compete for adsorption sites, further amplifies the effectiveness of these retention processes.

Industrial chemicals

The industrial chemicals showed removal similar to that of pesticides, with relatively limited attenuation (**Figure 30**). Compounds such as 2,3-benzotriazole and tributyl phosphate, known for their resistance to the chemical degradation, showed removal rates below 35% in the control CW system.

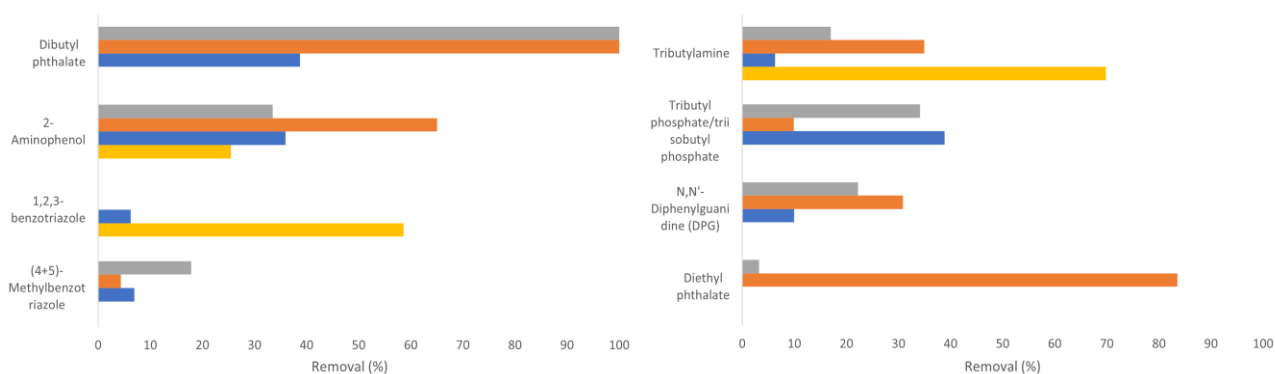


Figure 30. Industrial chemical removals by control CW system at Montornès del Vallès WWTP (April: yellow bar, May: blue bar, June: orange bar and July: grey bar)

The relatively low removal of phthalates, phosphates, and benzotriazoles in the control CW can be attributed to a combination of their physicochemical properties and the operational conditions of the system. Notably, dibutyl phthalate ($7.52 \pm 0.13 \mu\text{g/L}$) was detected in the construction material of the wetland, suggesting potential cross-contamination.

5.6.3 PFAS removal

Within the control CW system, no clear trend of long-chain and short-chain PFAS removal was observed (**Table 24** and **Table 25**). Several factors could contribute to this, including the selection of the plant species and the hydraulic residence time of the system.

Table 24. Average monthly sulfonic PFAS levels before (initial) and after (final) the control CW at Montornès del Vallés

Months	6:2 FTS (ng/L)		PFOS (ng/L)		PFHxS (ng/L)		PFBS (ng/L)	
	Initial	Final	Initial	Final	Initial	Final	Initial	Final
April	37.7	37.3	31.9	34.9	n.d.	n.d.	192.3	166.4
May	27.3	34.0	39.5	29.8	n.d.	n.d.	161.9	137.5
June	11.1	n.d.	13.5	12.9	10.8	9.8	255.4	207.0
July	21.7	16.7	38.2	61.5	11.7	8.7	47.3	61.4

n.d.: not detectable

Table 25. Average monthly carboxylic PFAS levels (initial) and after (final) the control CW at Montornès del Vallés

Months	PFNA (ng/L)		PFOA (ng/L)		PFHxA (ng/L)		PFBA (ng/L)	
	Initial	Final	Initial	Final	Initial	Final	Initial	Final
April	4.3	n.d.	17.2	13.5	n.d.	n.d.	n.d.	n.d.
May	4.8	97.1	23.8	21.6	n.d.	n.d.	n.d.	n.d.
June	3.2	n.d.	16.9	16.1	16.9	12.6	14.9	12.8
July	6.9	568.3	13.7	15.7	14.2	18.1	18.9	17.7

n.d.: not detectable

Certain plants have demonstrated high capacities for PFAS uptake and sequestration due to their physiological traits such as root structure and grow rate. For example, some plant species such as willow (*Salix* spp.) and sunflowers (*Helianthus annuus*) have demonstrated promising potential for PFAS removal in other studies (Sharma et al., 2020; Kavusi et al., 2023; Nassazzi et al., 2023). These species are known for their robust root systems and high biomass production. Willows have an extensive root network that interacts with the rhizosphere to enhance sorption and microbial activity, which may assist in PFAS immobilization. Another critical parameter to consider is the hydraulic residence time in the control CW system, as shorter values may not be sufficient to effectively remove PFAS compounds.

The increase in PFNA concentrations detected in both the control and post e-AOP CW systems suggests potential external contamination, possibly from the materials used in the construction of the wetland.

5.7 Compliance with Directive (EU) 2024/3019 on urban wastewater treatment

Directive 2024/3019 outlines the standards for advanced treatment of effluents from urban WWTPs. A minimum removal of 80% is required for specific micropollutants, which, even at low concentrations, can significantly impact water quality and the environment. The substances are classified into two categories, requiring different approaches for effective treatment and removal.

Category 1 (substances easily treated): amisulpride (CAS No 71675-85-9), carbamazepine (CAS No 298-46-4), citalopram (CAS No 59729-33-8), clarithromycin (CAS No 81103-11-9), diclofenac (CAS No 15307-86-5), hydrochlorothiazide (CAS No 58-93-5), metoprolol (CAS No 37350-58-6), and venlafaxine (CAS No 93413-69-5).

Category 2 (substances easily disposed of): benzotriazole (CAS No 95-14-7), candesartan (CAS No 139481-59-7), irbesartan (CAS No 138402-11-6) and a mixture of 4-methylbenzotriazole (CAS No 29878-31-7) and 5-methyl-benzotriazole (CAS No 136-85-6).

As specified in the Directive 2024/3019, the removal percentage must be calculated based on dry weather flow for at least six substances. Furthermore, the category 1 must contain twice as many substances as category 2. If fewer than six substances can be measured at sufficient concentrations, the relevant authority must designate alternative substances for the removal calculation if needed. The average of the specific removal percentages for each substance included in the calculation will be used to assess whether the 80% removal threshold has been achieved.

During the pilot plant pilot plant operation, four of the specific pollutants mentioned above were monitored: carbamazepine, venlafaxine, benzotriazole, and a mixture of 4-methylbenzotriazole and 5-methyl-benzotriazole. Apart from venlafaxine, all these specific substances exhibited removal rates below 80%. Nonetheless, out of the 41 PMTs analysed, eleven compounds achieved removal rates greater than 80% using EAOPs + CW system) (**Table 26** and **Table 27**).

Table 26. Summary of iPMTs data: EAOP inlet concentration and removal efficiencies

Pollutants	EAOP inlet concentration (µg/L)	EAOP removal (%)	EAOP + CW removal (%)	Control CW removal (%)
(4+5)-Methylbenzotriazole	0.904 ± 0.228	58.0 ± 28.9	47.7 ± 20.9	2.1 ± 17.4
(EDDP) / 2-ethyl-1,5-dimethyl-3,3-diphenylpyrrolinium	0.024 ± 0.021	25.1 ± 59.9	39.3 ± 42.8	29.7 ± 28.7
1,2,3-benzotriazole	2.697 ± 1.255	-3477.0 ± 13167.1	10.4 ± 50.5	-41.1 ± 80.7
1,8-Diazabicyclo [5.4.0]undec-7-ene (polycat dbu)	0.032 ± 0.051	90.4 ± 46.9	100.0 ± 51.5	86.1 ± 46.0
10,11-Dihydro-10,11-dihydroxycarbamazepine	0.520 ± 0.158	29.9 ± 12.8	32.8 ± 14.5	9.2 ± 13.6
2,4-Diaminotoluene	6.792 ± 6.786	72.4 ± 43.6	96.8 ± 49.9	74.7 ± 51.4
2-Aminophenol	1.540 ± 0.721	98.0 ± 2.6	93.8 ± 2.6	30.4 ± 28.9
2-Ethylhexyl diphenyl phosphate	1.511 ± 5.010	100.0 ± 26.7	100.0 ± 28.9	n.a.
2-Methoxy-5-methylaniline	n.a.	n.a.	n.a.	n.a.
3,5-di-tert-Butyl-4-hydroxybenzoic acid	0.367 ± 0.188	81.7 ± 23.4	49.7 ± 81.0	-121.6 ± 305.9
6-Methoxyquinoline	0.012 ± 0.012	100.0 ± 42.6	100.0 ± 38.9	24.0 ± 11.1
6-Methyl-2-pyridinemethanol+ 2-Amino-4-cresol	0.362 ± 0.385	-49.3 ± 65.8	-45.5 ± 106.0	9.9 ± 31.0
Bis(2-ethylhexyl)amine	0.009 ± 0.004	-10.6 ± 15.2	-140.4 ± 102.5	-0.9 ± 18.3
Caffeine	1.000 ± 0.769	54.6 ± 34.9	59.5 ± 35.3	56.3 ± 30.4
Caprolactam	0.149 ± 0.134	-52.5 ± 114.9	-44.8 ± 103.5	-43.9 ± 49.5
Carbamazepine	0.056 ± 0.013	67.3 ± 28.8	58.1 ± 20.8	-2.8 ± 10.6
Carbendazim	0.017 ± 0.030	-9.3 ± 235.7	-16.9 ± 282.1	11.3 ± 18.2
Dibutyl adipate	0.007 ± 0.024	100.0 ± 26.7	83.5 ± 24.1	n.a.
Dibutyl phthalate	0.403 ± 0.831	26.4 ± 109.7	-819.5 ± 2472.4	-584.1 ± 1637.1
Diethyl phthalate	1.396 ± 2.980	-111.1 ± 260.8	-67.4 ± 281.3	-46.8 ± 80.2
Diuron	0.017 ± 0.005	39.0 ± 40.7	16.5 ± 18.0	-2.2 ± 13.0
Erucamide	n.a.	n.a.	n.a.	n.a.

Pollutants	EAOP inlet concentration (µg/L)	EAOP removal (%)	EAOP + CW removal (%)	Control CW removal (%)
Flecainide	0.335 ± 0.537	70.0 ± 24.7	74.7 ± 23.5	22.4 ± 41.4
Galaxolidone	3.800 ± 1.540	16.7 ± 30.1	51.2 ± 17.7	23.4 ± 22.3
MDMA	1.843 ± 2.855	75.7 ± 34.2	75.4 ± 36.9	19.1 ± 63.7
Melamine	n.a.	n.a.	n.a.	n.a.
N,N'-Diphenylguanidine (DPG)	0.275 ± 0.088	93.3 ± 13.5	-3.3 ± 50.0	-82.0 ± 118.3
N-Phenyl-1-naphthylamine	n.a.	n.a.	n.a.	n.a.
O-Desmethyl venlafaxine	1.216 ± 0.251	98.0 ± 6.4	98.6 ± 1.8	62.8 ± 17.8
Ofloxacin	0.542 ± 0.841	77.3 ± 18.5	74.5 ± 14.5	57.2 ± 29.8
Secbumeton	0.001 ± 0.002	100.0 ± 26.7	n.a.	n.a.
Sitagliptin	0.823 ± 0.318	50.3 ± 23.8	85.4 ± 25.4	54.0 ± 28.2
Sulfamethoxazole	n.a.	n.a.	n.a.	n.a.
Sulpiride	0.300 ± 0.231	86.5 ± 23.7	86.4 ± 13.5	-3.6 ± 33.2
Temazepam	0.034 ± 0.006	13.6 ± 16.8	19.3 ± 13.5	2.1 ± 18.3
Terbutryn	0.038 ± 0.011	80.9 ± 26.1	77.6 ± 15.6	5.5 ± 12.6
Theophylline	0.540 ± 0.286	94.3 ± 36.4	96.1 ± 38.1	64.4 ± 36.0
Tributyl phosphate/triisobutyl phosphate	0.093 ± 0.063	-8.6 ± 61.0	-103.4 ± 101.9	-4.4 ± 45.0
Tributylamine	0.030 ± 0.019	37.2 ± 106.0	47.0 ± 54.7	4.0 ± 41.8
Triethyl phosphate	0.062 ± 0.071	5.1 ± 52.7	-209.7 ± 267.2	-92.9 ± 116.6
Tris(2-butoxyethyl) phosphate	0.298 ± 0.173	31.2 ± 19.5	31.4 ± 23.6	18.9 ± 33.3
Venlafaxine	0.427 ± 0.097	87.8 ± 22.3	92.6 ± 4.8	68.1 ± 17.6
Dibutyl hydrogen phosphate	0.117 ± 0.118	-164.1 ± 485.1	-150.0 ± 244.9	21.1 ± 62.1

n.a.: not available

Table 27. Summary of PFAS data: EAOP inlet concentration and removal efficiencies

Pollutants	EAOP inlet concentration (ng/L)	EAOP removal (%)	EAOP + CW removal (%)	Control CW removal (%)
PFBA	7.32 ± 10.38	21.5 ± 13.0	19.4 ± 15.2	n.a.
PFPeA	14.16 ± 12.88	-36.6 ± 123.9	27.2 ± 35.3	-6.6 ± 6.3
PFHxA	10.59 ± 11.98	8.3 ± 14.0	8.3 ± 13.8	-12.8 ± 9.0
PFHpA	7.86 ± 6.94	18,6 ± 33.8	-8.7 ± 12.0	-17.6 ± 10.3
PFOA	17.53 ± 4.56	11.0 ± 22.5	12.2 ± 27.4	-14.0 ± 15.8
PFNA	3.91 ± 2.39	-6.7 ± 58.6	-1765.5 ± 2545.3	-5659.5 ± 7273.7
PFDA	4.17 ± 2.99	-21.8 ± 55.1	3.8 ± 33.0	67.2 ± 51.5
PFuDA	n.a.	n.a.	n.a.	n.a.
PFDoA	n.a.	n.a.	n.a.	n.a.
PFTrDA	n.a.	n.a.	n.a.	n.a.
PFTeDA	n.a.	n.a.	n.a.	n.a.
FOSA	n.a.	n.a.	n.a.	n.a.
N-MeFOSAA	n.a.	n.a.	n.a.	n.a.
N-EtFOSAA	n.a.	n.a.	n.a.	n.a.
L-PFBS	156.86 ± 89.17	15.7 ± 29.0	-1.6 ± 19.3	-21.4 ± 22.4
L-PFPeS	4.07 ± 1.21	11.1 ± 21.6	9.0 ± 28.2	15.2 ± 35.0
L-PFHxS	3.15 ± 4.91	3.2 ± 30.7	-109.8 ± 106.7	-95.0 ± 49.2
L-PFHpS	1.67 ± 2.01	-11.1 ± 7.1	-4.9 ± 5.7	30.2 ± 46.8
L-PFOS	29.75 ± 10.00	17.3 ± 59.8	17.9 ± 36.7	-53.3 ± 86.4
L-PFNS	1.23 ± 2.28	66.7 ± 44.1	100.0 ± 5.7	n.a.
L-PFDS	n.a.	n.a.	n.a.	n.a.
L-PFDoS	n.a.	n.a.	n.a.	n.a.
4:2FTS	4.54 ± 8.40	-153.4 ± 68.0	-104.7 ± 49.2	n.a.
6:2FTS	15.06 ± 18.77	-56.6 ± 65.1	-95.9 ± 95.3	-129.5 ± 109.4
8:2FTS	0.02 ± 0.02	-187.8 ± 231.7	-19.3 ± 77.4	-30.6 ± 85.0

n.a.: not available

5.8 Challenges and adaptations during pilot plant operation

The operation of the pilot plant at the WWTP Montornès del Vallès represented a complex challenge, requiring careful adjustments to ensure successful operation. From unforeseen technical difficulties to the need for real-time monitoring, this section delves into the key challenges encountered during the operational stage within the PROMISCES project.

(i) **Varying treatment durations throughout the EAOP operation** introduced a notable challenge for result analysis. Since the oxidation equipment was operated at different times during various phases, establishing a consistent baseline for comparison was difficult. The inconsistencies in exposure times impacted the reliability of contaminant removal rates, complicating the assessment of the system's overall performance and effectiveness.

(ii) The **accumulation of struvite in the EAOP prototype** posed significant operational challenges, particularly in the pipes, pumps and on the electrodes of the electrochemical cell. This struvite buildup hindered the overall efficiency of the EAOP prototype, leading to flow obstructions and reduced electrochemical performance. To address these issues, a bi-monthly maintenance routine was established, involving thorough cleaning and inspection of the affected components. This regular maintenance was essential to ensure the continuous performance of the pilot plant, preventing disruptions and maintaining the integrity of the water of the water treatment process.

(iii) **Ozone quantification in the EAOP prototype** was conducted to measure the residual ozone, specifically the fraction not dissolved in the solution. Nevertheless, the lack of non-airtight conditions in the experiment setup prevented an accurate assessment of the ozone dosage within the system. To address this issue, an on-site ozone sensor should be installed to allow real-time monitoring of ozone levels during pilot operation, providing more precise data for optimizing the process.

(iv) **Evaporation and/or evapotranspiration in the constructed wetlands** involved challenges in accurately calculating the contaminant mass balance, hindering the evaluation of contaminant removal efficiency. The imbalance between incoming and outgoing water volumes further complicated accurate assessments. In addition, this variability affected comparison with the control wetland. Thus, the impact of evaporation and/or evapotranspiration on the wetland's treatment performance had to be carefully accounted for in the analysis.

(v) **Managing the inflow and outflow in wetlands** requires precise, manual control of valves to maintain optimal conditions. To prevent overflowing or full drainage, valves are manually adjusted and monitored daily, ensuring the substrate remains sufficiently saturated to support both plant growth and microbial processes. This approach allows for the careful balance of water retention, yet daily oversight is crucial to avoid surface flooding and maintain the desired equilibrium between moisture levels and flow.

(vi) The **unexpected presence of elevated PFNA concentrations in the treated effluent** indicated some construction materials utilized in the wetland may have contained PFAS (Figure 10). This situation complicates the assessment of PFAS removal efficiency, as the specific material composition is rarely provided in detail and often lacks explicit disclosures regarding PFAS content. Experiments to analyse iPMTs and PFAS in the leachates from the materials used in the CWs are currently underway.

6 Use of reclaimed water in vegetable crop irrigation

Over the past few decades, water scarcity has intensified into a critical global challenge, driven by the dual forces of climate change and escalating water demand associated with population growth (Ungureanu et al., 2020, Jurado et al., 2012). In response, the reuse of treated wastewater from wastewater treatment plants (WWTPs) for agricultural irrigation has emerged as a viable strategy to reduce reliance on freshwater resources (García Vara et al., 2023). Despite offering considerable advantages, this solution is accompanied by concerns about the environmental safety and potential risks, underscoring the importance of rigorous assessment and the implementation of robust mitigation measures.

Recent laboratory research on the effects of PFAS on maize has demonstrated that the uptake and distribution of these compounds within crops are influenced by factors such as chain length, functional groups, and the specific plant tissues involved (Ateia et al., 2019). Similarly, studies on strawberries and lettuce cultivated in both greenhouse and open-field conditions suggest that benzotriazoles can be absorbed, assimilated, and internally regulated by plants (LeFevre, 2017). Despite these findings, the understanding of the mechanisms governing the integration of PMT compounds into the water-soil-plant system and their potential impact on human health remains incomplete.

Innovative water reclamation technologies, such as the one explored in this study, hold promise for minimizing crop exposure to PMTs. Nevertheless, evaluating the effects of reclaimed water on crop productivity, quality, and metabolic processes becomes essential. Furthermore, determining whether residual PMTs in the water could accumulate in crop tissues and potentially impact human health warrants focused investigation.

6.1. Characteristics of the water used for irrigation

Table 28 presents the physicochemical characteristics of the irrigation waters used in this study, including control water: bottled water (BW), secondary wastewater effluent (WW), and reclaimed water: e-Peroxone + constructed wetland (RW). Four-week-old lettuce seedlings were transplanted into the pots and harvested after 42 days, once they reached commercial size. Daily irrigation frequency was adjusted to maintain soil moisture just below field capacity, effectively preventing leachate production.

Table 28. General water quality parameters for each type of irrigation water (n=5)

	Units	BW	RW	WW
pH	-	8.40 ± 0.60	7.90 ± 0.70	7.90 ± 0.90
Redox	mV	163.00 ± 58.00	158 ± 57	135.00 ± 73.00
Conductivity	μS/cm	344.00 ± 92.00	1717.00 ± 111.00	1601.00 ± 213.00
COD	mg/L	<2.00	24.15 ± 13.40	25.00 ± 20.00
TOC	mg/L	<1.00	2.00 ± 2.00	14.00 ± 10.00
NH₄⁺	mg/L	<0.01	0.30 ± 0.20	1.00 ± 0.80
NO₂⁻	mg/L	<0.01	0.44 ± 0.47	0.37 ± 0.12
NO₃⁻	mg/L	2.16 ± 0.02	2.41 ± 2.86	1.92 ± 2.39
PO₄³⁻	mg/L	<0.10	0.40 ± 0.33	0.47 ± 0.54
SO₄²⁻	mg/L	47.00 ± 15.00	107.00 ± 30.00	113.00 ± 42.00
K⁺	mg/L	5.00 ± 3.00	25.00 ± 23.00	30.00 ± 19.00

6.2. Uptake and distribution of contaminants in vegetable crops

6.2.1 iPM(T)s

The evaluation of contaminant uptake and distribution in lettuce samples irrigated with different water types was conducted using a targeted analysis method that focused on the same iPM(T) compounds identified in the water samples. **Table 29** shows the occurrence of iPM(T)s in irrigation waters and soil used for crop cultivation. As expected, some ubiquitous phthalates -though not the main target compounds-, including diethyl phthalate, were detected in all irrigation waters, including bottled water. Plastic bottled water was used to avoid the occurrence of PFAS, the main target group of compounds, from being introduced, rather than using glass bottles. Additionally, both diethyl and dibutyl phthalates were found at notable concentrations in soil, wastewater, and reclaimed water, underscoring the widespread presence of phthalate compounds in the environment (Net et al., 2015). Most of the PMTs studied, such as N,N'-diphenylguanidine (DPG), galaxolidone, and triethyl phosphate, were already present in the soil. However, pharmaceuticals and pesticides appeared to be more closely associated with wastewater sources. No PFAS were detected in bottled water or soil.

Table 29. Concentration of iPM(T)s in irrigation waters (n=3) and soil used for crop studies

Compounds	BW (ng/L)	RW (ng/L)	WW (ng/L)	Soil (ng/g)
Triethyl phosphate	n.d.	61 ± 17	24 ± 10	3.0 ± 0.4
Galaxolidone	n.d.	1618 ± 460	2507 ± 306	12 ± 1
Dibutyl adipate	40.38 ± 0.003	n.d.	n.d.	14 ± 1
Tris(2-butoxyethyl) phosphate	n.d.	299 ± 121	503 ± 81	n.d.
N,N'-Diphenylguanidine (DPG)	n.d.	208 ± 46	3491 ± 158	462 ± 19
Dibutyl phthalate	n.d.	159 ± 130	165 ± 158	49 ± 4
Diethyl phthalate	18419 ± 2	991 ± 614	2086 ± 2846	905 ± 15
Bis(2-ethylhexyl)amine	n.d.	20 ± 2	12 ± 3	n.d.
2-Ethylhexyl diphenyl phosphate	n.d.	n.d.	n.d.	n.d.
MDMA	n.d.	186 ± 201	2406 ± 2007	n.d.
O-Desmethyl venlafaxine	n.d.	19 ± 16	977 ± 315	n.d.
Venlafaxine	n.d.	34 ± 11	408 ± 95	n.d.
3,5-di-tert-Butyl-4-hydroxybenzoic acid	n.d.	387 ± 107	378 ± 66	n.d.
Carbendazim	n.d.	15 ± 16.22	16 ± 18	n.d.
(4+5)-Methylbenzotriazole	n.d.	510 ± 218	1008 ± 391	n.d.
1,8-Diazabicyclo [5.4.0]undec-7-ene	n.d.	<LOQ	6 ± 5	n.d.
PFBA	n.d.	15 ± 1	18 ± 2	n.d.
PFOA	n.d.	15 ± 5	16 ± 6	n.d.
PFHxS	n.d.	7 ± 4	7 ± 14	n.d.
PFOS	n.d.	27 ± 9	27 ± 11	n.d.
6:2 FTS	n.d.	30 ± 24	3 ± 6	n.d.

n.d.: not detectable

As can be seen in **Table 29**, the concentration of some compounds exhibited an increase after EAOP + CW treatment. Although this outcome may seem inconsistent, the values align with those reported in **Table 27**, showing negative removal and significant deviation. This could be attributed to analytical variability or matrix effects, which can influence the accuracy of the quantification.

Out of the 41 iPM(T)s evaluated, 16 compounds were detected in the lettuce samples (**Table 30**). The antidepressant venlafaxine and its metabolite O-desmethylvenlafaxine were only found in samples irrigated with effluent wastewater, suggesting residual concentrations in reclaimed water were too low to result in detectable levels in crop leaves. A similar trend was observed for the drug of abuse MDMA and the pesticide carbendazim. This suggests that the EAOP + CW successfully minimized the presence of these pollutants in both reclaimed water and the irrigated crops.

A different trend emerges for certain industrial chemicals, such as 2-ethylhexyl diphenyl phosphate and bis(2-ethylhexyl) amine, which were found at similar concentrations in crops irrigated with all water types, including in the control samples. These results are consistent with the detection of phthalates in all irrigation waters and some PMTs from industrial application found in the soil (**Table 29**). As a result, the presence of PMTs, including triethyl phosphate, galaxolidone, dibutyl adipate, N,N-diphenylguanidine, dibutyl and diethyl phthalates, in all lettuce samples, including those irrigated with BW, appears to be directly linked to their presence in the soil.

Table 30. Overview of the iPM(T)s compounds in lettuce samples irrigated with bottled water (BW), secondary effluent wastewater (WW), and reclaimed water (RW)

Compounds	LOD (ng/g)	LOQ (ng/g)	Average concentration (ng/g)			Frequency of detection (/30)
			BW	RW	WW	
Triethyl phosphate	0.17	0.57	29 ± 6.5	28 ± 7	22 ± 5.0	30
Galaxolidone	1.1	3.7	7.9 ± 3.1	8.1 ± 3.2	5.5 ± 4.0	29
Dibutyl adipate	0.18	0.61	1.5 ± 0.88	3.3 ± 1.9	3.2 ± 2.6	24
Tris(2-butoxyethyl) phosphate	0.07	0.22	0.24 ± 0.08	0.13 ± 0.08	0.43 ± 0.18	22
N,N'-Diphenylguanidine (DPG)	0.22	0.71	1.1 ± 0.06	0.99 ± 0.01	1.1 ± 0.03	19
Dibutyl phthalate	0.79	2.6	70 ± 32	30 ± 17	51 ± 30	15
Diethyl phthalate	3.4	11	123 ± 88	13 ± 12	741	14
Bis(2-ethylhexyl)amine	0.04	0.15	0.06 ± 0.02	0.01 ± 0.007	n.d.	11
2-Ethylhexyl diphenyl phosphate	0.88	2.9	3.3 ± 2.3	3.5 ± 0.35	4.2 ± 2.7	10
MDMA	0.12	0.39	n.d.	n.d.	1.3 ± 0.59	10
O-Desmethyl venlafaxine	0.15	0.51	n.d.	n.d.	0.24 ± 0.13	10
Venlafaxine	0.09	0.31	n.d.	n.d.	1.2 ± 0.61	10
Carbendazim	0.04	0.13	n.d.	n.d.	0.25 ± 0.03	4
(4+5)-Methylbenzotriazole	0.10	0.33	n.d.	n.d.	0.05 ± 0.05	3
1,8-Diazabicyclo [5.4.0]undec-7-ene	0.04	0.12	n.d.	0.15 ± 0.04	n.d.	3

n.d.: not detectable

6.2.2 PFAS

The assessment of contaminant uptake and distribution in lettuce samples irrigated with different water types was performed using the analytical procedure detailed in section 4.7. Out of the entire set of PFAS analysed, only five compounds were detected and quantified in at least one sample (**Table 31**).

Table 31. Overview of the PFAS compounds in lettuce samples irrigated with bottled water (BW), secondary effluent wastewater (WW), and reclaimed water (RW) (n=10)

Compounds	LOD (ng/g)	LOQ (ng/g)	Average concentration (ng/g)			Frequency of detection (/10)
			BW	RW	WW	
PFBA	0.023	0.070	0.44 ± 0.11	1.16 ± 0.7	0.71 ± 0.21	50% BW 100% RW 50% WW
PFOA	0.015	0.045	0.05 ± 0.01	0.09 ± 0.07	n.d.	30% BW 40% RW 0% WW
PFHxS	0.013	0.039	0.09 ± 0.04	0.1 ± 0.04	0.85 ± 0.79	100% BW 100% RW 100% WW
PFOS	0.025	0.074	0.18 ± 0.16	0.14 ± 0.07	7.21 ± 6.95	100% BW 100% RW 100% WW
6:2 FTS	0.043	0.130	0.25 ± 0.05	0.22 ± 0.09	0.22 ± 0.21	100% BW 100% RW 90% WW

The results reveal notable differences between the PFAS levels reported in the irrigation waters used in the experiments (detailed in the section 5.5.4.) and the uptake profile observed in the lettuce samples. Only two acids and three sulfonates were detected in the samples. The sulfonates PFHxS, PFOS and 6:2 FTS were the most frequently identified, consistent with their higher log Kow values (2.98, 5.61, and 3.12, respectively), indicating greater potential for uptake and accumulation.

The results demonstrated the use of reclaimed water from the combined EAOP + CW technology reduced the concentrations of PFOS and PFHxS in crop leaves. More specifically, the concentration of PFOS in lettuce leaves decreased from 7.21 to 0.14 ng/g when irrigated with WW instead of RW, while PFHxS levels dropped from 0.85 to 0.1 ng/g. Although most PFAS were detected in lettuce leaves irrigated with BW, concentration levels were very close to the method's LOQ, considering the standard deviation values reported in **Table 31**. Furthermore, the presence of PFAS may stem from other alternative sources, such as the soil used for growing the lettuce crops - a presumably pristine site where no agricultural or industrial activities have occurred in the past-, as previously discussed regarding the other iPM(T)s.

6.3. Impact on crop yield and quality

6.3.1 Crop productivity and quality

Figure 31a illustrates that crop productivity, measured by dry weight, was not significantly affected by the quality of the irrigation water. Other agricultural parameters followed a similar trend, with no notable impact on humidity (**Figure 31b**) or leaf height (**Figure 31c**).

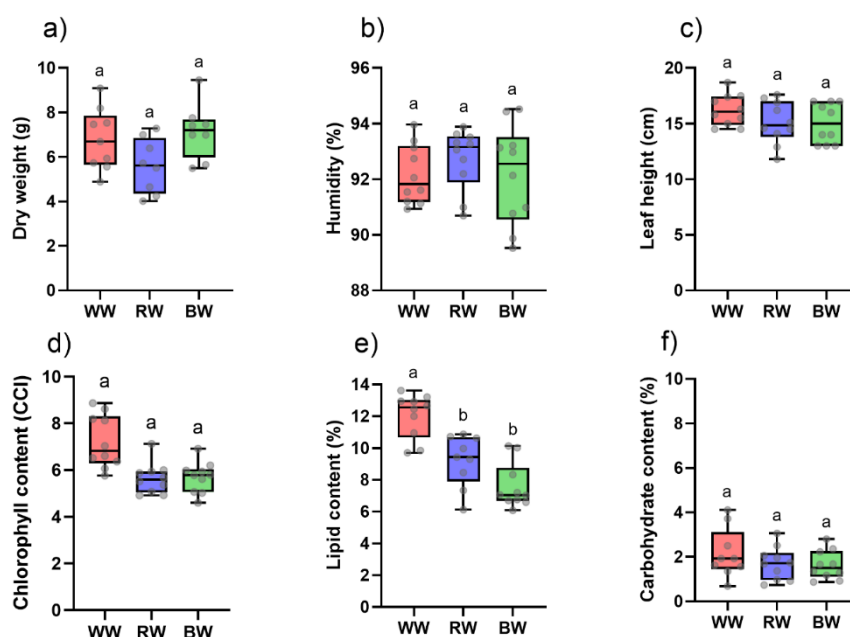


Figure 31. Agronomical parameters of lettuce crops irrigated with different water types (n=10)

Regarding the lipid and carbohydrate content (**Figure 31e** and **Figure 31f**), the use of WW for irrigation increased lipid levels compared to crops irrigated with BW or RW, with carbohydrate content remaining unaffected. The increase in the plant lipid concentration is not negative outcome and even, it may indicate enhanced production of essential fatty acids or stress-related secondary metabolites. However, if driven by the oxidative stress, contamination, or the buildup of harmful substances, it raises concerns about potential adverse effects. To explore this in greater depth, a metabolomics analysis has been carried out.

For chlorophyll content (**Figure 31c**), no significant differences were observed between treatments. However, the WW treatment resulted in higher chlorophyll levels compared to the other two. Although an increase in chlorophyll can enhance photosynthesis, it may also be induced by stress. Therefore, chlorophyll content should be considered alongside other agronomic parameters. In this case, both lipid content and chlorophyll levels seem to be impacted by the WW treatment.

Considering all parameters together, the results suggest that compounds present in WW, such as iPM(T)s and PFAS, may have significantly contributed to the increase in lipid content. Reclaimed water had no notable effect on lettuce agronomics compared to control water, secondary treated wastewater influenced lipid levels.

These results suggest that the developed EAOP + CW technology plays a role in mitigating the impact of wastewater constituents on lettuce.

6.3.2 Crop metabolomics

For the metabolomics analysis, intermediate leaves from three lettuce plants per treatment were collected using an 8-mm leaf punch. These samples were immediately frozen in dry ice and transported to the laboratory within two hours, where they were stored at -80°C until analysis.

The metabolomic profiling focused on lettuce grown with the three different irrigation water treatments. Leaf extraction followed a modified version of previously established protocols. Ten mg of homogenized lettuce tissue were placed in an Eppendorf tube, to which 400 μL of methanol was added. The samples were vortexed, sonicated, and centrifuged using a methanol-chloroform-water mixture based on the methodology outlined by Hurtado et al. (2017). The resulting extracts were vacuum-dried, followed by derivatization with methoxyamine in pyridine (20,000 mg/L) and N-methyl-N-(trimethylsilyl) trifluoroacetamide (MSTFA) containing 1 % trimethylchlorosilane (TMCS) according to Jorge et al. (2016). Triphenylamine was added to the samples before analysis.

GC-Orbitrap analysis was performed using an instrument equipped with a Zebtron ZB-5HT Inferno column (30 m \times 0.25 mm \times 0.25 μm). The oven temperature program started at 70°C for 2 minutes, then increased to 100°C at a rate of $7^{\circ}\text{C}/\text{min}$, followed by a rise to 260°C at $5^{\circ}\text{C}/\text{min}$, and finally to 320°C at $10^{\circ}\text{C}/\text{min}$.

Data from the GC-MS analysis were processed using Thermo Scientific's TraceFinder 5.1 software. Peak detection, spectral deconvolution, alignment, and library searches were carried out through the TraceFinder plug-in. A minimum total ion chromatogram (TIC) intensity threshold of 1×10^3 and an ion overlap window of 98% were applied to ensure data accuracy. Feature peak areas of the samples were uploaded to the MetaboAnalyst 5.0 platform (<http://www.metaboanalyst.ca>) for further analysis. Data normalization was performed using the triphenylamine feature peak, followed by Pareto scaling.

Metabolomics data were initially analyzed using univariate analysis (Kruskal-Wallis test) to identify potential significant differences in features. Subsequently, principal component analysis (PCA) was applied to detect distinct patterns and visualize variations in the data (**Figure 32**).

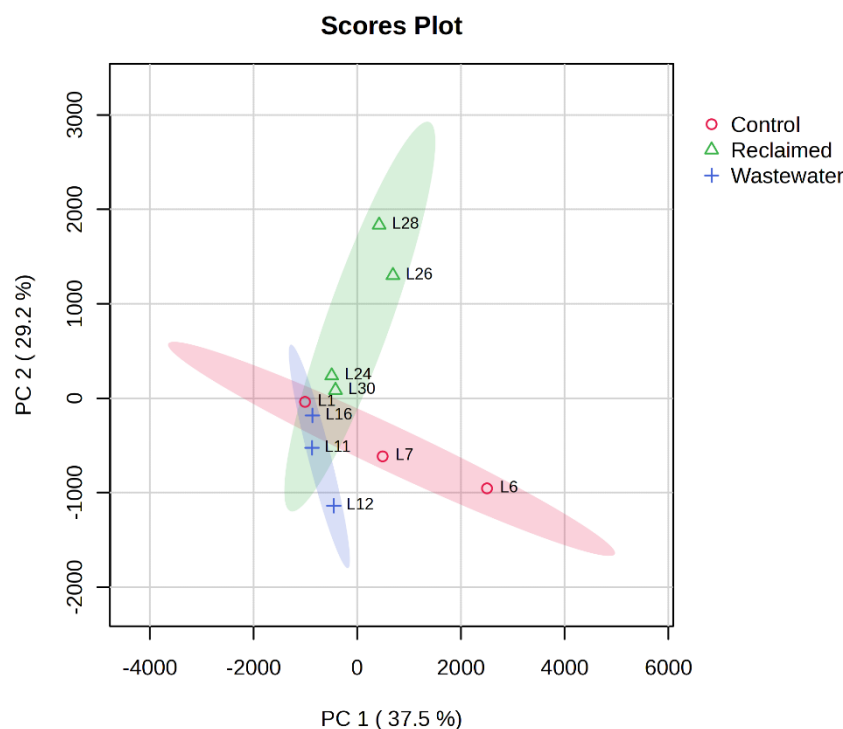


Figure 32. Score plot with samples normalized using the triphenylamine feature and data scaled via Pareto scaling. A PCA was then conducted. The shaded area represents the 95% confidence interval.

None of the features showed a significant difference in univariate analysis (p -value < 0.05 , non-parametric test) across the three treatment groups. Additionally, the PCA of the metabolome did not reveal any noticeable separation between lettuces irrigated with the different water types (**Figure 32**). The results show no significant metabolomic changes in the lettuce plants, even though varying contaminant concentrations were detected in the samples during this initial growth cycle. This limited impact of irrigation water quality could be attributed to the combined influence of the soil, the lettuce plants, and the diverse microbial communities inhabiting the root zone (rhizosphere). These microorganisms and their associated genes are known for their remarkable diversity and their crucial role in enhancing plant resilience to abiotic stresses caused by soil contaminants (Chaudhry et al., 2005). Additionally, the rhizosphere exhibits a superior capacity for pollutant breakdown compared to unplanted soil (Olson et al., 2003).

6.4. Environmental and health implications

6.4.1 iPM(T)s

The ecotoxicological risk of the 38 iPM(T)s identified in influent and effluent water from the WWTP and the e-Peroxone effluent was evaluated through risk quotients (RQs). These RQs were determined by calculating the ratio between the maximum measured concentrations (MECs) and the predicted no-effect concentrations (PNECs) for freshwater, as published by the NORMAN network (<https://www.norman-network.com/nds/ecotox/lowestPnecsIndex.php>) (**Table 32**).

Based on the established risk categories, considering reclaimed water, fourteen compounds fall under the “no risk” classification for aquatic organisms, with RQ values below 0.1. Fourteen compounds are categorized as “low risk”, exhibiting RQ values between 0.1 and 1. Six compounds

show a “**moderate risk**” potential, with RQ values ranging from 1 to 10, while four compounds are identified as “**high risk**” with RQ values exceeding 10.

Compared to the influent (WW) of the WWTP, a decrease in the number of compounds categorised as “**high risk**” can be observed, due to a decrease in their concentration, 1) when applying the conventional treatment in the Montornès del Vallès WWTP (secondary effluent wastewater, WW) and 2) after the e-Peroxone (reclaimed water, RW).

Table 32. Risk quotient (RQs) values for iPMT compounds detected in untreated wastewater (uWW), secondary effluent wastewater (WW) and reclaimed water (RW)

Compounds	PNEC (ng/L)	uWW		WW		RW	
		MECs (ng/L)	RQ	MECs (ng/L)	RQ	MECs (ng/L)	RQ
Galaxolidone	100	4.9E+03	49	4.2E+03	42	2.1E+03	21
MDMA	216	1.2E+05	551	1.1E+04	50	2.7E+03	12
O-Desmethyl venlafaxine	6	2.3E+03	370	1.6E+03	267	71	12
Venlafaxine	6	569	93	658	108	70	11
Ofloxacin	26	2.1E+03	80	720	28	223	8.6
Caffeine	100	2.4E+04	240	3.2E+03	32	705	7
Bis(2-ethylhexyl) amine	14	45	3.2	18	1.3	52	3.7
Tris(2-butoxyethyl) phosphate	1.4E+02	1.3E+03	9.0	584	4.2	479	3.4
Theophylline	1.0E+02	2.0E+04	196	1.2E+03	12	203	2.0
3,5-di-tert-Butyl-4-hydroxybenzoic acid	1.1E+03	1.1E+03	1.0	574	0.5	1.3E+03	1.1
Flecainide	640	22	0.03	1.7E+03	2.6	536	0.8
(EDDP) / 2-ethyl-1,5-dimethyl-3,3-diphenylpyrrolinium	85	145	1.7	79	0.9	41	0.5
1,2,3-benzotriazole	7.8E+03	2.7E+03	0.4	4.8E+03	0.6	3.6E+03	0.5
Temazepam	71	345	4.9	42	0.6	32	0.4
2,4-Diaminotoluene	1.2E+04	5.1E+04	4.3	1.6E+04	1.3	5.2E+03	0.4
N,N'-Diphenylguanidine (DPG)	1.1E+03	237	0.2	555	0.5	448	0.4
Dibutyl phthalate	1.0E+04	1.6E+03	0.2	1.2E+03	0.1	4.1E+03	0.4
Diuron	70	28	0.4	26	0.4	22	0.3
Terbutryn	65	45	0.7	83	1.3	20	0.3
10,11-Dihydro-10,11-dihydroxycarbamazepine	1.9E+03	2.1E+04	11.0	739	0.4	516	0.3
Carbendazim	150	32	0.2	133	0.9	39	0.3
(4+5)-Methylbenzotriazole	8.0E+03	1.4E+03	0.2	1.5E+03	0.2	869	0.1
Diethyl phthalate	1.6E+04	5.1E+03	0.3	6.3E+03	0.4	1.6E+03	0.1
2-Aminophenol	4.0E+03	2.8E+04	7.0	2.4E+03	0.6	263	0.1
Sulpiride	4.1E+03	407	0.1	887	0.2	114	0.03
Secbumeton	48	n.d.	n.d.	n.d.	n.d.	1	0.02
Carbamazepine	2.0E+03	62	0.03	79	0.04	41	0.02

		uWW		WW		RW	
Compounds	PNEC (ng/L)	MECs (ng/L)	RQ	MECs (ng/L)	RQ	MECs (ng/L)	RQ
6-Methyl-2-pyridinemethanol + 2-Amino-4-cresol	4.6E+04	612	0.01	1.5E+03	0.03	935	0.02
Dibutyl hydrogen phosphate	5.6E+04	5.8E+04	1.0	1.0E+03	0.02	567	0.01
Caprolactam	6.7E+04	8.5E+03	0.1	329	0.005	548	0.01
Dibutyl adipate	7.0E+03	n.d.	n.d.	n.d.	n.d.	49	0.01
Tributyl phosphate/triisobutyl phosphate	6.6E+04	4.9E+04	0.7	566	0.009	331	0.005
Sitagliptin	8.4E+04	2.8E+03	0.03	1.4E+03	0.02	304	0.004
Triethyl phosphate	6.3E+05	43	0.0001	224	0.0004	551	0.0009
Tributylamine	8.8E+04	49	0.0006	63	0.0007	38	0.0004
Melamine	3.6E+05	208	0.001	353	0.001	82	0.0002
1,8-Diazabicyclo [5.4.0]undec-7-ene (polycat dbu)	1.7E+04	86	0.005	132	0.008	n.d.	n.d.
6-Methoxyquinoline	3.9E+04	33	0.001	25	0.0006	n.d.	n.d.

Furthermore, diuron (maximum concentration: 22 ng/L) and terbutryn (maximum concentration: 20 ng/L), both with RQ values of 0.3, remain well below the Environmental Quality Standards (EQS) for surface waters set by Directive 2013/39/EC. For diuron, these limits are 200 ng/L (annual average, AA) and 1800 ng/L (maximum allowable concentration, MAC), while for terbutryn, the thresholds are 65 ng/L (AA) and 340 ng/L (MAC).

In the analysed lettuce samples (**Table 33**, max (ng/g) in lettuce), no maximum residue limits (MRLs) are established for any of the detected compounds, except for carbendazim, which has an MRL of 100 ng/g (Reg. (EU) No 559/2011). However, the maximum concentration of carbendazim found in the samples was significantly lower than this limit.

To evaluate potential health risks associated with the presence of iPM(T)s in the lettuce, the threshold of toxicological concern (TTC) approach was applied. This method is useful when toxicity data are limited, relying on structural alerts to categorize compounds into toxicity classes using the Cramer classification decision tree in Toxtree software (<http://toxtree.sf.net/predict>). The iPM(T)s detected in lettuce were classified into Class I (least toxic, TTC = 30 µg/kg/day), Class II (TTC = 9 µg/kg/day), and Class III (most toxic, TTC = 1.5 µg/kg/day) according to Munro et al. (1996) (**Table 33**).

To determine the worst-case scenario, the daily consumption (DC) of lettuce required to reach the TTC value was calculated by multiplying the TTC by an average adult body weight of 70 kg and dividing by the maximum concentration of each compound in the lettuce. The resulting DC values (**Table 33**) are significantly higher than the estimated daily intake (DI) of lettuce (0.01 kg/day/person, MAPA, 2022). This indicates that the presence of iPM(T)s in the lettuce samples poses no significant risk to human health.

Table 33. Threshold of toxicological concern (TTC) analysis results for detected compounds

Compounds	max (ng/g)	Risk Class	TTC value (µg/Kg/day)	DC (Kg/day/person)
Triethyl phosphate	40	III	1.5	3
Galaxolidone	13	III	1.5	8
Dibutyl adipate	7.6	I	30	276
Tris(2-butoxyethyl) phosphate	0.72	III	1.5	146
N,N'-Diphenylguanidine (DPG)	1.1	III	1.5	95
Dibutyl phthalate	124	I	30	17
Diethyl phthalate	741	I	30	3
Bis(2-ethylhexyl)amine	0.09	I	30	23333
2-Ethylhexyl diphenyl phosphate	6.8	III	1.5	15
MDMA	2.2	III	1.5	48
Venlafaxine	2.5	I	30	840
O-Desmethyl venlafaxine	0.44	I	30	4773
3,5-di-tert-Butyl-4-hydroxybenzoic acid	9.0	II	9	70
Carbendazim	0.29	III	1.5	362
1,8-Diazabicyclo [5.4.0]undec-7-ene (polycat dbu)	0.20	III	1.5	525
(4+5)-Methylbenzotriazole	0.10	III	1.5	1050

6.4.2 PFAS

Regarding the health implications of PFAS, the EFSA established the tolerable weekly intake (TWI) safety threshold for PFAS in food in 2020, including PFOA, PFOS, PFNA, and PFHxS, at 4.4 ng/kg of body weight per week (Bignami et al., 2020). Based on this, the Weekly Intake (WI) was calculated for the sum of PFOA, PFOS, and PFHxS, using the main results from CW, RW and WW. Notably, PFNA was not detected in the lettuce, so it was excluded from the WI calculation. The calculation assumed that an adult weighing 60 kg consumes one lettuce (approximately 300 g) per week (**Table 34**). As shown, nearly all samples irrigated with direct WW exceed safe consumption levels. However, no risk to consumers was observed using RW or BW, according to the TWI set by EFSA.

Table 34. Weekly intake for PFAS (sum of PFOA, PFOS and PFHxS)

Sample code	Weekly Intake (ng/kg bw per week)	Risk for consumer
RW	1,38 ± 0,55	-
WW	40,3 ± 35,39	YES
CW	1,36 ± 0,96	-

7 Conclusions and recommendations

7.1 Key findings on process operation

The PROMISCES project has yielded significant insights into the EAOP + CW operation, particularly regarding their efficiency, challenges and potential for real-world application. These key findings highlight essential aspects of performance, optimization, and sustainability. For a clearer and more concise overview, the conclusions are presented in the following bullet points.

Operation (EAOP + CW)

- The operation of post EAOP CW system depends on the performance of the e-Peroxone process. High iPM(T)s removal efficiencies in the EAOP involve minimal further removal by the CW, as most of the contaminants are already eliminated.
- Oversizing CW design results in longer retention time, enhancing the degradation efficiency and reducing the burden on the EAOP. Although pollutant removal over longer periods in the CW system has not been evaluated during the pilot operation, the existing literature suggests that both hydraulic retention time and CW type are positively correlated with PFAS removal. Additionally, placing a larger or more efficient CW a pretreatment step to the EAOP could lower the concentrations of co-contaminants, organic matter, suspended solids, and other substances that negatively affect the EAOP efficiency.

Risk assessment (crop uptake and RQs)

- Tertiary wastewater treatment effluent should be preferred for irrigation over water from secondary treatment due to the presence of contaminants in the latter, which pose potential health risks. Irrigation with different qualities of water led to varying concentrations of pollutants in lettuce, pharmaceuticals (such as O-Desmethyl venlafaxine and venlafaxine) and some PFAS (including PFOS and PFHxS) were detected at higher concentrations in crops irrigated with secondary-treated effluent.
- Agricultural studies also suggest a potential uptake of PMTs by crops from the soil, although no human health risk based on calculated TTC values was observed. Nevertheless, this source of pollution in crops should be acknowledged.
- Agronomic and metabolomic results for the irrigated crops showed no differences between the irrigation water sources used, indicating the pollutant concentrations in the crops were too low to induce any noticeable changes.

7.2 Recommendations for optimizing the treatment and crop studies

Based on results from the pilot plant's operation at Montornès del Vallés WWTP, this section outlines some key recommendations for enhancing the efficiency and effectiveness of the treatment process. These suggestions offer a strategic approach to optimizing current operations, tackling potential inefficiencies, and ultimately contributing to the development of more robust and scalable treatment solutions.

(i) This **initial testing** was conducted exclusively during warm weather, which may have influenced the CW process due to **higher ambient temperatures**. To gain a complete understanding of the system's resilience and effectiveness, conducting tests across all seasons is essential. Seasonal temperature variations can affect microbial activity, chemical reaction rates, and overall treatment efficiency. Testing under diverse weather conditions allows us identifying potential performance

fluctuations, optimize for a wider range of environmental factors, and ensure reliable, year-round operation of the treatment process.

(ii) In this initial testing, the plants were still in early stages of growth, with **limited aerial and root biomass**. Consequently, the data gathered may not yet reflect the full treatment potential of the system. As plants mature, their larger root networks and denser foliage rise contaminant removal, oxygen transfer, and microbial activity within the wetland. Therefore, testing should be extended across all seasons to capture the entire annual biological cycle of the plants.

(iii) Due to EAOP prototype limitations, the **continuous operation is not feasible**, which prevents precise alignment of constructed wetland sampling with the completion of the eAOP process. This constraint requires careful strategic planning to ensure samples are collected at intervals that best reflect the treatment process and provide reliable data for analysis. Moreover, finding commercial pumps or flowmeters capable of accurately handling such low flow rates is challenging.

(iv) The **design and operation of the CW systems** encountered several critical challenges. The daily manual measurement of inflow and outflow in the CW was time-consuming: the flow was very low and not piston-like, leading to non-homogeneous water flow. Additionally, more heterogeneous backfill materials could enhance root development, ensuring the formation of the rhizosphere and biofilm, which are crucial for supporting a diverse microbial community capable of degrading pollutants. Furthermore, the secondary effluent has high electrical conductivity, indicating elevated salinity levels, which are intensified by the e-Peroxone process and therefore, lead to a decrease in nutrient concentrations.

(v) The **crop study** had some operational limitations due to its scale. The experiments were carried out in a greenhouse using soil sourced from a presumably pristine location, which was later found to contain trace amounts of some PMTs. Additionally, RW and WW were collected from the pilot plant and transported in plastic containers to prevent PFAS contamination. However, this inadvertently led to contamination from plasticizers. The presence of plasticizers did not present a significant issue, as they were of low toxicity (**Table 33**) and not the focus of the study. Future studies should be conducted at a field scale, ideally using plots irrigated with different water qualities sourced directly from the production site. This would help minimize cross-contamination during the transportation of water or soil.

7.3 Future considerations for system scalability

Looking ahead, the scalability of the system is a key factor for broader application. Although the current design and performance provides promising results, scaling the system to meet demands of larger operations presents both exciting opportunities and significant challenges. Tackling these considerations will be essential for optimizing the system and ensuring its successful development across a range of real-world conditions.

(i) A **potentially effective configuration** could be **wetland + EAOPs + wetland**. In this approach, the first wetland serves to remove nutrients prior to their oxidation, while the post-treatment wetland focuses on eliminating the inorganic ions generated during the oxidative process under anoxic conditions. Previous studies reported the inhibitory effect of nitrate on perchlorate removal, with oxygen being considered the major inhibitor of the perchlorate reduction (Tan et al, 2004). This configuration considerably reduces the nutrient load before the e-Peroxone treatment, thereby decreasing the deposition of struvite.

(ii) The formation of chlorate and perchlorate is an inherent issue of the oxidation process in waters with relatively high chloride concentrations. Adjusting the ozone dose during the oxidation process reduces their concentration; however, removing these inorganic ions necessitates complementary technologies, such as ion exchange processes, reverse osmosis membranes, or nature-based solutions operating under anoxic conditions.

(iii) Integrating **resource recovery strategies** (struvite precipitation) enhances both the sustainability and economic viability of the system. This approach offers dual advantages, reducing nutrients concentration in treated water while simultaneously yielding struvite-a valuable slow-release fertilizer for agriculture applications. By transforming nutrient-rich wastewater into a resource, this method supports the circular economy model.

(iv) A **thorough toxicity analysis of the treated effluent** should extend beyond just PFAS and iPM(T)s. Although these contaminants are significant, they constitute only a fraction of the wider range of potential pollutants present in wastewater. A global bioassay and/or ecotoxicological test could ensure the overall safety of the treated water used in irrigation, safeguarding the aquatic life, plants and humans.

(v) A **potentially improved wetland configuration** could involve adding a third flume wetland without plants to assess the nutrient removal capacity of bacteria, excluding the influence of the rhizosphere, and to investigate the clogging dynamics to better understand the system's lifespan.

(vi) The **potential accumulation of some iPM(T)s in the soil** due to the continuous use of reclaimed or wastewater for crop irrigation warrants further evaluation. This study focused exclusively on the target pollutants present in the irrigation water, without considering transformed or conjugated compounds. Moving forward, research should expand to analyze these substances and incorporate toxicological bioassays on lettuce to guarantee the long-term safety of the crop.

8 References

- Allen, D.J.; Huang, J.; Farrell, M.; Mosley, L.M. (2023) Novel insight into ammonium, phosphate and iron (II) dynamics in the sediment porewater of a constructed wetland under artificial aeration through the diffusive equilibrium in thin films technique. *Environmental Research*, 236, 1, art. 116746.
- Amado-Piña, D.; Roa-Morales, G.; Molina-Mendieta, M.; Balderas-Hernández, P.; Romero, R.; Barrera Díaz, C.E.; Natividad, R. (2022) E-peroxone process of a chlorinated compound: Oxidant species, degradation pathway and phytotoxicity. *Journal of Environmental Chemical Engineering*, 10 (4), art. 108148.
- Ateia, M.; Maroli, A.; Tharayil, N.; Karanfil, T. (2019) The overlooked short- and ultrashort-chain poly- and perfluorinated substances: A review. *Chemosphere*, 220, pp. 866-882.
- Barbosa, M.O.; Ratola, N.; Homem, V.; Pereira, M.F.R.; Silva, A.M.; Ribeiro, A.R.; Llorca, M.; Farré, M. (2023) Per- and poly-fluoroalkyl substances in Portuguese rivers: spatial-temporal monitoring. *Molecules*, 28(3), art. 1209.
- Barco, A. and Borin, M. (2017) Treatment performance and macrophytes growth in a restored hybrid constructed wetland for municipal wastewater treatment. *Ecological Engineering*, 107, pp. 160-171.
- Barisci, S. and Suri, R. (2020) Electrooxidation of short and long chain perfluorocarboxylic acids using boron doped diamond electrodes. *Chemosphere*, 243, art. 125349.
- Béalu, Z.; Walther, J.; Abufasia, A.; Altmann, K.; Meurer, M.; Gretzschel, O.; Schäfer, M.; Steinmetz, H. (2024) Removal of organic micropollutants and microplastics via ozonation followed by granular activated carbon filtration. *Environments*, 11 (11), 241.
- Bignami, M.; Bodin, L.; Chipman, J.K.; del Mazo, J.; Grasl-Kraupp, B.; Hogstrand, C.; Hoogenboom, L.R.; Leblanc, J.C.; Nebbia, C.S.; Nielsen, E.; Ntzani, E.; Petersen, A.; Sand, S.; Schrenk, D.; Schwerdtle, T.; Vleminckx, C.; Wallace, H. (2020) Risk to human health related to the presence of perfluoroalkyl substances in food. *EFSA Journal*, 18 (9), art. e06223.
- Casierra-Martínez, H.A.; Madera-Parra, C.A.; Vargas-Ramírez, X.M.; Caselles-Osorio, A.; Torres-López, W.A. (2020) Diclofenac and carbamazepine removal from domestic wastewater using a constructed wetland-solar photo-Fenton coupled system. *Ecological Engineering*, 153, art. 105699.
- Cedillo-Herrera, C.I.G.; Roé-Sosa, A.; Ramírez, K.; Rochín-Medina, J.; Amabilis-Sosa, L.E. (2020) Efficient malathion removal in constructed wetlands coupled to UV/H₂O₂ pretreatment. *Applied Sciences*, 10 (15) art. 5306.
- Chaudhry, Q.; Blom-Zandstra, M.; Gupta, S.; Joner, E.J. (2005) Utilising the synergy between plants and rhizosphere microorganisms to enhance breakdown of organic pollutants in the environment. *Environmental Science and Pollution Research*, 12, pp. 34-48.
- Deliverable D1.4. GC- and LC-HRMS methods and data treatments workflows for suspect screening and retrospective identification of relevant CECs in the water cycle and for identifying transformation products of PFAS during remediation process (DOI: [10.5281/zenodo.14629045](https://doi.org/10.5281/zenodo.14629045)).
- Furini, L.N.; Constantino, C.J.L.; Sanchez-Cortes, S.; Otero, J.C.; López-Tacón, I. (2016) Adsorption of carbendazim pesticide on plasmonic nanoparticles studied by surface-enhanced Raman scattering. *Journal of Colloid and Interface Science*, 465, pp.183-189.

- García Vara, M., Orlando Véliz, D., Bonansea, R. I., Postigo, C., & de Alda, M. L. (2023) Prioritization of organic contaminants in a reclaimed water irrigation system using wide-scope LC-HRMS screening. *Journal of Hazardous Materials*, 459, art. 132119.
- Hollender, J.; Zimmermann, S.G.; Koepke, S.; Krauss, M.; McArdell, C.S.; Ort, C.; Singer, H.; von Gunten, U.; Siegrist, H. (2009) Elimination of organic micropollutants in a municipal wastewater treatment plant upgraded with a full-scale post-ozonation followed by sand filtration. *Environmental Science and technology*, 43 (20), pp. 7862-7869.
- Hurtado, C.; Parastar, H.; Matamoros, V.; Piña, B.; Tauler, R.; Bayona, J.M. (2017) Linking the morphological and metabolomic response of *Lactuca sativa* L exposed to emerging contaminants using GC × GC-MS and chemometric tools. *Scientific Reports*, 7, art. 6546.
- Jaffer, Y.; Clark, T.A.; Pearce, P.; Parsons, S.A. (2002) Potential phosphorous recovery by struvite formation. *Water Research*, 36 (7), pp. 1834-1842.
- Jorge, T.F.; Mata, A.T.; António, C. (2016) Mass spectrometry as a quantitative tool in plant metabolomics. *Philosophical Transactions of the Royal Society A: Mathematical, Physical and Engineering Sciences*, 374, art. 20150370.
- Jurado, A.; Vázquez-Suñé, E.; Carrera, J.; de Alda, M.L.; Pujades, E.; Barceló, D. (2012) Emerging organic contaminants in groundwater in Spain: a review of sources, recent occurrence and fate in a European context. *Science of the Total Environment*, 440, pp. 82-94.
- Kavusi, E.; Ansar, B.S.K.; Ebrahimi, S.; Sharma, R.; Ghoreishi, S.S.; Nobaharan, K.; Abdoli, S.; Dehghanian, Z.; Lajayer, B.A.; Senapathi, V.; Price, G.W.; Astatkie, T. (2023) Critical review on phytoremediation of polyfluoroalkyl substances from environmental matrices: Need for global concern. *Environmental Research*, 217, art. 114844.
- Kékedi-Nagy, I.; Teymouri, A.; Herring, A.M.; Greenlee, L.F. (2020) Electrochemical removal and recovery of phosphorous as struvite in an acidic environment using pure magnesium vs. the AZ31 magnesium alloy as the anode. *Chemical Engineering Journal*, 380, art. 122480.
- Kumarathilaka, P.; Oze, C.; Indraratne, S.P.; Vithanage, M. (2016) Perchlorate as an emerging contaminant in soil, water and food. *Chemosphere*, 150, pp. 667-677.
- LeFevre, G.H.; Lipsky, A.; Hyland, K.C.; Blaine, A. C.; Higgins, C.P.; Luthy, R.G. (2017) Benzotriazole (BT) and BT plant metabolites in crops irrigated with recycled water. *Environmental Science: Water Research and Technology*, 3, pp. 213-223.
- Lin, Z.; Yao, W.; Wang, Y.; Yu, G.; Deng, S.; Huang, J.; Wang, B. (2016) Perchlorate formation during the electro-peroxone treatment of chloride-containing water: Effects of operational parameters and control strategies. *Water Research*, 88, pp.691-702.
- Margenat, A.; Matamoros, V.; Díez, S.; Cañameras, N.; Comas, J.; Bayona, J.M. (2018) Occurrence and bioaccumulation of chemical contaminants in lettuce grown in peri-urban horticulture. *Science of Total Environment*, 637-638, pp. 1166-1174.
- Matamoros, V.; Puigagut, J.; García, J.; Bayona, J.M. (2007) Behaviour of selected priority organic pollutants in horizontal subsurface flow constructed wetlands: A preliminary screening. *Chemosphere*, 69, 9, pp. 1374-1380.

- Matamoros, V.; Escolà-Casas, M.; Pastor, E.; Tadić, Đ.; Cañameras, N.; Carazo, N.; Bayona, J.M. (2022) Effects of tetracycline, sulfonamide, fluoroquinolone, and lincosamide load in pig slurry on lettuce: Agricultural and human health implications, *Environmental Research*, 215 (1), art. 114237.
- Meffe, R.; de Santiago-Martín, A.; Teijón, G.; Martínez Hernández, V.; López-Heras, I.; Nozal, L.; de Bustamante, I. (2021) Pharmaceutical and transformation products during unplanned water reuse: Insights into natural attenuation, plant uptake and human health impact under field conditions. *Environmental International*, 157, art. 106835.
- Mirabediny, M.; Sun, J.; Yu, T.T.; Åkermark, B.; Das, B.; Kumar, N. (2023) Effective PFAS degradation by electrochemical oxidation methods-recent progress and requirement. *Chemosphere*, 321, art. 138109.
- Munro, I.C.; Ford, R.A.; Kennepohl, E.; Sprenger, J.G. (1996) Correlation of a structural class with no observed-effect levels: a proposal for establishing a threshold of concern. *Food and Chemical Toxicology*, 34, pp. 829–867.
- Nassazzi, W.; Wu, T.C.; Jass, J.; Lai, F.Y.; Ahrens, L. (2023) Phytoextraction of per- and poly-fluoroalkyl substances (PFAS) and the influence of supplements on the performance of short-rotation crops. *Environmental Pollution*, 333, art. 122038.
- Net S; Sempéré R.; Delmont A.; Paluselli A.; Ouddane B. (2015) Occurrence, Fate, Behavior and Ecotoxicological State of Phthalates in Different Environmental Matrices. *Environmental Science & Technology*, 49, pp. 4019–4035
- Olson, P. E., Reardon, K. F., & Pilon-Smits, E. A. H. (2003) Chapter 10: Ecology of rhizosphere bioremediation. In: *Phytoremediation: transformation and control of contaminants*, Ed. John Wiley & Sons, Inc., pp. 317-353.
- Radjenovic, J.; Duinslaeger, N.; Avval, S.S.; Chaplin, B.P. (2020) Facing the challenge of poly- and perfluoroalkyl substances in water: is electrochemical oxidation the answer? *Environmental Science and Technology*, 54 (23), art. 14815.
- Sachdeva, S.; Chowdari, J.; Patro, A.; Mittal, S.; Sahoo, P.K. (2023) Emerging Aquatic Contaminants, Chapter 9. Efficacy of biotic components in constructed wetlands for mitigating pesticides, pp. 235-276.
- Sanders, Laura L. (1998) *A manual of field hydrogeology*. Prentice-Hall, Inc., 113 Sylvan Ave. Englewood Cliffs NJ 07632 USA. 381.
- Santos Sanchez, A. and Martins, G. (2021) Nutrient recovery in wastewater treatment plants: Comparative assessment of different technological options for the metropolitan region of Buenos Aires. *Journal of Water Process engineering*, 41, art. 122076.
- Schymanski, E.L.; Jeon, J.; Gulde, R.; Fenner, K.; Ruff, M.; Singer, H.P.; Hollender, J. (2014) Identifying small molecules via high resolution mass spectrometry: Communicating confidence. *Environmental Science and Technology*, 48 (4), pp. 2097-2098.
- Sharma, N.; Barion, G; Shrestha, I.; Ebinezer, L.B.; Trentin, A.R.; Vamerali, T.; Mezzalira, G.; Masi, A.; Ghisi, R. (2020) Accumulation and effects of perfluoroalkyl substances in three hydroponically grown *Salix L.* species. *Ecotoxicology and Environmental Safety*, 191, art. 110150.
- Singh, R.K.; Multari, N.; Nau-Hix, C.; Woodard, S.; Nickelsen, M.; Thagard S.M.; Holsen, T.M. (2020) Removal of Poly- and Per-Fluorinated compounds from ion exchange regenerant still bottom samples in a plasma reactor. *Environmental Science & Technology*, 54(21), pp. 13973-13980
- Ungureanu, N.;

- Vlăduț, V.; Voicu, G. (2020) Water scarcity and wastewater reuse in crop irrigation. *Sustainability*, 12(21), art. 9055.
- Savvidou, P.; Dotro, G.; Campo, Coulon, F.; Lyu, T. (2024) Constructed wetlands as nature-based solutions in managing per-and poly-fluoroalkyl substances (PFAS): Evidence, mechanisms and modelling. *Science of the Total Environment*, 934, art. 173237.
- Tan, K.; Jackson, W.A.; Anderson, T.A.; Pardue, J.H. (2004) Fate of perchlorate-contaminated water in upflow wetlands. *Water Research*, 38, pp. 4173-4185.
- Vymazal, J. (2011) Plants used in constructed wetlands with horizontal subsurface flow: a review. *Hydrobiology*, 674, pp. 133-156.
- Wang, Y.; Yu, G.; Deng, S.; Huang, J.; Wang, B. (2018) The electro-peroxone process for the abatement of emerging contaminants: mechanisms, recent advances, and prospects. *Chemosphere*, 208, pp. 640-654.
- WHO (2016a) Perchlorate in Drinking-Water Background. World Health Organization.
- WHO (2016b) Chlorine Dioxide, Chlorite and Chlorate in Drinking-Water Background Document for Development of WHO Guidelines for Drinking-Water Quality. World Health Organization.
- Yang, J.; Dong, Z.; Jiang, C.; Wang, C.; Liu, H. (2019) An overview of bromate formation in chemical oxidation processes: Occurrence, mechanism, influencing factors, risk assessment, and control strategies. *Chemosphere*, 237, art. 124521.
- Yao, W.; Fu, J.; Yang, H.; Wang, Y (2019) The beneficial effect of cathodic hydrogen peroxide generation on mitigating chlorinated by-product formation during water treatment by an electro-peroxone process. *Water Research*, 157, pp. 209-2017.